D1.6 – Improved ASR-Coastal Reference site

Improved ASR-Coastal reference sites in Nootdorp and Westland, the Netherlands (TRL8)

SUBSOL has received funding from the European Union's Horizon 2020 research and innovation programme under grant agreement No 642228

Title:	Improved ASR-Coastal Reference sites (TRL8)

Grant agreement no:	642228
Work Package:	WP1.3
Deliverable number:	D1.6
Partner responsible:	KWR Watercycle Research Institute
Deliverable author(s):	Dr. Koen Zuurbier, Teun van Dooren MSc, Steven Ros MSc
Quality assurance:	Prof. Dr. Pieter Stuyfzand (KWR),
Planned delivery date:	30 September 2017
Actual delivery date:	13 August 2018
Dissemination level:	PU *PU = Public* *PP = Restricted to other programme participants (including the Commission Services)* *RE = Restricted to a group specified by the consortium (including the Commission Services)* *CO = Confidential, only for members of the consortium (including the Commission Services)*

Table of contents

Executive Summary

At two field sites, ASR-Coastal set-ups have been operating between 2012 and 2017 to store (very) fresh rainwater in a brackish to saline sandy aquifer (10 to 40 m deep). Both sites showed distinct characteristics, but followed the same basic ASR-Coastal strategy: water could be infiltrated and recovered via various independently operated well screens in different segments of the aquifer to increase the recovery of freshwater.

The Nootdorp ASR-Coastal system functioned rather smoothly and was always able to supply sufficient irrigation water to the local horticulturist (~ 7 200 m^3/yr after infiltration of ~14 000 m^3/yr). The required maintenance was limited and the recovered water quality was very constant after Cycle 1 and met the owners demands. With total costs of 0.59 euro/m^3, the ASR-Coastal system provided a significantly cheaper source of high-quality freshwater compared to alternatives. The owner will keep using the system as only source of irrigation water.

The Westland ASR-Coastal system functioned satisfactorily, but clearly suffered from saltwater leakage via a nearby older borehole, which reduced the recovery efficiency from 40% to 22.5%. Per year, 7 500 to 16 000 m^3 could be supplied, while 28 000 to 70 000 m^3/yr was infiltrated. The system was not able to meet the yearly demand of the local horticulturist. Additionally, yearly cleaning of the infiltration system and ASR wells was required at the start-up of the system after long periods without infiltration. Despite these additional obstructions, the total costs were acceptable (0.84 euro/m^3). The owner will keep using the system as additional supply, together with aboveground rainwater storage and brackish water reverse osmosis.

The two sites show that the ASR-Coastal technique is mature and robust (TRL8) and can be further implemented. It also shows that local conditions and mode of operation can lead to differences in performance and operational costs, and should therefore be taken into account.

1. Introduction

Two ASR-Coastal pilots have been operated in close cooperation with greenhouse horticulturists. The aim of these ASR-Coastal systems is (1) to maximize the recovery of infiltration water using the flexible multiple partially penetrating wells by fine-tuning of the infiltration / recovery scheme, and (2) to intercept (and use) mixed infiltration/brackish water by deep wells to protect the shallower freshwater.

The Nootdorp pilot has a yearly infiltration capacity of about 15 m^3/h of roof-collected, treated rainwater. The rainwater is stored into a brackish groundwater aquifer located at a depth of 10-40 m. The pilot system has been running since 2012, and the recovery of the stored freshwater during summer met the needs for high-quality irrigation water of both the orchid grower and a neighbouring grower. The Westland pilot is a larger scale system, harvesting rainwater from rooftops of 4 adjacent tomato growers. The capacity of the system (in operation since 2013), is around 30 m^3/h.

The aims at the ASR-Coastal reference sites were to:

- Enable improved testing of the resilience of ASR-Coastal under varying hydrological conditions by additional data collection and monitoring. This will also provide new data to conclude on the expected lifespan and maintenance costs.
- Control and monitor the pre-treatment, infiltration, and recovery in ASR-coastal system using an automated central controlling unit. This requires conversion of knowledge and knowhow from models and scientific expertise into operational software. Automated ASR-Coastal control will facilitate (new) end-users in implementation and optimization of ASR-Coastal
- Further optimize the ASR recovery, by combining ASR-Coastal with the Freshkeeper concept. This work is initiated in the national pilot, and SUBSOL allows for testing during multiple cycles, including additional data-analysis, modelling and documentation. Possibilities to desalinate (RO) and use the intercepted brackish water will be studied, including an extensive review of the quality of this water and the effects of RO concentrate disposal (deep well infiltration) on the local and regional groundwater system. This latter work is to be undertaken in close dialogue with local authorities.

1.1. Aims (this report)

The aim is to present the documented use of ASR-Coastal in two on-going national pilots at a Technical Readiness Level 8 (TRL8): Nootdorp and Westland between 2012 and 2017.

1.2. Note

Information on and description of the set-up and aquifer characterisation, as presented in earlier studies and publications, was used to compile Chapters 2, 0, 10 and 11 of this report.

2. Set-up of the ASR-Coastal system in Nootdorp

2.1. ASR-strategy

The ASR-Coastal system in Nootdorp was installed to improve freshwater management in brackish or saline coastal areas by aquifer storage and recovery (ASR), using multiple partially penetrating wells (MPPWs). This application allows to preferably inject freshwater through the deepest well screens and to recover it again through the shallower well screens in times of demand (Figure 2.1). Consequently, it reduces freshwater losses resulting from buoyancy forces on the 'light' injected freshwater.

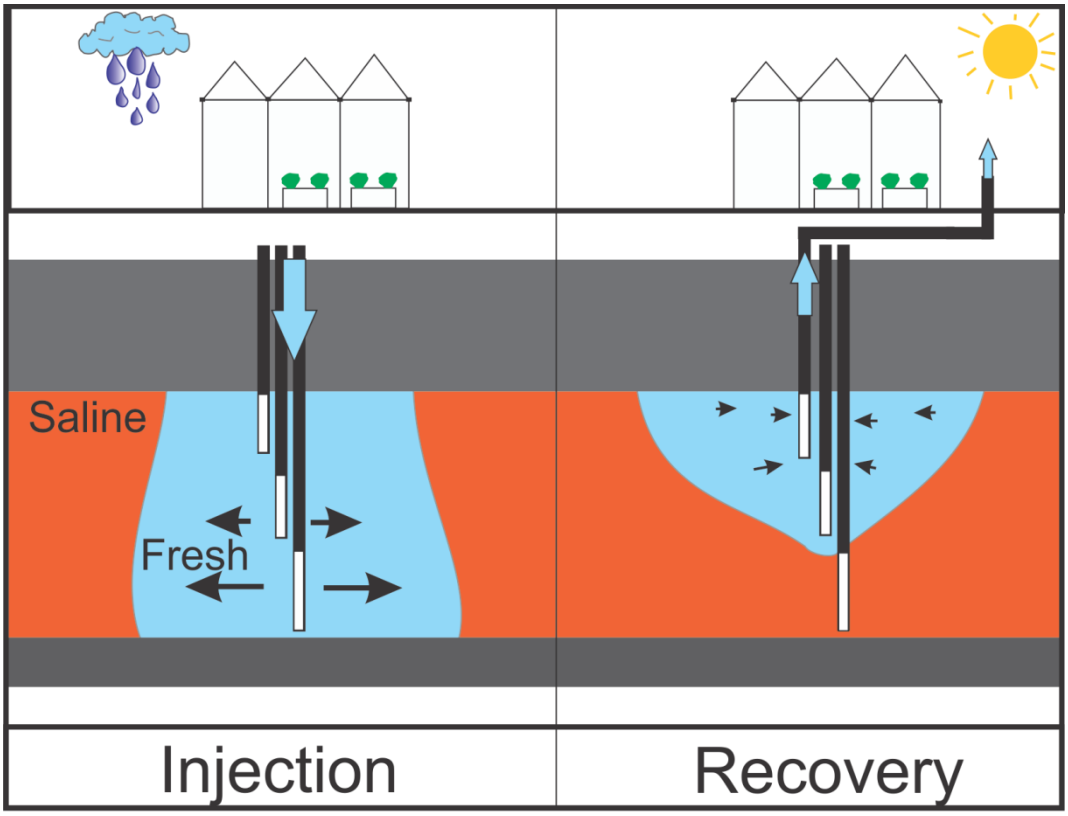

Figure 2.1: Concept of ASR-Coastal with multiple partially penetrating wells (MPPWs) in Nootdorp.

2.2. Location

Nootdorp is located in the western coastal province of Zuid Holland in The Netherlands, between the cities of The Hague and Rotterdam (Figure 2.2). The study area is dominated by greenhouse horticulture with a typical high water demand and high quality standards concerning salinity. The ASR site is situated in a deep polder with brackish seepage to the surface waters (de Louw et al., 2010), but with negligible lateral background flow. Chloride concentrations in the target aquifer are typically around 1000 mg/L (Figure 2.2). The local surface level has an elevation of 3.8 meters below sea level (m BSL).

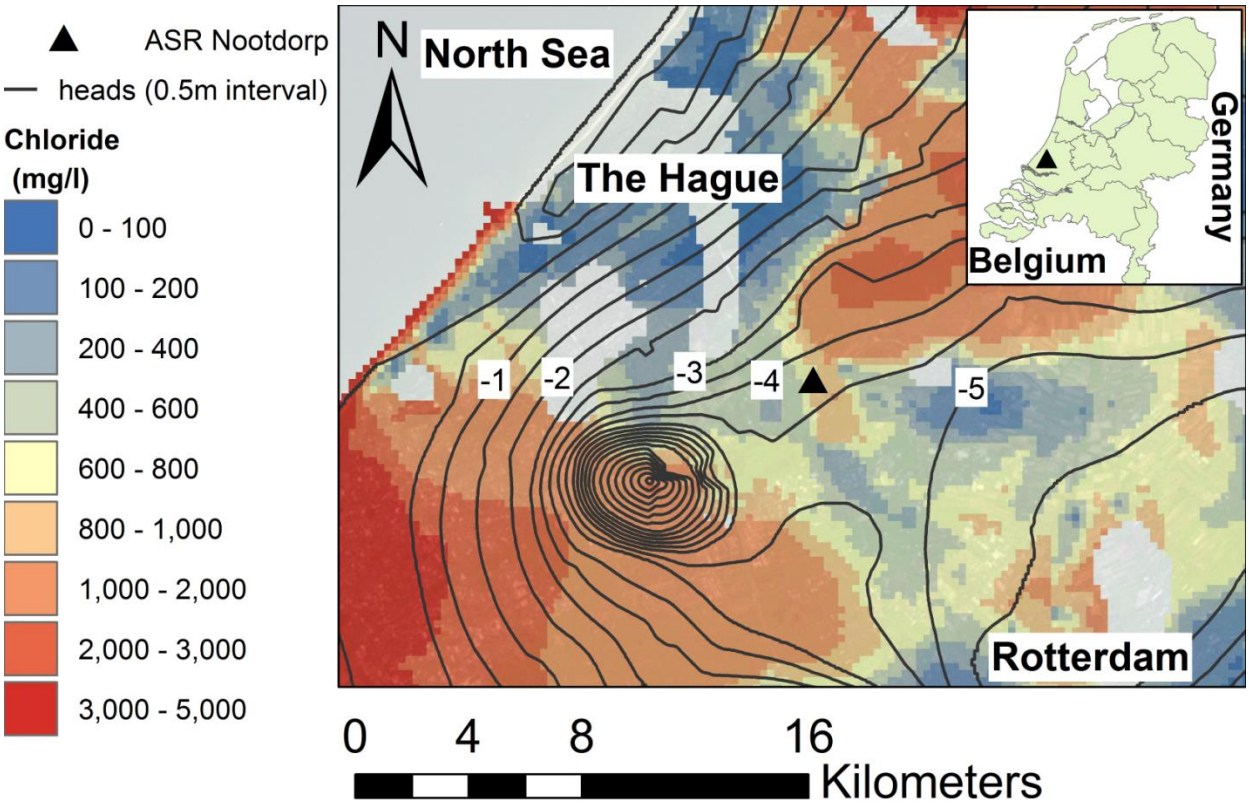

Figure 2.2: Regional piezometric head contours (TNO, 1995) and chloride concentrations (Oude Essink et al., 2010) at mid depth of the ASR target aquifer, with location of the Nootdorp ASR field trial (black triangle).

2.3. The ASR-facility

The ASR system has been installed to supply a greenhouse with a roof surface of 20,000 m^2 and with an estimated yearly water demand of 400 mm (8,000 m^3/yr), in an area with a mean gross annual precipitation of 853 mm (Royal Netherlands Meteorological Institute) or 17,060 m^3/yr. However, the water recovered from the aquifer after storage must have a chlorinity <0.5 mmol/l (~18 mg/l Cl) as water quality requirements are strict. This means that only 1.5% of ambient brackish water is allowed in the recovered water.

In the target aquifer, a 34 m deep, 350 mm diameter borehole was drilled by reverse-circulation rotary in November 2011, in which the MPPWs with a diameter of 75 mm

(screens 1- 3) and 90 mm (screen 4) are installed at different depth intervals (Figure 2.3 and Table 2.1). Bentonite clay plugs of 0.4 to 0.7 m thickness were installed using pellets at a minimum vertical distance of approximately 0.5 m away from each screen top or where clay layers were pierced. Each well was equipped with a valve in the infiltration and recovery pipeline, allowing manual adjustment of infiltration and recovery rates per well. Rainwater collected by the greenhouse roof was stored in a 400 m^3 rainwater storage tank, which could thus store 20 mm of rainfall. Prior to infiltration, the roofwater was pre-treated by rapid and slow sand filtration to prevent well clogging by suspended particles (Figure 2.3).

ASR operation started in February 2012. Infiltration automatically started with a rate of ~12 m^3/h once a predefined level in the rainwater storage tank was reached (30%, to prevent overflow during intense rainfall). Infiltration ceased when a set minimum level (20%) was reached. Recovery started automatically with a pumping rate of ~8 m^3/h when the predefined minimum level (40%) in a 90 m^3 irrigation water tank was reached, and was stopped once the predefined maximum level in this tank was reached (60%).

The size of the tanks, their predefined minimum and maximum levels, and the precipitation distribution resulted in a highly dynamic ASR operation with frequent alternation of infiltration and recovery stages. The whole process of infiltration, storage and recovery was automated and electronically logged via a central control unit with a programmable logical controller, which could be operated using a touch screen and via an internet connection.

2.4. Monitoring wells

Three bailer drilled boreholes (MW 1-3, Figure 2.3 and 3) with a diameter of 219 mm were realized at locations aligned at 5, 15, and 40 meters from the ASR-well, respectively. There were six (MW1) or five (MW2 and 3) separate piezometers with 1 m screen length installed in each borehole at different depth intervals (Table 2.1). Bentonite clay plugs of 1 to 2 m thickness were installed using pellets at a minimum vertical distance of 0.5 meter from the screen top, or where clay layers were pierced. These monitoring wells allowed to determine the distribution of and interaction between the fresh- and saltwater bodies during operation of the ASR-Coastal system (Figure 2.3 and 4). The depth intervals of these monitoring well screens are included in Table 2.1.

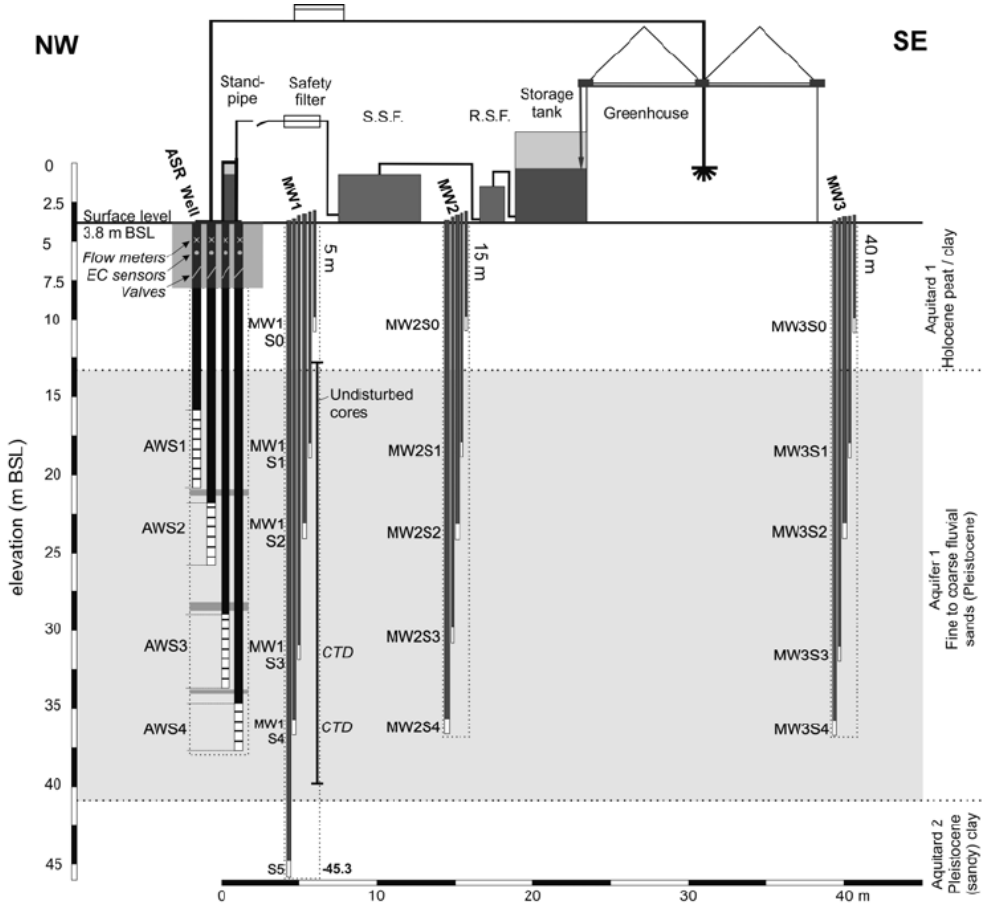

Figure 2.3: Schematic overview of the ASR-Coastal set-up at Nootdorp. MW = monitoring well, CTD = electrical conductivity, temperature, and pressure datalogger, R.S.F. = rapid sand filtration, S.S.F. = slow sand filtration.

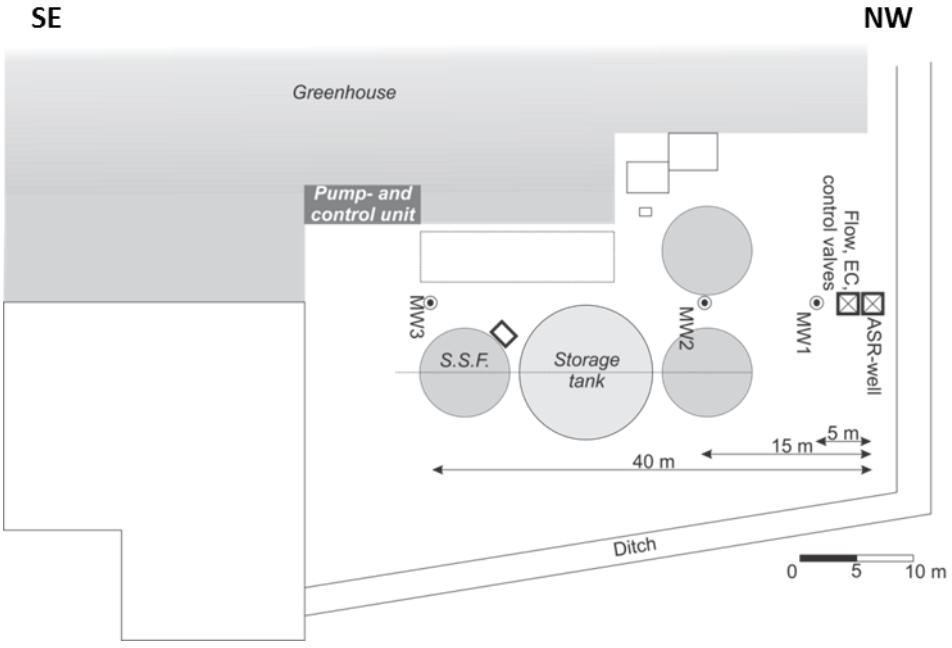

Figure 2.4: Schematic plan view of the ASR-Coastal set-up at the Nootdorp pilot site. MW = monitoring well, EC = electrical conductivity, temperature, and pressure datalogger, S.S.F. = slow sand filtration.

Table 2.1: Depth intervals of the MPPW-ASR well screens (AW#) and the monitoring well screens (MW#-S#) of the ASR-Coastal set-up in Nootdorp (Figure 2.3 and 4).

Monitoring Well-Screens	Well screen top (m BSL)	Well screen bottom (m BSL)
AW1	-15.8	-20.8
AW2	-21.8	-25.8
AW3	-29.2	-33.7
AW4	-34.7	-37.7
MW1-S0	-9.82	-10.82
MW1-S1	-17.97	-18.97
MW1-S2	-23.12	-24.12
MW1-S3	-30.92	-31.92
MW1-S4	-35.72	-36.72
MW1-S5	-44.82	-45.82
MW2-S0	-9.77	-10.77
MW2-S1	-17.77	-18.77
MW2-S2	-23.22	-24.22
MW2-S3	-29.77	-30.77
MW2-S4	-35.62	-36.62
MW3-S0	-9.92	-10.92
MW3-S1	-17.72	-18.72
MW3-S2	-23.27	-24.27
MW3-S3	-31.02	-32.02
MW3-S4	-35.72	-36.72

2.5. Photographic impression

A photographic impression of the ASR-Coastal set-up in Nootdorp is presented in Figure 2.5 to Figure 2.8.

Figure 2.5: ASR-Coastal well field Nootdorp: infiltration well and monitoring equipment in front (white covers), and monitoring wells (steel cases) and storage tanks (one for rainwater, others for water reuse) in the background.

Figure 2.6: Multiple partially penetrating well heads at ASR-Coastal Nootdorp

Figure 2.7: Tank of the of the slow sand filter (left) and the rainwater storage tank (right). Green tank is for heat storage, not water supply.

Figure 2.8: ASR pump and control unit, including the rapid sand filter (blue tank) and the pressure standpipe used to provide a constant pressure for infiltration (right).

3. Characterization of the target aquifer

3.1. Approach

A detailed characterization of the target aquifer was obtained by:

- Using a core catcher (Oele et al., 1983) and thin-wall tubes of 1 m length and 0.1 m diameter to obtain a 27 m long (12.8 to 39.8 m BSL) continuous, undisturbed core at MW1 (Figure 2.3 and Figure 2.4). A total of 114 samples was taken from these thin-wall tubes, at intervals of 0.2 m or smaller where different lithological units appeared.
- Taking samples from the bailer every meter at the other depth intervals of MW1 (n = 14) and over the full depth of MW2 and 3 (n = 29 and n = 28, respectively).
- Preparing the samples using the method of Konert and Vandenberghe (1997).
- Using a HELOS/KR laser particle sizer (Sympatec GmbH, Germany) to derive the grain size distributions of the prepared samples in the range of 0.12 - 2000 µm.
- Correcting the obtained grain size distribution for the gravel contribution by oven-drying samples containing gravel and sieving them with a 1600 µm sieve to obtain the fraction > 2000 µm, taking elongated particles into account.
- Using Bear (1972) to initially assess the hydraulic conductivity (K) of the target aquifer from the measured grain size distribution. Several pumping stages were also performed to calibrate the hydraulic conductivity (and specific storage, S_s) from the freshwater head response with a numerical density dependent groundwater flow model (Chapter 0).
- Using chloride breakthrough curves and the same density dependent groundwater flow model to calibrate the effective porosity (n_e) and dispersivity (D) in the aquifer.

A detailed characterization of the native groundwater in the target aquifer was obtained by:

- Recording the electrical conductivities in the aquifer at two locations (MW2 and MW3) prior to ASR operation (January 18, 2012) by geophysical borehole logging using a Robertson DIL-39 probe (‘EM-39’) (McNeill et al., 1990). This allows to determine the exact location of the fresh-salt interface. The 2.3 m long probe could not be lowered into the target aquifer through MW1 due to a slight curve in the standpipe.
- Sampling at all monitoring screens prior to ASR operation (December 19, 2011), and analysing the samples for the same parameters as during the water quality monitoring (see Chapter 5.2).

3.2. Aquifer characterization

The target aquifer for the ASR-Coastal pilot in Nootdorp is underlain by a compacted silty loam layer. According to the regional geological model (TNO-NITG), the base of this unit can be found at 55 m BSL, while the vertical hydraulic conductivity (K_v) should be ~0.02

m/d. The base of the target aquifer (~ 31 to 41 m BSL) is characterized by fine to gravelly very coarse sands and marked by Unit 1f to 1i (Figure 3.1). Most estimated K-values of these units (based on the grain size distributions) are well above 20 m/d, with a maximum of 100 m/d at the basal 1 m (well sorted gravel and coarse sand, Unit 1i). Thin clay layers, reworked peat, and clay pebbles (with a diameter of 1 to 10 cm in the cores of MW1, and mollusks were found in a matrix of middle coarse sand in the central part of the aquifer (Unit 1e, 28 to 31 m BSL). This unit is not considered a continuous clay layer separating the aquifer into two (semi-)confined aquifers (Busschers et al., 2005). A mean K of ~5 to 10 m/d was estimated based on the grain size distributions for this Unit. The top of the target aquifer (Unit 1a to 1c, ~ 13 to 28 m BSL) consists of relatively homogeneous, mainly middle coarse fluvial sands. The estimated K of those units is 5 - 15 m/d. The Holocene cover (3.8 to ~ 13 m BSL) consists of marine silty clay and silty loam with thin peat layers. The K_v based on grain size distributions of this upper confining unit was estimated 0.01 m/d. The K and S_s values based on freshwater head response in the aquifer are given in Figure 3.1. All K-values are in line with K-values known for the specific sediments (Bear, 1972). The deduced total transmissivity (1,900 m^2/d) was significantly higher than indicated by the geological model (TNO-NITG), which predicted a much thinner target aquifer with a maximum depth of 35 m BSL. The clay aquitards were considered anisotropic (K_h / K_v = 10). Unit 1e was considered slightly anisotropic (K_h / K_v = 2), to incorporate the clayey intervals in the model. The vertical anisotropy of the whole target aquifer based on the values derived for K_v and K_h is 1.9, indicating the aquifer is relatively isotropic. Effective porosities in the aquifer ranged from 0.25 (intervals containing gravel) to 0.35 (pure sands).

3.3. Native groundwater characterization

Baseline groundwater in the target aquifer prior to ASR operation showed a clear salinity stratification (Figure 3.1). Relatively fresh groundwater was observed at the top of the aquifer (Cl: 115 mg/l), allowing a mixing ratio (f) of 0.8 here to comply with irrigation water demands. At the base, however, chloride concentrations ranged from 860 to 1001 mg/l. This means f should remain >0.98 here, allowing no more than 2% of ambient groundwater to be admixed in the water recovered from the deepest ASR well. The vertical TDS zonation in the aquifer was dominated by a NaCl water type at the base of the aquifer, and by a $CaHCO_3$ water type in the upper aquitard. Both water types show a positive Base Exchange Index (BEX) (Stuyfzand, 1993; Stuyfzand, 2008), indicating that the originally saline aquifer was flushed with fresh groundwater.

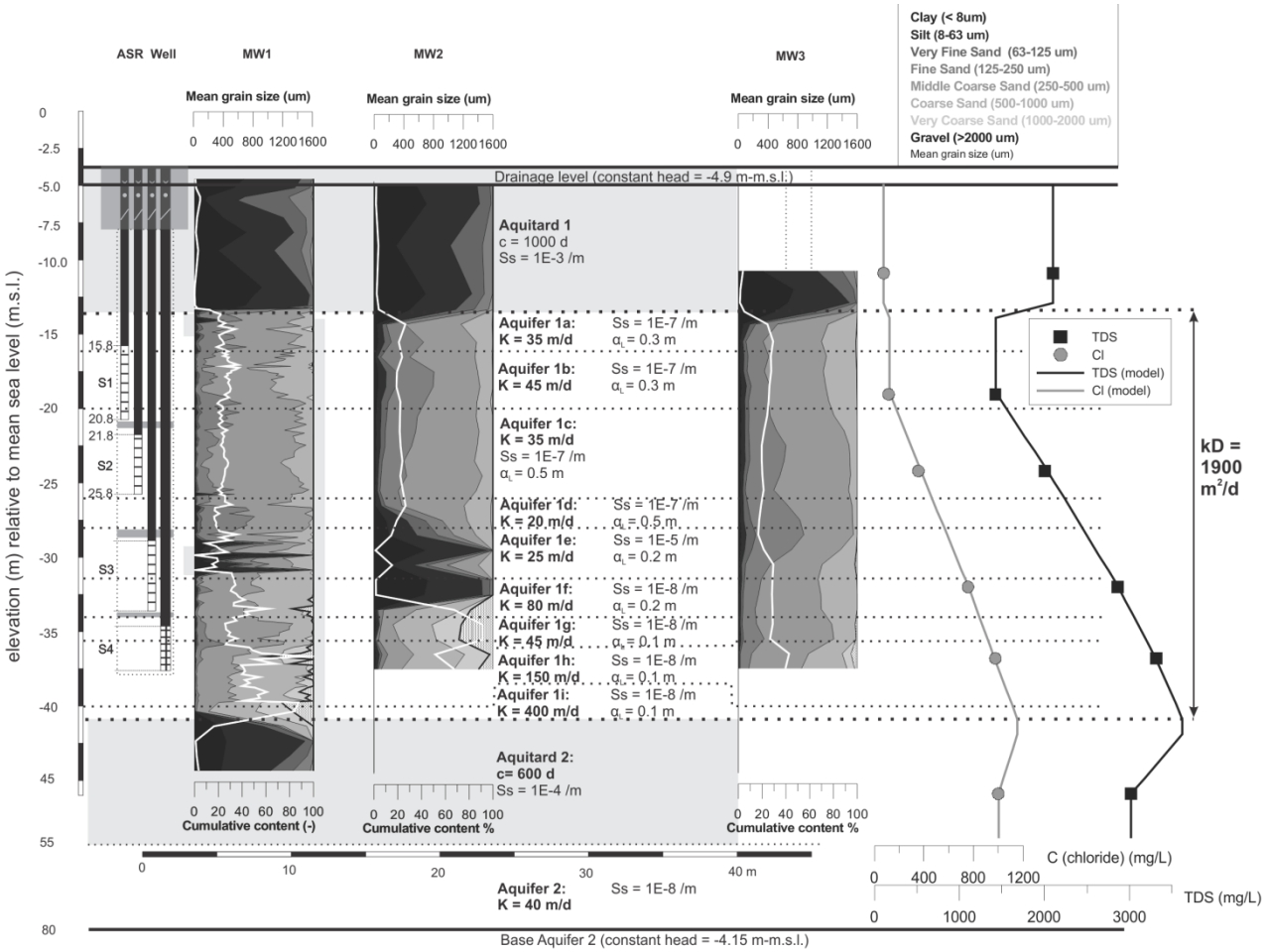

Figure 3.1: Physical characterization of the target aquifer in the monitored flow direction, groundwater salinity (measured at MW1), and calibrated aquifer properties. c = hydraulic resistivity, S_s = specific storage, α_L = longitudinal dispersivity, Cl = chloride concentration, and TDS = concentration of total dissolved solids.

4. Groundwater model set-up

4.1. Model set-up

An axial-symmetric homogeneous SEAWAT (Langevin et al., 2007) model was built for the ASR-Coastal system in Nootdorp to calibrate the geohydrological parameters. A schematization of the model is shown in Figure 4.1. For detailed information on the SEAWAT model, the reader is referred to Zuurbier et al. (2014). The final model includes daily stress periods from 13 January 2012 until 5 August 2017 to accurately model the dynamic subsurface infiltration and abstraction. The daily pumping rates of each well were based on the daily logged cumulative volumes of infiltration and abstraction.

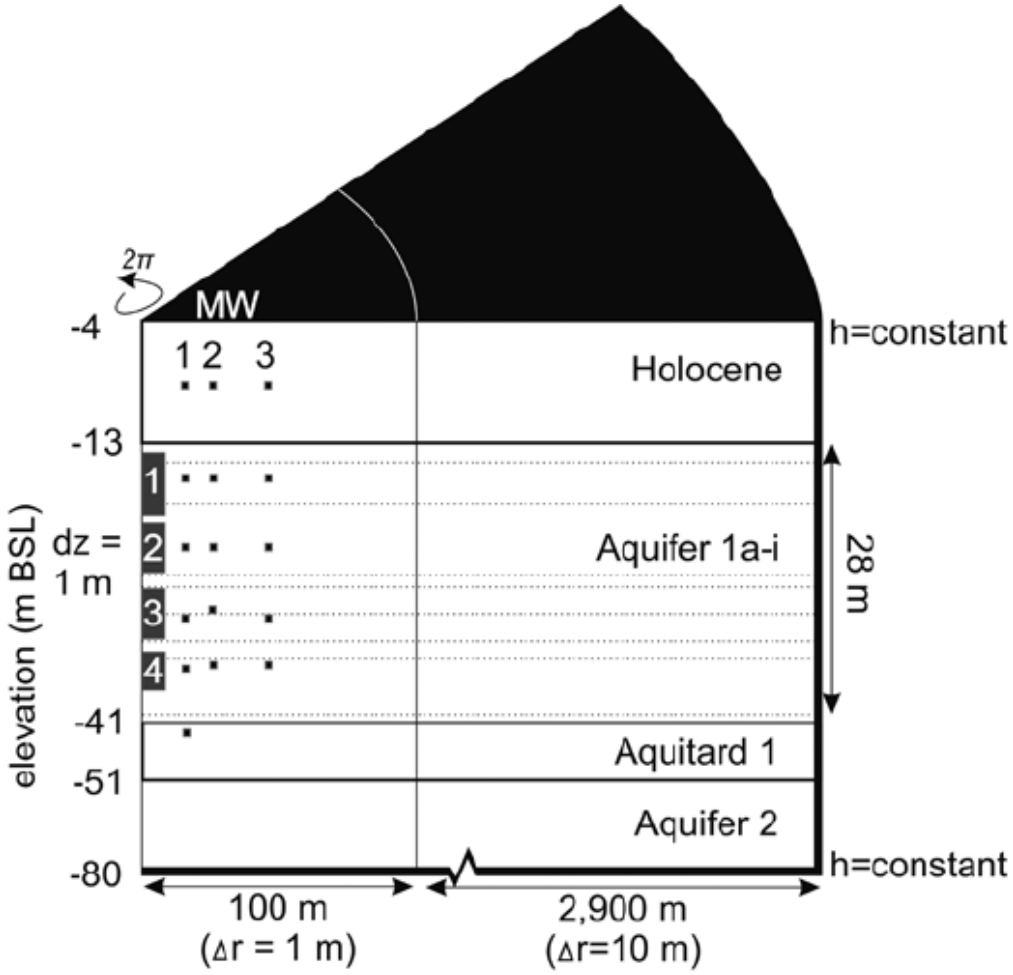

Figure 4.1: Set-up of the axial-symmetric SEAWAT model for the ASR-Coastal pilot in Nootdorp.

4.1. Modelling strategy

The results from grain size analyses were used to define geohydrological units and to estimate hydraulic conductivities (K). Field measurements of head responses to pumping and breakthrough curves of chloride at MW1 were used to calibrate the model for K and specific storage (S_s), and dispersivity (D) and effective porosity (n_e), respectively. The calibrated aquifer parameters were already given in Figure 3.1.

The final SEAWAT run was compared with field measurements of e.g. chloride at AW1, MW1 and MW2, to validate its capability to predict the future performance at the field site.

5. Monitoring during operation (2012-2017)

5.1. Water quantity

Operation of the ASR-Coastal system was monitored by electronic data logging with a 30 minutes interval. This included: ASR cycle registration (operating phase), injected volumes per well (based on pipe diameters and flow velocities from Signet 515 Rotor-X Paddlewheel Flow Sensors (Georg Fischer Signet LLC, USA)), recovered volumes per well (idem), EC of recovered water per well (ELMECO, The Netherlands), and the total operation period per pump.

5.2. Water quality

Water samples were frequently (2012-2013: monthly, 2015-2017: bimonthly) obtained from the infiltration water, the ASR-well, and the monitoring well. All samples were analysed in the field in a flow-through cell for EC (GMH 3410, Greisinger, Germany), pH and temperature (Hanna 9126, Hanna Instruments, USA), and dissolved oxygen (DO) (Odeon Optod, Neotek-Ponsel, France). The samples were filtrated using 0.45 µm cellulose acetate membranes (Whatman FP-30, UK) in the field and sent to the VU University Water Lab (2012-2015) and the WUR University Water Lab (2015-2017). There, the macrochemical composition was analysed. Samples were stored in two 10-ml plastic vials, of which one was acidified with 100 µl 65% HNO_3 (Suprapur, Merck International) for analysis of cations (Na, K, Ca, Mg, Mn, Fe, S, Si, P, and trace elements) using ICP-OES (Varian 730-ES ICP OES, Agilent Technologies, U.S.A.). The other 10 ml vial was used for analysis of F, Cl, Br, NO_2, NO_3, PO_4, and SO_4 using the Dionex DX-120 IC (Thermo Fischer Scientific Inc., USA), and NH_4 using the LabMedics Aquakem 250 (Stockport, UK). All samples were cooled to 4°C and stored dark immediately after sampling. At the WUR university, 100 ml samples with filtrated samples were used for ICP-AES (Al, Ca, Fe, K, Mg, Mn, Na, P, S, Zn, Si) and ICP-MS (As) upon Aqua-Regia extraction, Segmented Flow Analyzer (NH_4, NO_3+NO_2, PO_4), Flow Injection Analyzer (Cl), and Shimadzu analyzer (TC, IC).

5.3. Hydrological effects

Two combined electrical conductivity and pressure transducers (CTD) and two regular pressure transducers (Divers from Schlumberger Water Services, USA) were installed at MW1 (S1-4). Manual head measurements were performed prior to each sampling round to validate the head observations by the Divers.

5.4. Geophysical measurements

Electrical conductivity profiles were constructed for MW1, MW2, and MW3 by geophysical borehole logging (EM-39) during different phases of consecutive ASR cycles in 2012 and 2016. Changes in formation conductivity outside the standpipe of the well should indicate a change in electrical conductivity of the groundwater, as the lithology remains constant (Metzger and Izbicki, 2013). Therefore, these profiles can be used to determine the

development and distribution of the freshwater body during operation of the ASR-Coastal system in Nootdorp.

6. Results: Monitoring

6.1. Water quantity analysis

The cumulative volumes of freshwater infiltrated through and recovered from the ASR-well, and the resulting net volume of infiltrated freshwater are given in Figure 6.1 for the complete operation period of the ASR-Coastal set-up in Nootdorp. The data is also plotted per year in Figure 6.2 to Figure 6.7. In addition, the statistics of these figures are tabulated in Table 6.1.

The first year of operation (2012/2013) was a relatively wet year, which is why there is initially a large amount of infiltration. On the contrary, 2015 had a relatively dry springtime, which explains the 100% recovery in the summer of 2015. It should be noted that the system is highly dynamic with multiple ASR cycles each year. Freshwater is infiltrated whenever there is a temporary surplus of precipitation, and is recovered again at any time of demand. This implies that an ASR cycle at the ASR-Coastal site in Nootdorp can even last for only one day. The recovery of freshwater therefore depends on the freshwater demand rather than on the recovery potential. This means that the recovery efficiency (RE) is mainly a reflection of the freshwater demand (unless the demand exceeds the RE).

On average, the ASR-Coastal set-up in Nootdorp infiltrated 13,530 m^3 of freshwater and recovered 7,224 m^3 of freshwater each Nootdorp ASR year. The recovery efficiency of the set-up therefore equals 54.5%. The remaining volume of infiltrated freshwater (on average 6,306 m^3/year) was not needed for irrigation and would partly be unrecoverable due to mixing with ambient brackish water.

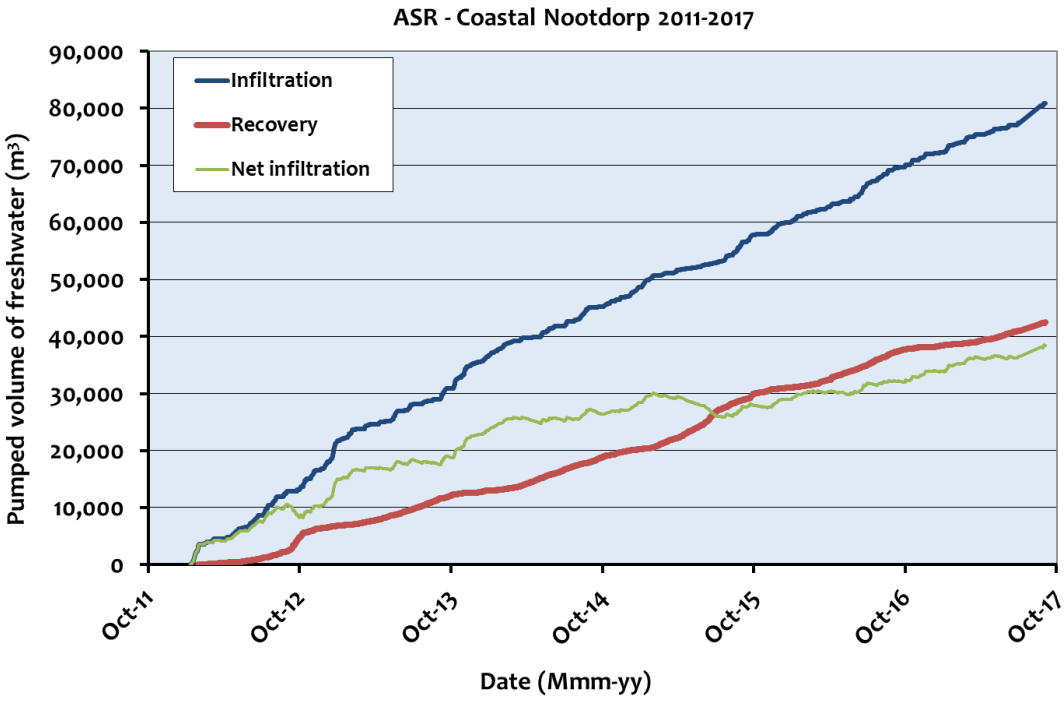

Figure 6.1: Cumulative volume (m^3) of freshwater infiltrated (blue) and recovered (red) through the ASR-well from 2012 until 2017. The resulting net volume (m^3) of freshwater infiltrated through the ASR-well is given in green.

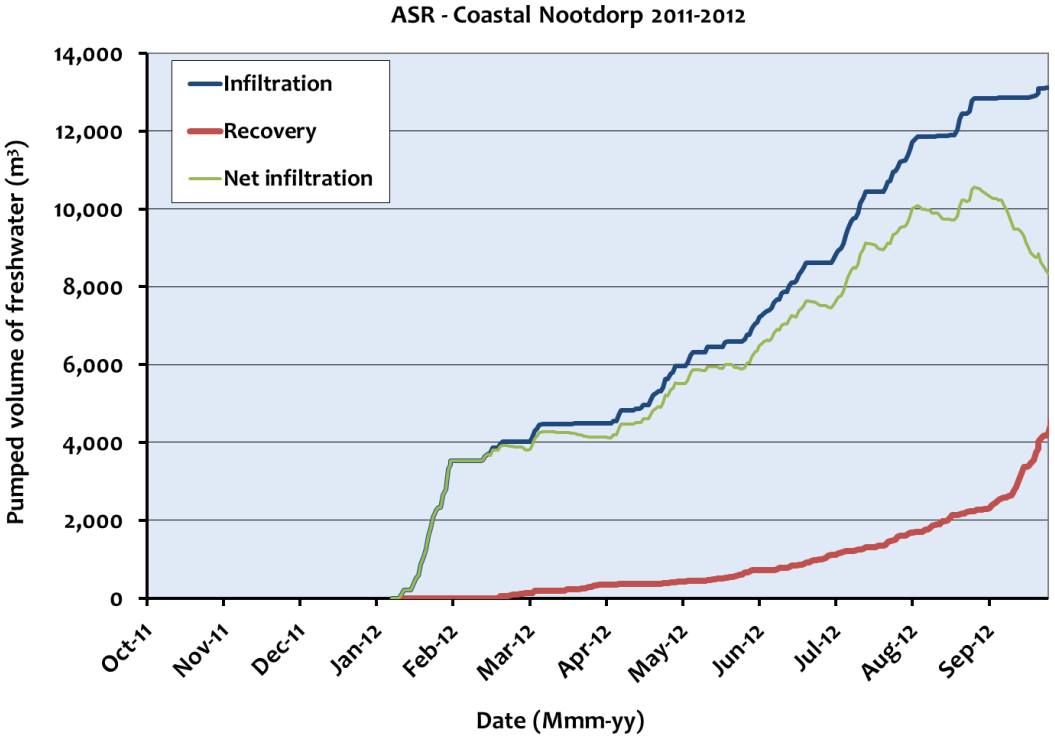

Figure 6.2: Cumulative volume (m^3) of freshwater infiltrated (blue) and recovered (red) through the ASR-well during the Nootdorp ASR year 2011/2012. The resulting net volume (m^3) of freshwater infiltrated through the ASR-well is given in green.

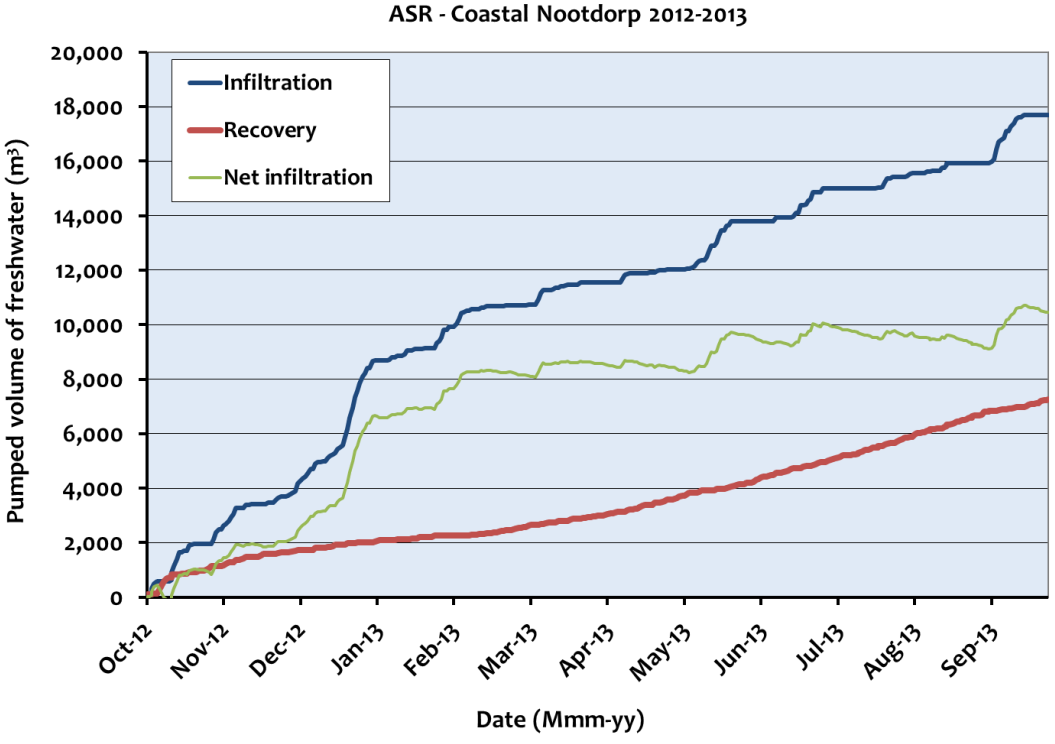

Figure 6.3: Cumulative volume (m^3) of freshwater infiltrated (blue) and recovered (red) through the ASR-well during the Nootdorp ASR year 2012/2013. The resulting net volume (m^3) of freshwater infiltrated through the ASR-well is given in green.

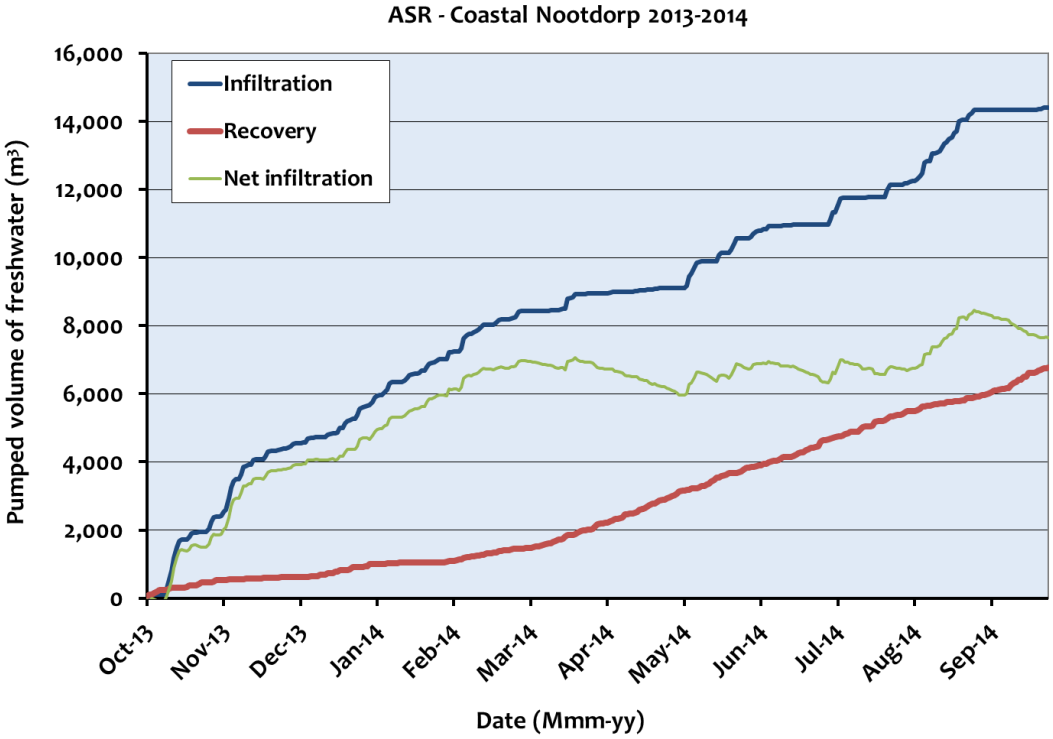

Figure 6.4: Cumulative volume (m^3) of freshwater infiltrated (blue) and recovered (red) through the ASR-well during the Nootdorp ASR year 2013/2014. The resulting net volume (m^3) of freshwater infiltrated through the ASR-well is given in green.

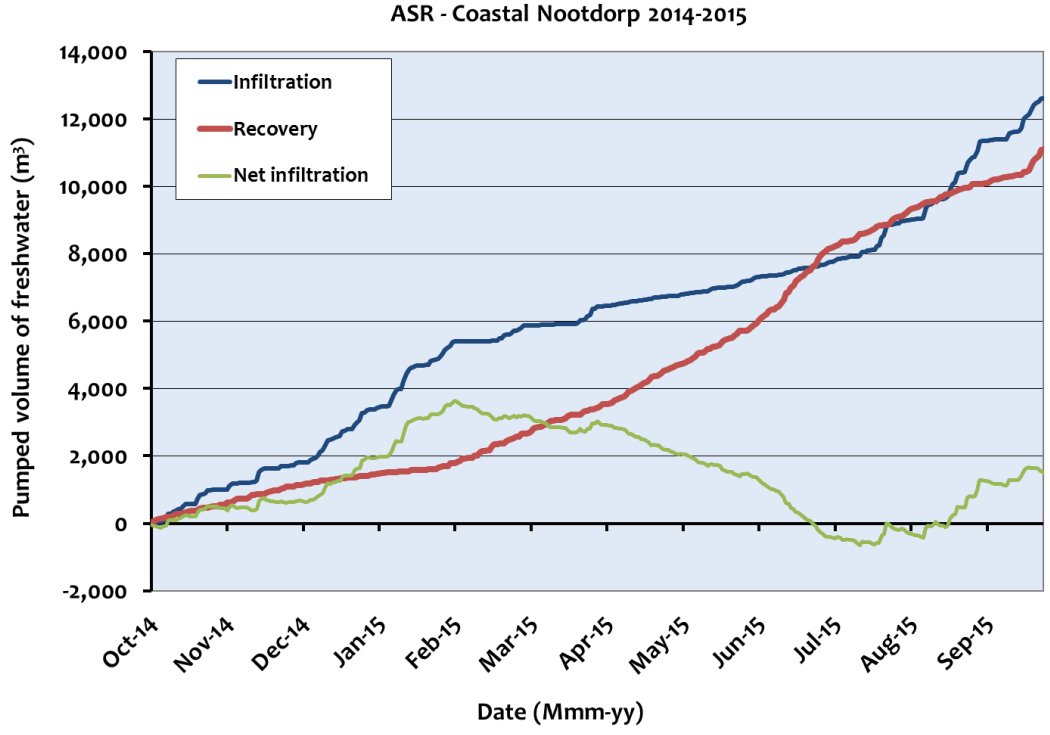

Figure 6.5: Cumulative volume (m^3) of freshwater infiltrated (blue) and recovered (red) through the ASR-well during the Nootdorp ASR year 2014/2015. The resulting net volume (m^3) of freshwater infiltrated through the ASR-well is given in green.

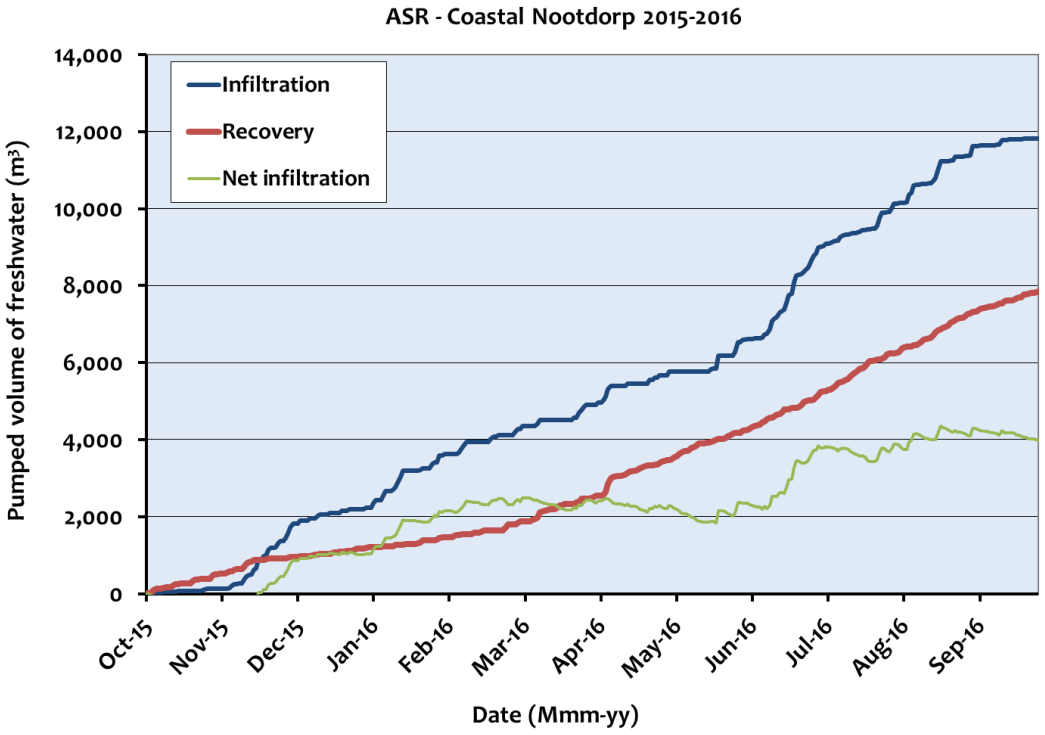

Figure 6.6: Cumulative volume (m^3) of freshwater infiltrated (blue) and recovered (red) through the ASR-well during the Nootdorp ASR year 2015/2016. The resulting net volume (m^3) of freshwater infiltrated through the ASR-well is given in green.

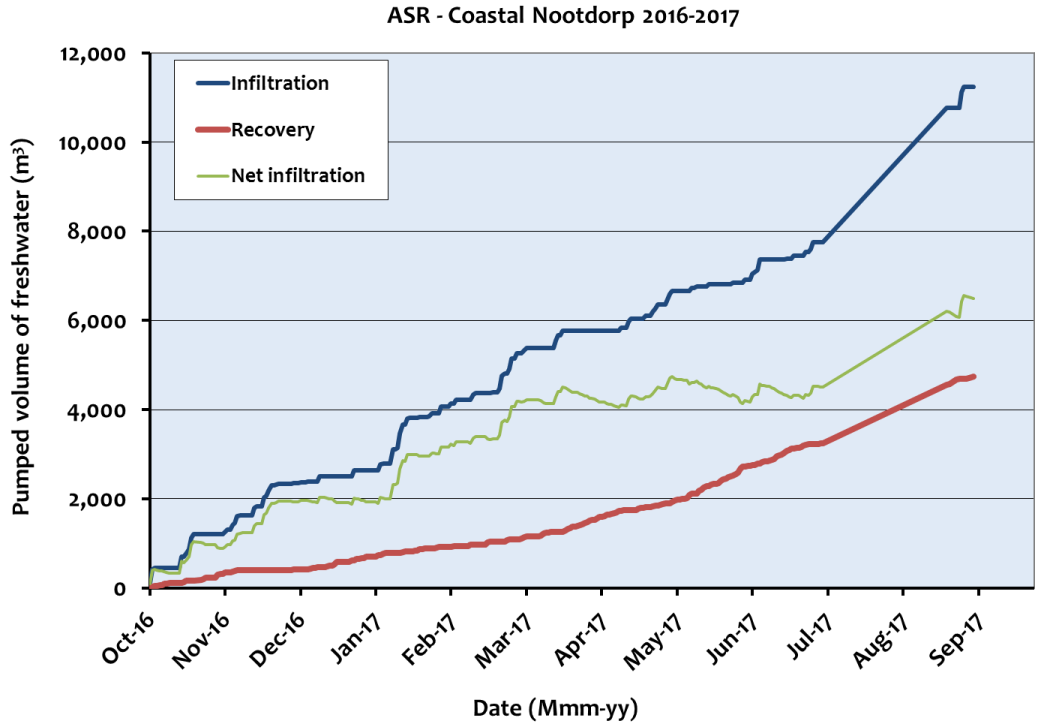

Figure 6.7: Cumulative volume (m^3) of freshwater infiltrated (blue) and recovered (red) through the ASR-well during the Nootdorp ASR year 2016/2017. The resulting net volume (m^3) of freshwater infiltrated through the ASR-well is given in green. Due to adjustments in the installation, there are no measurements between July 5 and August 24.

Table 6.1: Operational performance of the ASR-Coastal system in Nootdorp for each Nootdorp ASR year (Oct 1 – Sep 30) From January 12, 2012 until September 5, 2017. The recovery efficiency is calculated as the percentage of injected freshwater that is recovered by the MPPWs.

Nootdorp ASR year (Oct 1 – Sep 30)	Volume of freshwater infiltrated (m^3)	Volume of freshwater recovered (m^3)	Net volume of freshwater infiltrated (m^3)	Recovery efficiency
2011/2012	13116	4768	8348	36.4 %
2012/2013	17709	7254	10455	41.0 %
2013/2014	14412	6767	7645	47.0 %
2014/2015	12610	11097	1513	88.0 %
2015/2016	11824	7849	3974	66.4 %
2016/2017	11242	4750	6492	42.3 %
Total (m^3)	**80912**	**42485**	**38427**	**52.5 %**
Average (m^3/year)	**13530**	**7224**	**6306**	**53.4 %**

6.2. Water quality analysis: infiltration water

The average quality of the infiltration water is based on 19 samples taken between 2012 and 2017 (Table 6.2). In addition, the temporal variation of the infiltration water quality is shown in Figure 6.8-Figure 6.10.

The EC is constantly very low, indicating freshwater. This is confirmed by the low concentrations of Na and Cl. EC and pH are relatively constant, but the temperature has a seasonal variation.

The concentration of most dissolved substances in infiltration water decreased slightly from 2012 to 2017, potentially indicating a reduced leaching of the sand in the slow sand filter. Zinc is the only exception, increasing in concentration during the operation of ASR-Coastal, which may indicate an increase of Zn leaching from the greenhouse rainwater collection system. Nevertheless, all average concentrations of the infiltrated freshwater remain below the legal limits set by the Water Act of The Netherlands in 2017.

The presence of pesticides was monitored twice every year (Summer / Winter). Generally, no pesticides were found above there detection limits in the infiltration water, except for the Summer of 2016, when 9 pesticides were detected in low concentration. Two pesticides were found in concentrations >0.1 µg/l. The sum of pesticides always remained <0.5 µg/l. In the following winter, no pesticides were observed in the infiltration water.

Table 6.2: Observed infiltration water quality averaged over 34 measurements between 2012 and 2017, divided in two periods of 3 years (2012-2014 and 2015-2017) and tabulated together with the legal limits set by the Water

Act of The Netherlands in 2017. EC-25 Field is the electrical conductivity measured in the field with a reference temperature of 25°C.

Sample code	Average 2012-2014	Average 2015-2017	Legal limits Water Act, The Netherlands, 2017
EC-25 Field (µS/cm)	82	51	-
Temperature (°C)	10.5	10.6	-
pH (Field)	7.4	7.6	-
DO (mg/L)	9.9	6.6	-
Na (mg/L)	2.9	2.0	120
K (mg/L)	0.3	0.1	-
Ca (mg/L)	14.5	7.4	-
Mg (mg/L)	0.6	0.4	-
Fe (mg/L)	0.0	0.0	-
Mn (mg/L)	0.0	0.0	-
NH_4 (mg NH_4/L)	0.6	0.0	3.2
Cl (mg/L)	4.5	3.7	200
SO_4 (mg SO_4/L)	3.5	1.7	150
HCO_3 (mg HCO_3/L)	48.0	20.8	-
NO_3 (mg N/L)	5.5	4.2	24.8
PO_4-t (mg P/L)	0.2	0.1	1.25
As (µg/L)	0.8	0.5	10
Zn (µg/L)	9.4	15.8	65

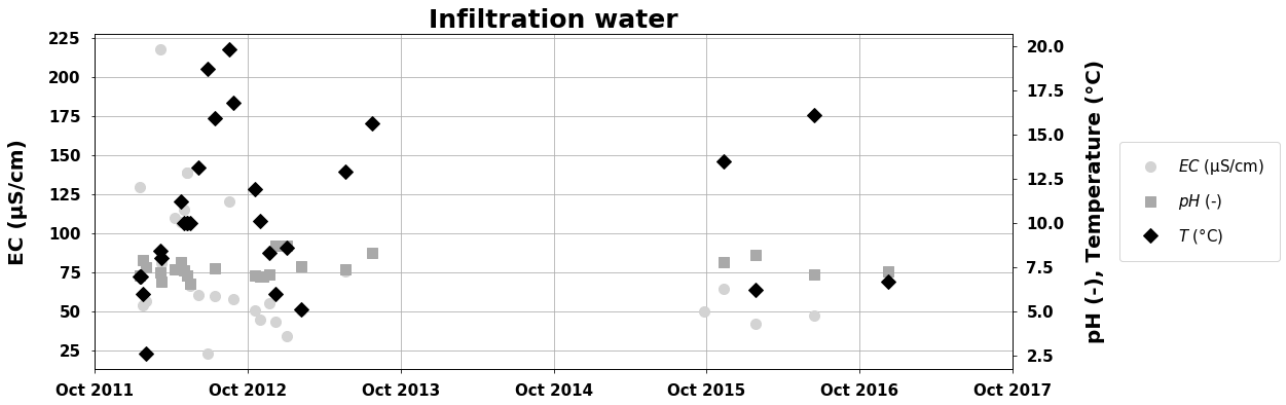

Figure 6.8: Electrical conductivity (EC in µS/cm), pH (-), and temperature (Temp in °C) of the freshwater infiltrated into the brackish target aquifer through the MPPW-ASR well.

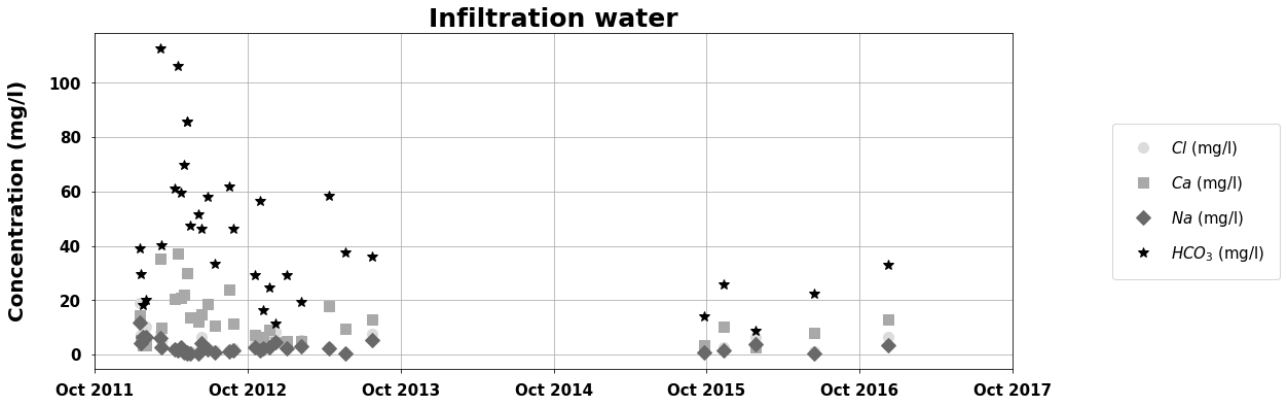

Figure 6.9: Concentrations of Cl, Ca, Na, and HCO_3 in the freshwater infiltrated into the brackish target aquifer through the MPPW-ASR well.

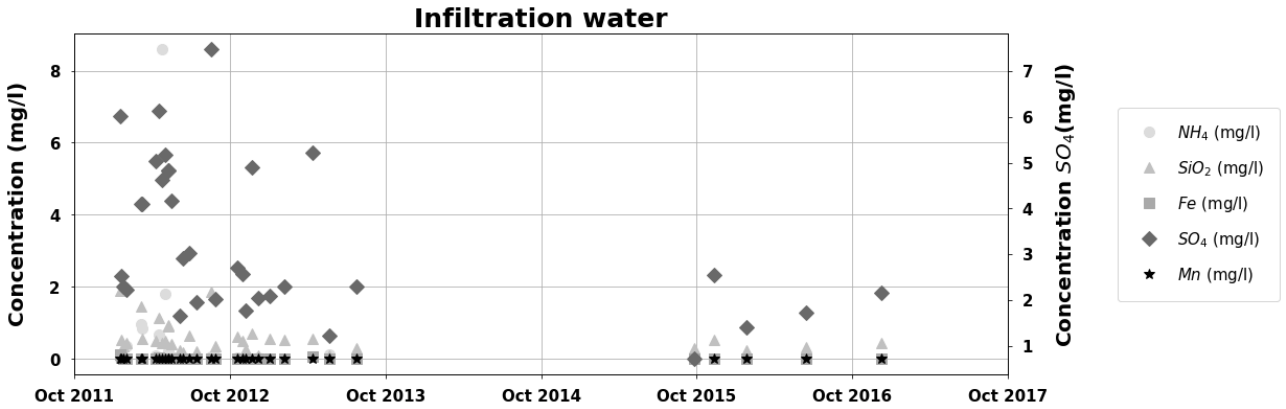

Figure 6.10: Concentrations of NH_4, SiO_2, Fe, SO_4, and Mn in the freshwater infiltrated into the brackish target aquifer through the MPPW-ASR well.

6.3. Water quality analysis: recovered freshwater

For quality assurance of the freshwater recovered via the upper two well screens of the ASR-well in times of demand, the hydrogeochemical composition of this water was monitored over time (Figure 6.11-Figure 6.16).

Except for the seasonal variation of temperature, there is not much variation visible in the water quality. The EC and concentrations of dissolved species remain fairly constant throughout the operation of the ASR-Coastal system, which was considered a clear advantage by the greenhouse owner. This can be attributed to the dynamics of the ASR-Coastal system in Nootdorp. Every year has many short ASR-cycles, controlled by the timing of freshwater surplus and demand. Only in the first year of operation, salinization was observed, at the end of the summer season, when a large volume was abstracted for research purposes.

The average water quality recovered through both well screens is given in Table 6.3. As indicated, the average recovered water quality improves over time, which can be related to the improvement of the infiltration water (Table 6.2) and a potentially by the continuous use of the ASR-Coastal system. Zn is the only dissolved specie that does not follow this

trend and increases in concentration during operation of the ASR-Coastal system. SO_4 is mobilized throughout the operation, which indicates ongoing pyrite oxidation (Zuurbier et al., 2016). Potential mobilisation of Zn and As by this process was however identified as a threat for the irrigation water quality and tended to decrease over time (Table 6.3).

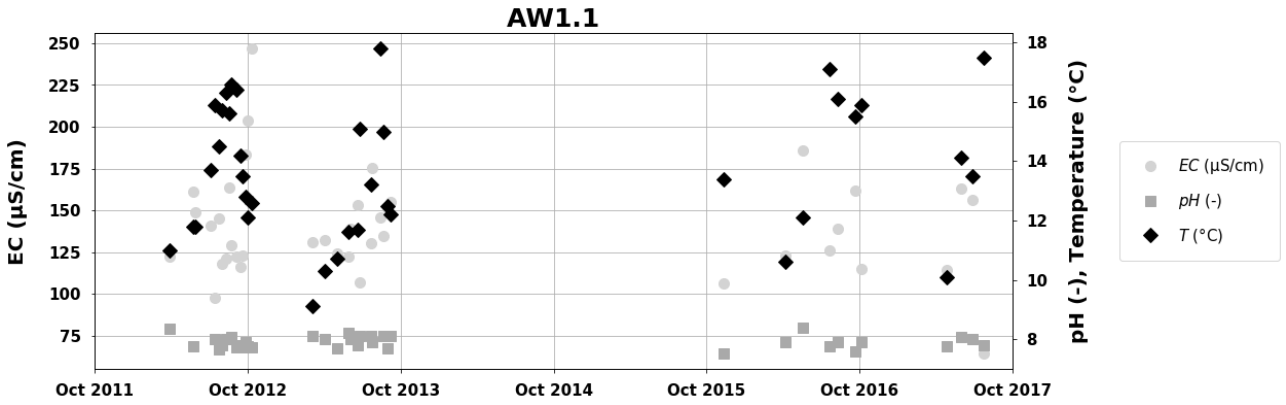

Figure 6.11: Electrical conductivity (EC in µS/cm), pH (-), and temperature (Temp in °C) of water recovered through AW1.1.

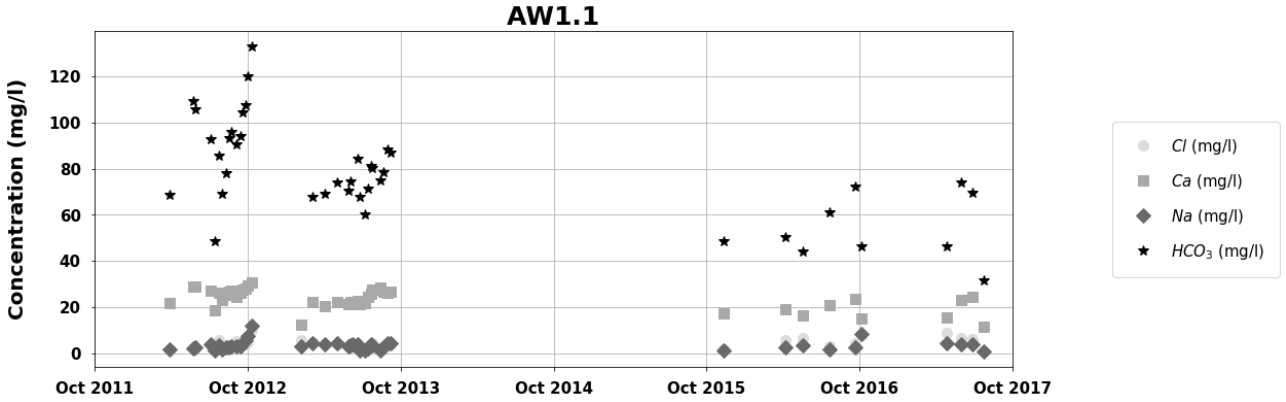

Figure 6.12: Concentrations of Cl, Ca, Na, and HCO_3 in water recovered through AW1.1.

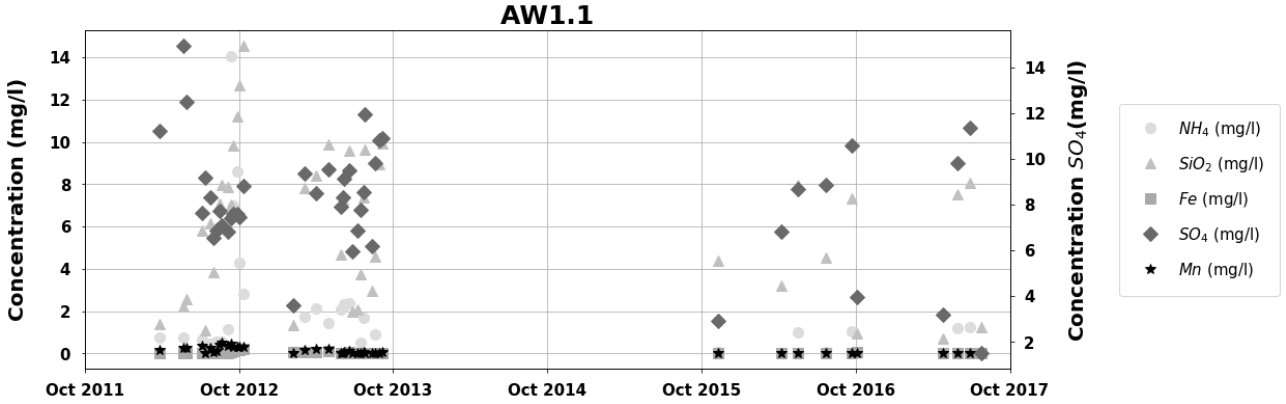

Figure 6.13: Concentrations of NH_4, SiO_2, Fe, SO_4, and Mn in water recovered through AW1.1.

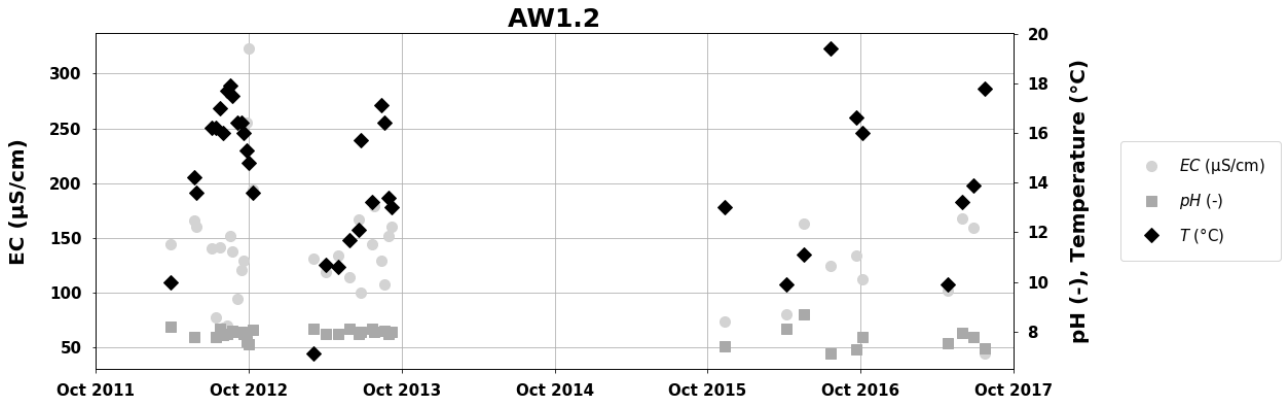

Figure 6.14: Electrical conductivity (EC in µS/cm), pH (-), and temperature (Temp in °C) of water recovered through AW1.2.

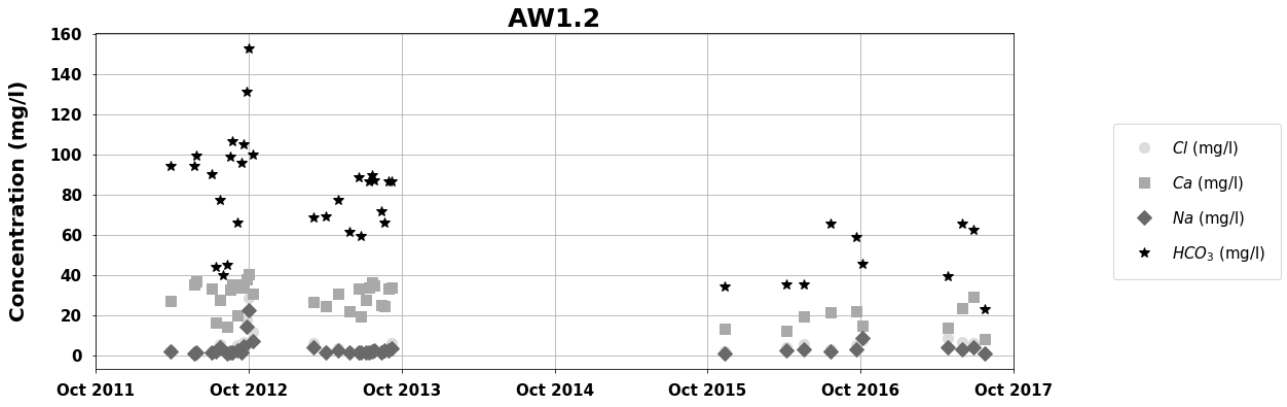

Figure 6.15: Concentrations of Cl, Ca, Na, and HCO_3 in water recovered through AW1.2.

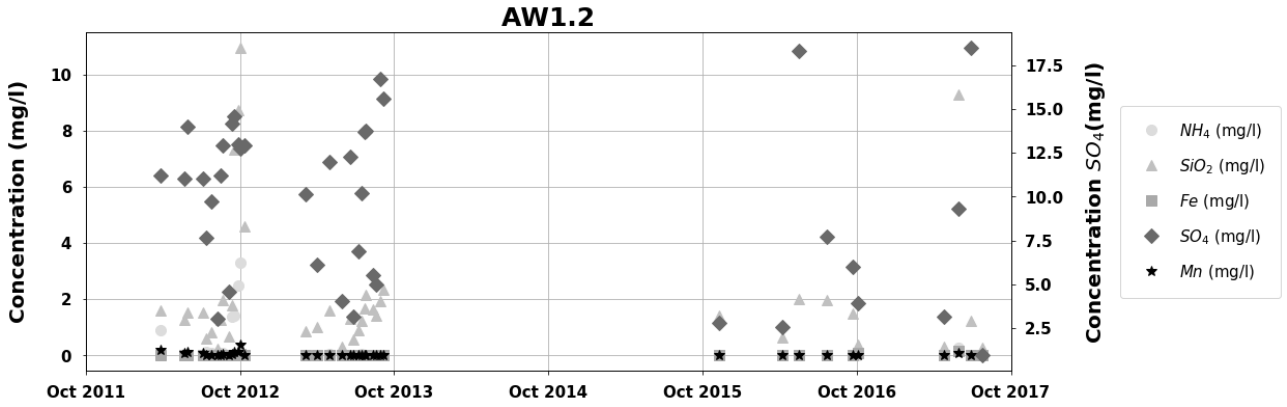

Figure 6.16: Concentrations of NH_4, SiO_2, Fe, SO_4, and Mn in water recovered through AW1.2.

Table 6.3: Quality of water recovered through the upper two well screens of the ASR-well, averaged over measurements between 2012 and 2017, tabulated for the two monitoring periods. EC-25 Field is the electrical conductivity measured in the field with a reference temperature of 25°C.

Sample code	AW1 Average	AW1 Average	AW2 Average	AW2 Average

	2012-2014	2015-2017	2012-2014	2015-2017
EC-25 Field (µS/cm)	143	132	143.1	116
Temperature (˚C)	13.5	14.2	14.4	14.1
pH (Field)	7.9	7.9	7.9	7.7
DO (mg/L)	0.5	2.9	1.7	4
Na (mg/L)	3.6	3.7	3.3	3.2
K (mg/L)	1.1	0.6	0.5	0.3
Ca (mg/L)	24.8	19.0	29.6	17.5
Mg (mg/L)	1.5	1.1	1.0	0.7
Fe (mg/L)	0.0	0.0	0.0	0.0
Mn (mg/L)	0.2	0.0	0.1	0.0
NH_4 (mg NH_4/L)	2.1	0.5	0.4	0.0
Cl (mg/L)	3.6	5.6	4.4	5.2
SO_4 (mg SO_4/L)	8.6	6.8	10.3	7.3
HCO_3 (mg HCO_3/L)	84.7	54.4	84.1	46.4
NO_3 (mg N/L)	0.9	2.8	1.8	3.3
PO_4-t (mg P/L)	0.7	0.4	0.2	0.2
As (µg/L)	6.9	2.5	2.2	0.8
Zn (µg/L)	6.7	15.7*	7.6	25.7**

** One observation of 121 µg/l increased the average concentration, which would otherwise be 4 µg/l.*
*** One observation of 196 µg/l (4-10-2016) increased the average concentration, which would otherwise be 6.8 µg/l.*

6.4. Hydrological effects

The hydraulic heads observed at MW1-S2 in 2012 are given in Figure 6.17, together with several manual observations for validation. The short-term variation in hydraulic heads in the target aquifer are mainly controlled by infiltration and recovery of water by the ASR-Coastal system and are in the range of 10 cm at only 5 m from the ASR-well. The natural variation as a response to the dry/wet periods is in the range of 30 cm. These observed responses to pumping were used to calibrate the groundwater model.

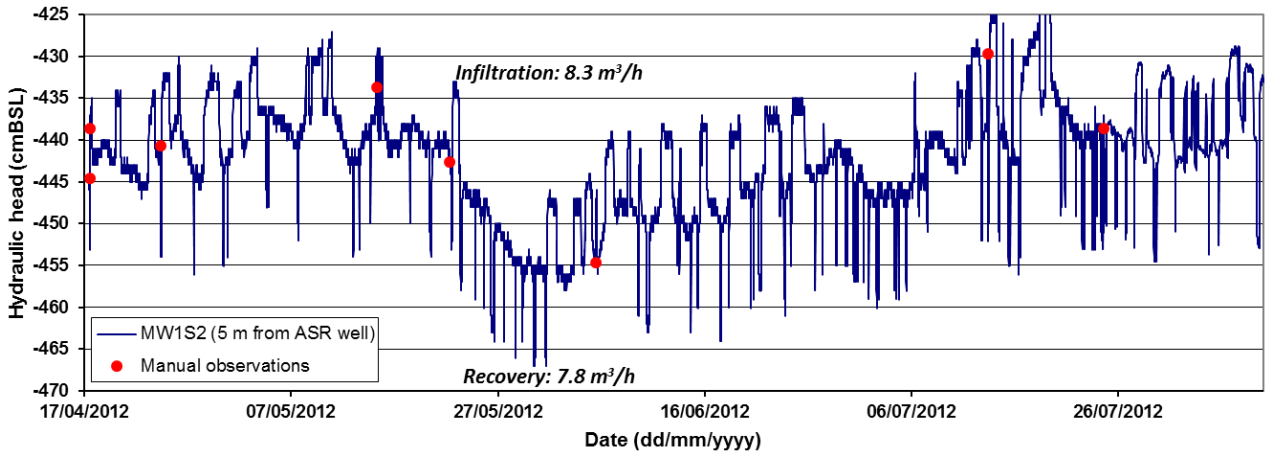

Figure 6.17: Hydraulic head in the target aquifer observed at MW1-S2 by a continuous pressure transducer (blue solid line) and by manual observations (red dots).

6.5. Geophysical measurements: EM-39

Geophysical logging of the subsurface with EM-39 provided detailed information about the local (MW1, MW2, and MW3) changes at the interface of freshwater and saltwater (Figure 6.18-59). Only the upper ~15 m of MW1 could be measured, because MW1.6 had a curved standpipe. Based on the results, it can be concluded that:

1. The coarser fractions of the aquifer are freshened as a result of the infiltration of freshwater;
2. Finer fractions of the aquifer and the clayey aquitards freshened to a lesser extent (32 m BSL) or not at all (28 m BSL and 5-12 m BSL);
3. Freshening of the aquifer top also occurred at MW3, located at a distance of 40 m from the ASR-well;
4. Freshening occurred mainly at the top of the target aquifer and to a lesser extent at the bottom of the aquifer. This was a result of buoyancy effects;
5. Every year, the target aquifer at MW2 became more fresh because the volume of unrecovered freshwater increased after subsequent ASR-cycles.

Altogether, the results underline that buoyancy effects at the site are strong, such that the ASR-Coastal strategy is important to recover the freshwater unmixed. It is also shown that

even close to the ASR-well, clayey segments of the aquifers are still containing brackish water. Based on the recovered water quality, (diffusion from) these layers do not threat the performance of the system.

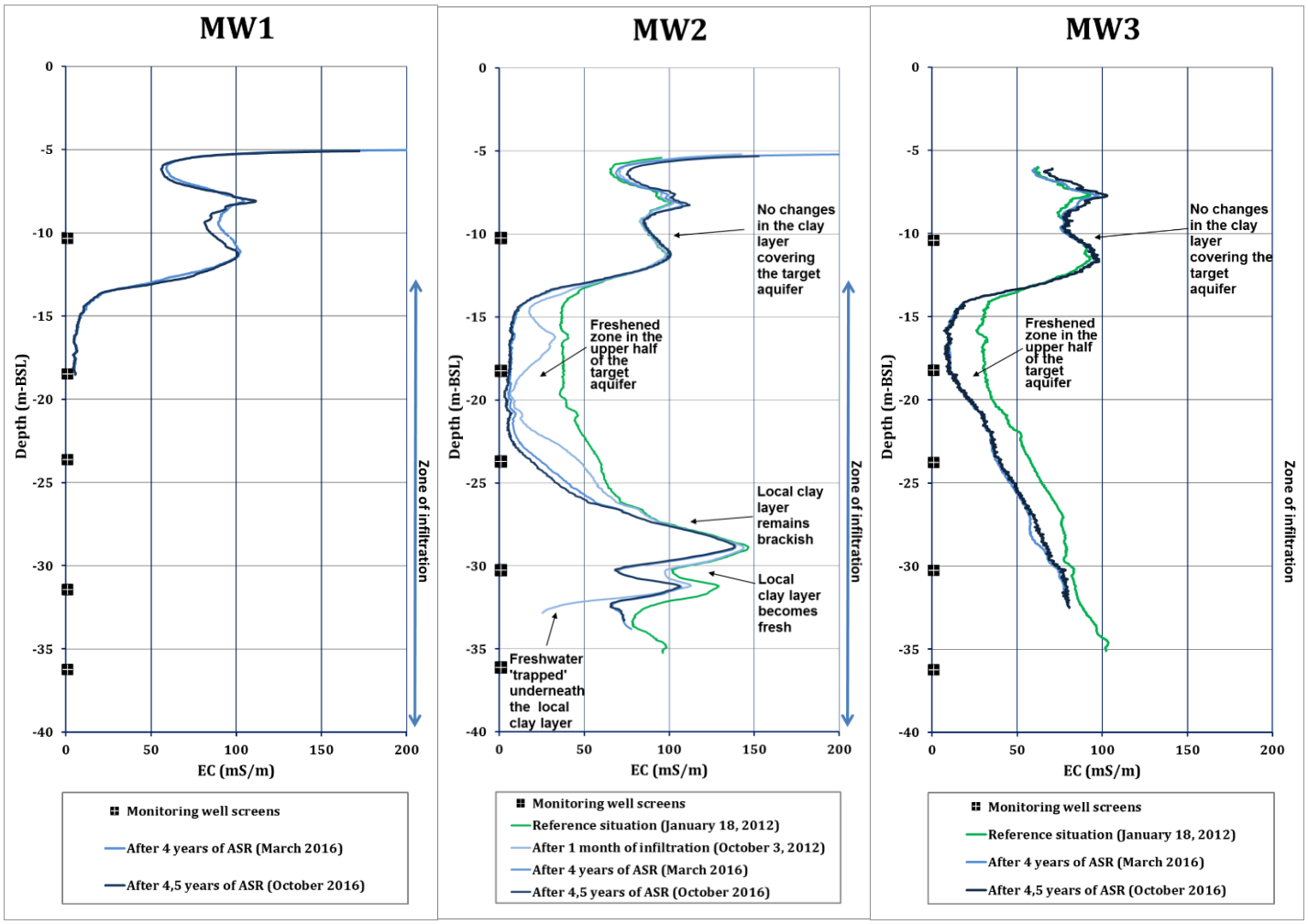

Figure 6.18:Conductivity profile (EC [mS/m] vs. Depth [m BSL]) measured in MW1 (left), MW2 (middle) and MW3 (right) during different phases of the ASR operation in Nootdorp.

7. Results: Modelling

7.1. Comparison field data and groundwater modelling

A calibrated density-dependent axial-symmetric groundwater flow model was used to simulate the ASR-Coastal implementation at the Nootdorp field site over the period of 13 January 2013 until 5 September 2017. Model results are here compared with field data to validate its capability to predict future performance. Therefore, measured chloride concentrations at MW1, 2, and at the ASR well (AW1) were plotted together with modelled values (Figure 7.1 to Figure 7.3).

In addition, (axial-symmetric) cross-sections through the ASR well have been included to visualize the dynamic chloride distribution in the subsurface. The initial chloride distribution (13 January 2012) is given in Figure 7.4. The chloride distribution in the subsurface after a long period of infiltration (31 January 2015) and abstraction (7 July 2015) are shown in Figure 7.5 and Figure 7.6, respectively. The final situation (5 September 2017) is given in Figure 7.7.

The following observations were made regarding the performance of the model with regards to the field observations:

- The general trends observed via groundwater analysis and EM-39 borehole logging are well reproduced by the model;
- The dynamics of the system were not reproduced in the complex geological intervals with intervening clay layers (especially MW1.4, MW1.5, MW2.4);
- Field measurements generally show lower chloride concentrations compared to model at AW1.1 to AW1.3.
- Salinization of upper well screens still occurred during prolonged periods of abstraction according to the model, but was not observed in the field;
- The lower well screens (AW4, MW1.5) salinize more rapidly than predicted by the model during recovery of freshwater.

Potential causes can be

- The chloride concentration of the infiltrated rain water has been slightly overestimated in the input of the model;
- The complexity by the local and highly variable clay layers in the lower part of the aquifer has definitively impacted the groundwater flow around the observation wells here, but cannot be incorporated in the model. However, they have a severe impact on the flow patterns by forcing more water into the more permeable zones (mainly around MW1.2, 1.3, 2.2, 2.3) and can prevent upconing of saltwater from deeper zones of the aquifer;

- The model was set up as an axial-symmetric model – assuming zero lateral background flow. Brackish groundwater extractions for reverse osmosis around the ASR site may have induced some lateral flow during summer
- The regional background lateral regional flow (directed southwest, towards MW1, MW2 and MW3) may have resulted in the lower chloride concentrations at the observation wells during field measurements. This cannot explain however, the lack of salinization at AW1.1 and AW1.2 during long recovery phases.

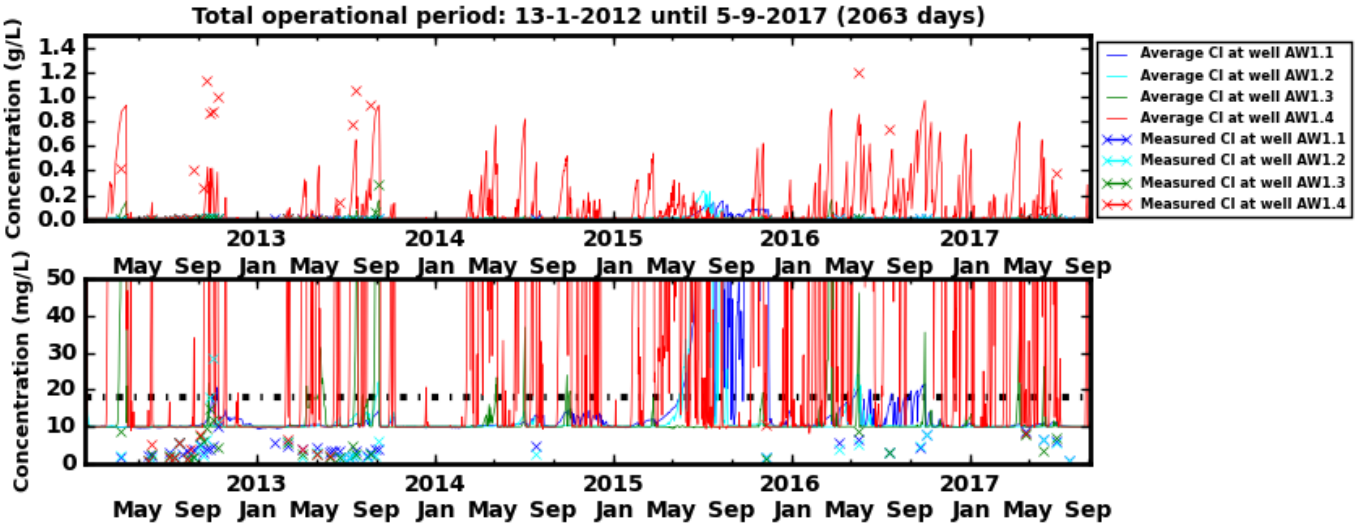

Figure 7.1: Measured (crosses) and modelled (solid lines) chloride concentration in water in the different well screens of the ASR-well (AW1) in Nootdorp from 13 January 2012 until 5 September 2017. 'Average Cl' = modelled Cl concentration. Dashed line indicates the limit set for Cl.

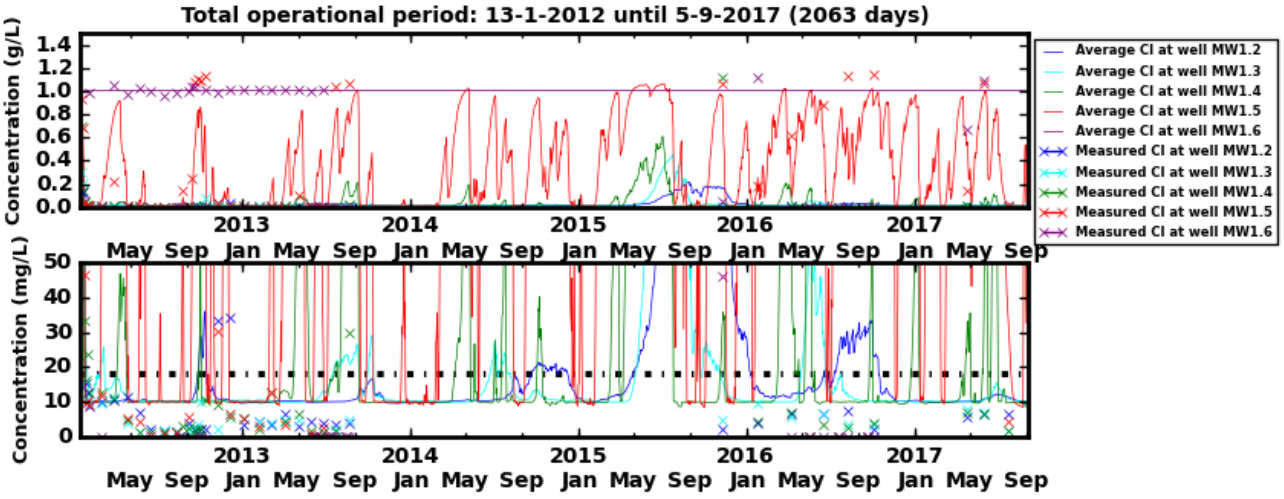

Figure 7.2: Measured (crosses) and modelled (solid lines) chloride concentration in water in the different well screens of monitoring well 1 (MW1) in Nootdorp from 13 January 2012 until 5 September 2017. 'Average Cl' = modelled Cl concentration. Dashed line indicates the limit set for Cl.

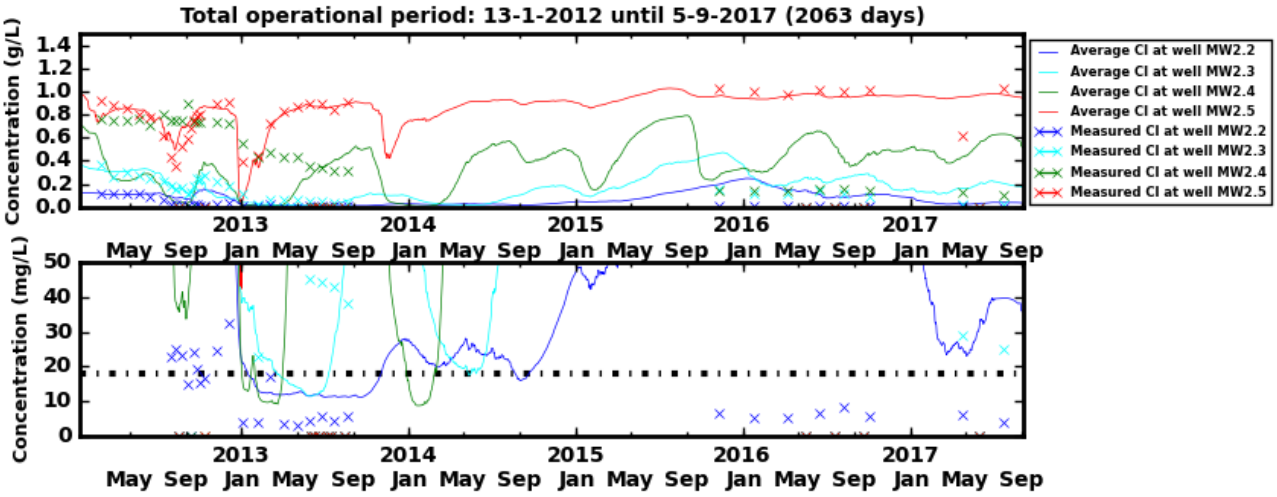

Figure 7.3: Measured (crosses) and modelled (solid lines) chloride concentration in water in the different well screens of monitoring well 2 (MW2) in Nootdorp from 13 January 2012 until 5 September 2017. 'Average Cl' = modelled Cl concentration. Dashed line indicates the limit set for Cl.

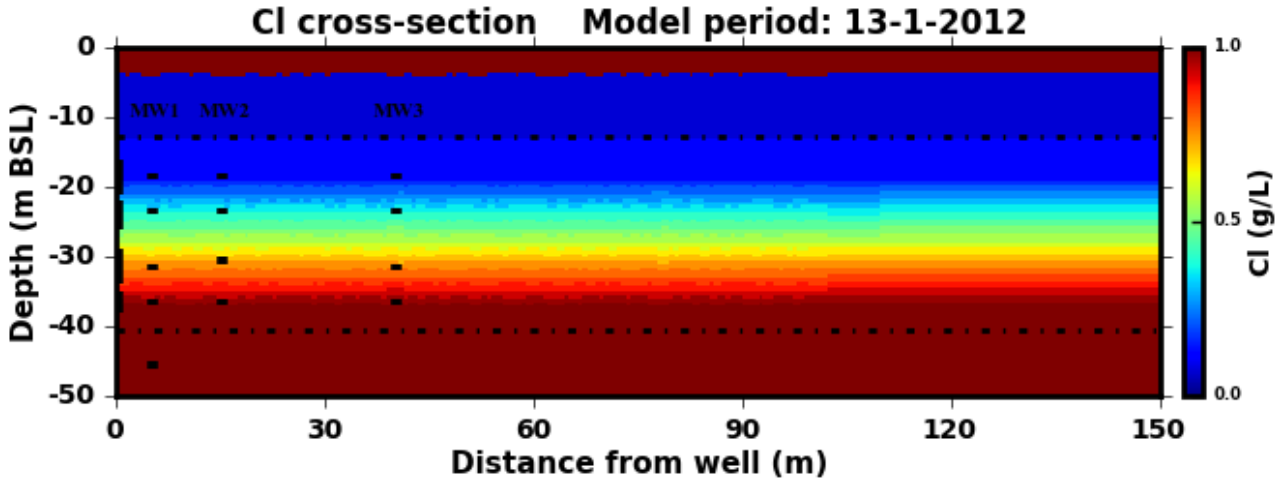

Figure 7.4: Initial modelled chloride concentrations for a cross-section of the subsurface through the ASR-well (left edge) for the initial situation (13 January 2012).

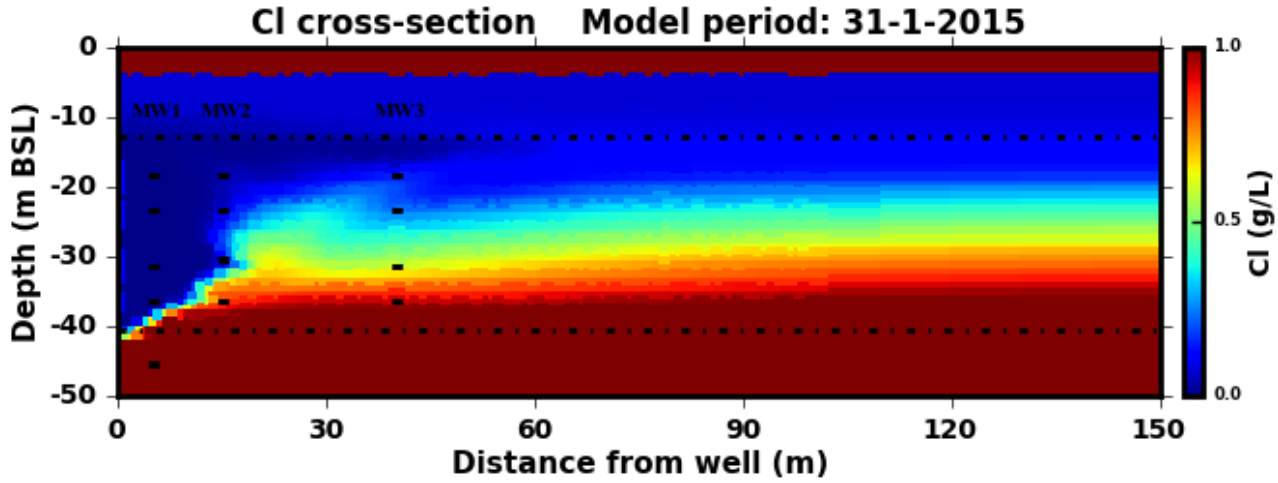

Figure 7.5: Modelled chloride concentrations for a cross-section of the subsurface through the ASR-well (left edge) after a prolonged period of infiltration (31 January 2015).

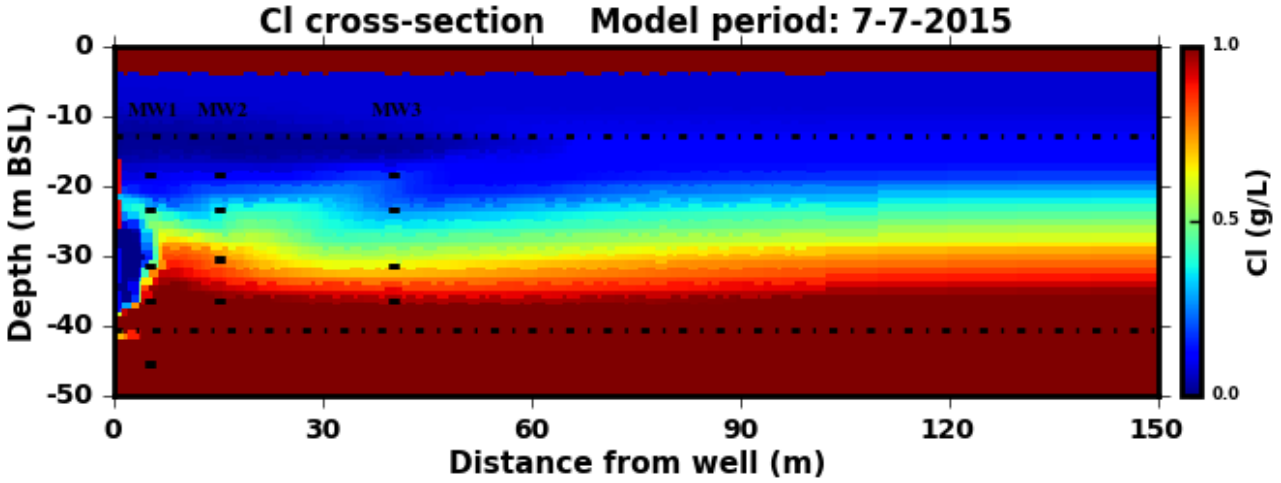

Figure 7.6: Modelled chloride concentrations for a cross-section of the subsurface through the ASR-well (left edge) after maximal recovery when brackish water is abstracted by the well (7 July 2015).

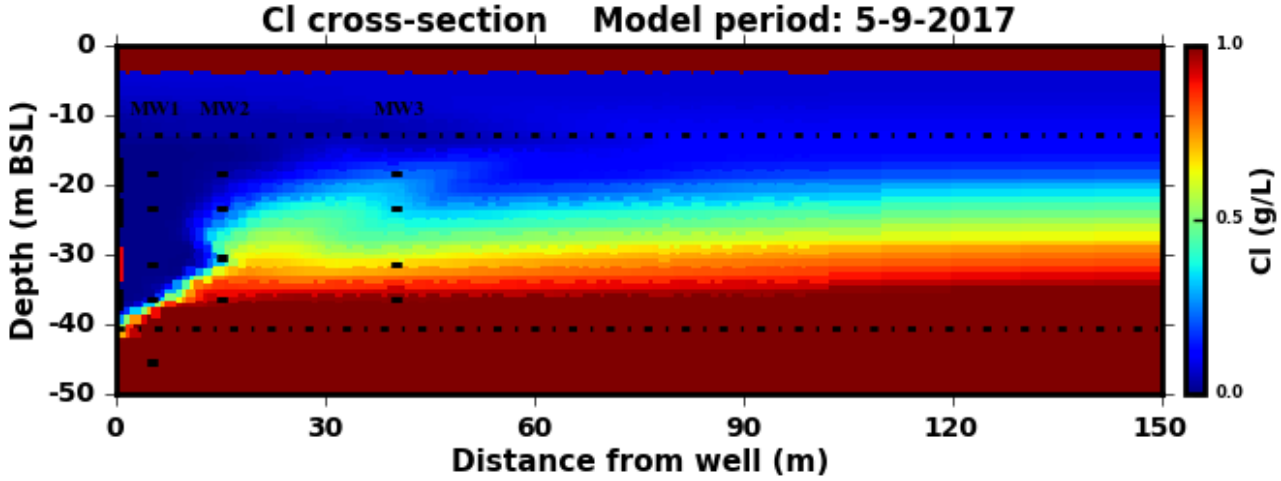

Figure 7.7: Final modelled chloride concentrations for a cross-section of the subsurface through the ASR-well (left edge) for the most recent situation (February 2017).

8. Pre-treatment and well clogging

8.1. Functioning of the pre-treatment

The combination of rapid and slow sand filtration successfully functioned as pre-treatment of the collected rainwater:

- Only once a year, cleaning of the top layer of the slow sand filter is required (staff of the greenhouse needed approximately 4 working hours);
- The rapid sand filter successfully maintains its initial capacity of 25 m3/h when it is back flushed for 3 minutes every 12 hours;
- The MFI of the infiltration water after pre-treatment was between 1.0 and 3.5 s/l^2, which is below the required 4.0 s/l^2 for infiltration via infiltration wells;
- Once a year the 130 micron safety filter which is installed in the infiltration line required cleaning, mainly because dirt washed into the floater box (unfavourably placed in a low area) behind the slow sand filter during intense rainfall events (Figure 8.1).

Figure 8.1: Rainwater in the low area around the floater box of the slow sand filter.

8.2. Condition of the ASR wells (2016)

No cleaning (mechanically or chemically) of the ASR wells was applied in Nootdorp throughout its operation. Around twice a year, the deepest well screens (AW1.3, AW1.4) were shortly backflushed with the recovery pump (maximum rate: 10 m^3/h). The ASR well showed no particular decline in the infiltration rate at the constant infiltration pressure (0.4 bar). The observed actual rate was around 12 m^3/h at the start of the operation, and around 17 m^3/h in the Summer of 2017. In Figure 8.2, the infiltration (per day) is shown,

which is however not suitable to determine the maximal infiltration rate, since the rainfall virtually never lasted long enough to infiltrate throughout a whole (calendar) day.

On July 21, 2016, the ASR well was inspected with a camera to examine its condition. It was found that the different well screens showed quite distinct features (Table 8.1). The observed brownish material in the slots at AW1.3 and 1.4 appears to be related with biogrowth caused by nutrients and some AOC (10 µg/l) in the infiltration water. At AW1.1 (mainly recovery), however, a potential combination with Fe-precipitation may be present. It was not succeeded to collect proper samples of the clogging material. Altogether, the wells are in a relatively good condition after years of operation without cleaning.

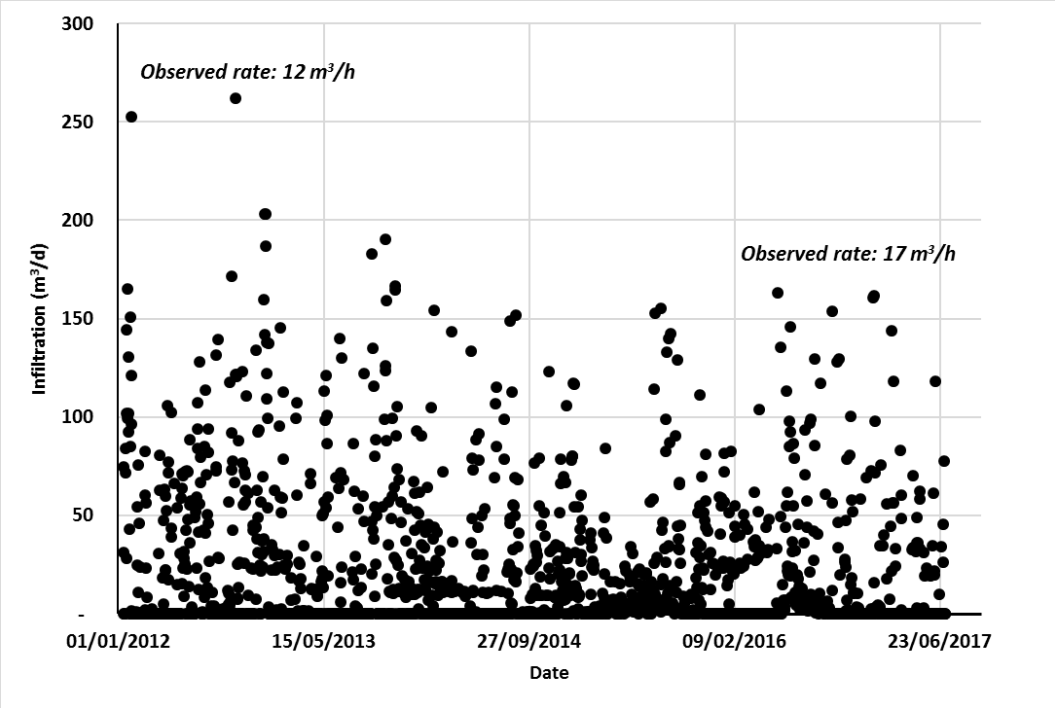

Figure 8.2: Infiltrated water in m^3/d: 2012-2017

Table 8.1: Observations during camera inspections (July 21, 2016)

Well	Observation
AW1.1	• Most recovery of freshwater, least freshwater injection (net abstraction) • Recovery of Fe and Mn observed in first cycles in water infiltrated via AW1.3 and AW1.4 (see figure above), potentially simultaneous abstraction with oxic water injected at AW1.2. • Upon purging with 20 m^3/h: opening of slots at the base of the well. Release of clogging material. • White worms observed
AW1.2	• Infiltration exceeds recovery (net infiltration) • Recovered water normally free of Fe, Mn. At the start of recovery: DO, NO_3
AW1.3	• Infiltration exceeds recovery significantly, virtually no recovery during last cycles. • Water injected in this section quickly attains high levels of Fe, Mn. Therefore: no

	recovery. • White worms observed
AW1.4	• Infiltration exceeds recovery significantly, no recovery, only backflushing (twice a year). The well was backflushed for 5 minutes before the camera inspection took place; • This well regularly salinizes with brackish water containing high levels of Fe, Mn. • Base of the well is much cleaner than the top

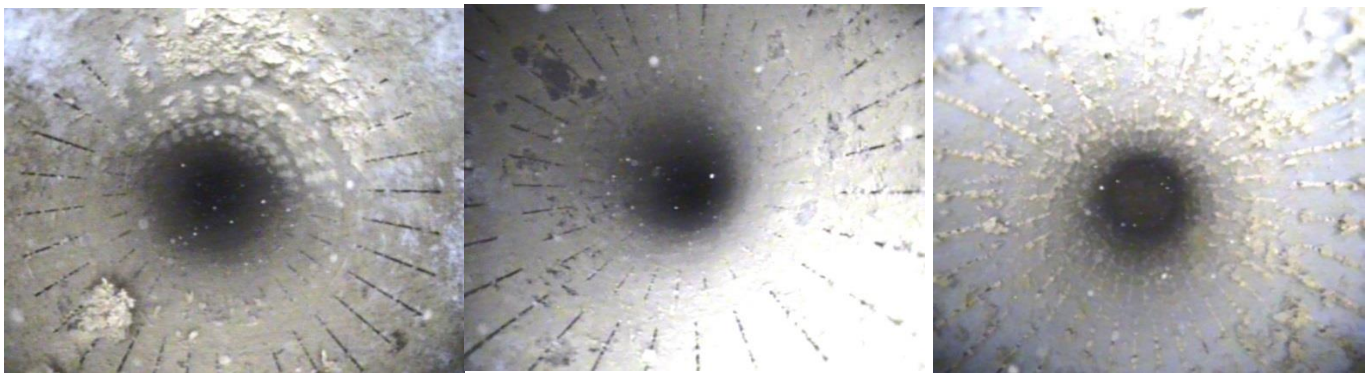

Figure 8.3: Top, centre, and bottom of AW1.1

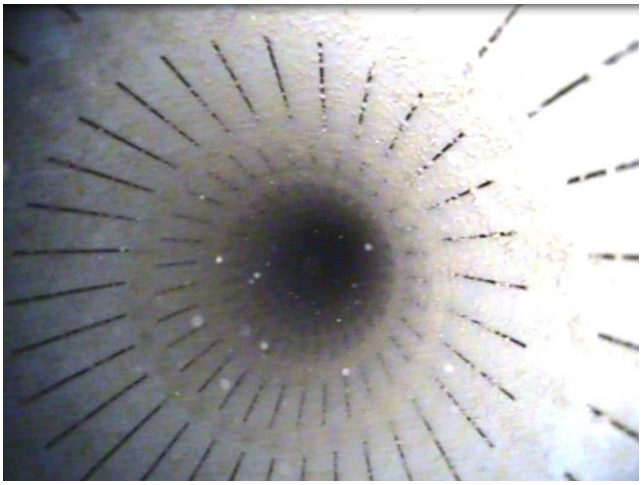

Figure 8.4: Typical condition of AW1.2.

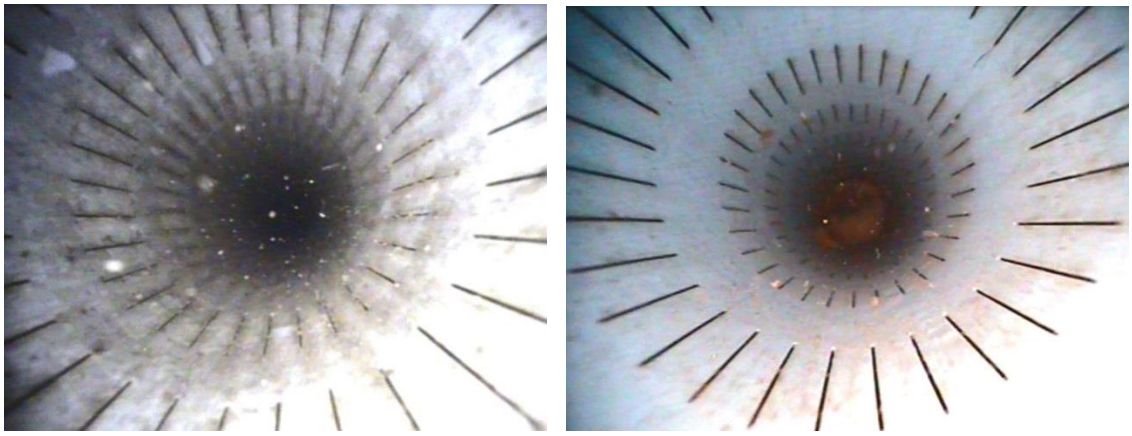

Figure 8.5: Top and bottom of AW1.3.

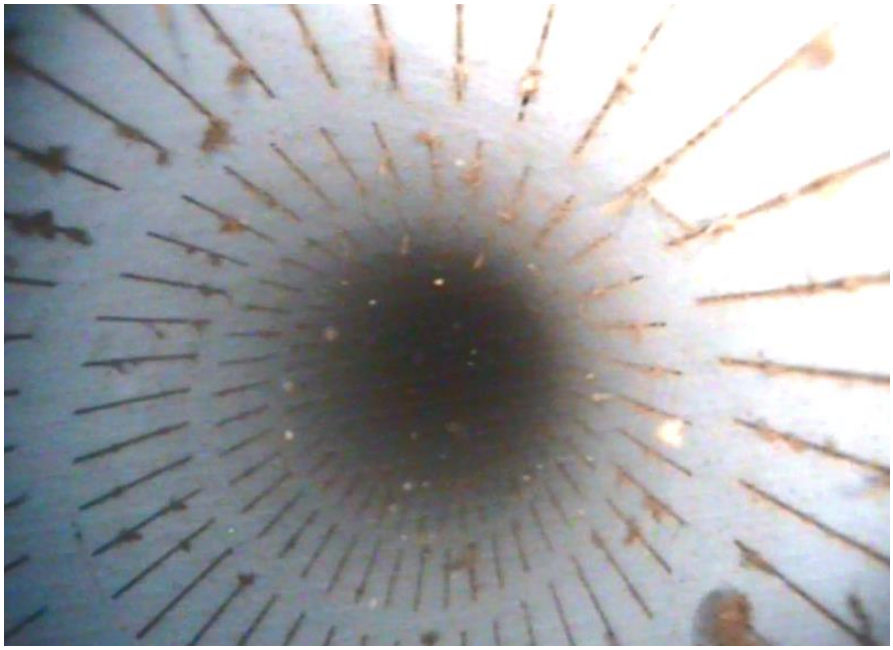

Figure 8.6: Top of AW1.4

9. Cost analysis ASR-Coastal Nootdorp

The costs of the ASR-Coastal system in Nootdorp were analysed, taking into account:

- The true costs required to build the current installation;
- National subsidies for investment in sustainable technologies like ASR (MIA/Vamil);
- Operational and energy costs;
- Depreciation (in 10 years);
- Re-investments to keep the scheme running (pumps).
- Tax shield: as a consequence of depreciation, less profit tax has to be payed;
- Financing (incl. interest);
- Costs discounted at a discount rate of 3%;
- An economic lifespan of 20 years (wells, pipelines, central control unit should make this without re-investments);
- The total production of freshwater during the lifespan,

The alternative (an aboveground basin) was also analysed with the same model, taking into account the loss of net income by the claim on aboveground agricultural land (greenhouse) into account (Table 9.1).

Table 9.1: Input for ASR-Coastal Nootdorp cost analysis

Parameter	Unit	Input
ASR-Coastal		
Lifespan ASR-system	yr	20
Yearly recovery	m^3/yr	7 224
Yearly infiltration	m^3/yr	13 530
Depreciation period	yr	10
Discount rate	%	3
Energy price	€/kWh	0.16
Maintenance/monitoring	€/yr	800
Initial investment	€	76 000
Basin		
Lifespan Basin	yr	15
Depreciation period	yr	10
Loss of net income	€/m^2	3.6
Basin volume	m^3	4 000
Basin surface	m^2	2 400
Costs for realisation	€/m^3	6.15
Loan duration	yr	5
Interest	%	3

It was found that the ASR-Coastal system produces cheaper water (Table 9.2) than the current alternative for storage (above ground basins), which is primarily due to the longer lifetime and the absence of loss of production by a spatial claim. Initial investments and operational costs are higher, compared to the alternative. Piped river water is available from the drinking water distribution system, but is also more expensive per m^3 and relatively saline (57 mg/l Na and 53 mg/l Cl) and thus not fit for use.

Table 9.2: Cost price of the produced irrigation water at the ASR-Coastal Nootdorp site

Water source	ASR-Coastal	Aboveground basin	Piped water
Costs / m^3	0.61	1.16	1.02

ASR-Coastal in Westland

10. Set-up of the ASR-Coastal system in Westland

10.1. ASR-strategy

The ASR-Coastal system in Westland was installed to improve freshwater management in coastal areas by aquifer storage and recovery (ASR), using multiple partially penetrating wells (MPPWs), similar to the system in Nootdorp. However, the system was later complemented with a Freshkeeper and reverse osmosis (ASRRO) to further improve the recovery of freshwater (Figure 10.1). The ASRRO-concentrate is disposed through a well screen in a deeper and more saline aquifer.

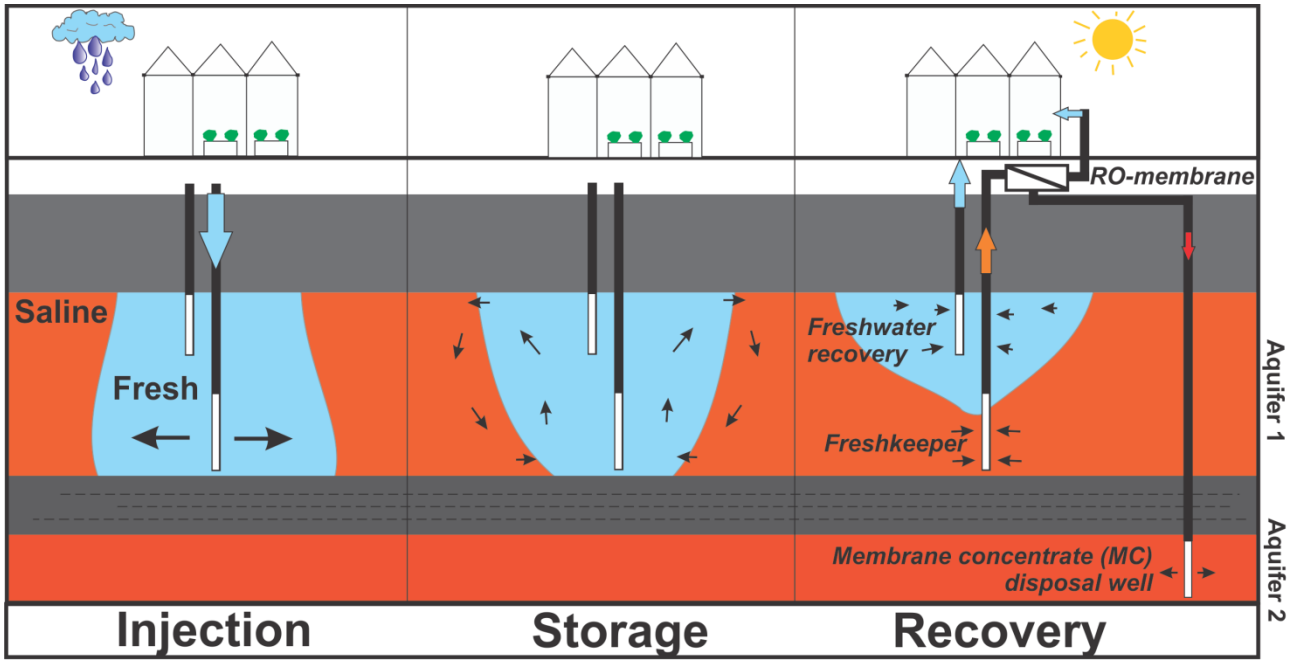

Figure 10.1: Concept of ASR-Coastal in Westland with multiple partially penetrating wells (MPPWs) and the Freshkeeper.

10.2. Location

The Westland ASR-Coastal site is situated in the coastal province of Zuid-Holland, in the western part of The Netherlands. The study area is dominated by greenhouse horticulture with a typical high water demand and strict quality standards concerning salinity. Rainwater from greenhouse roofs is therefore used as the main irrigation water source. Chloride concentrations in the target aquifer are typically around 4000 mg/L (Figure 10.2). The local surface level has an elevation of 0.5 m above sea level (m ASL).

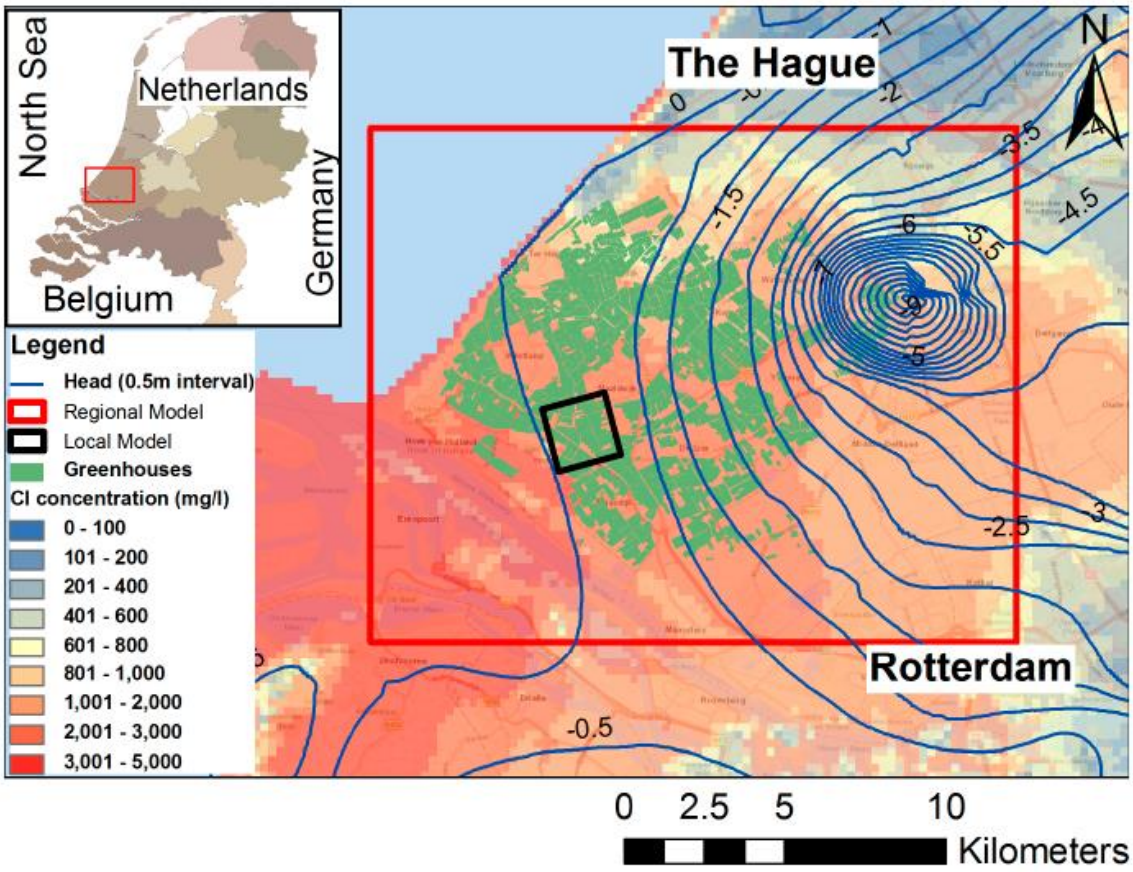

Figure 10.2: Regional piezometric head contours (TNO, 1995) and chloride concentrations (Oude Essink et al., 2010) in the centre of the ASR target aquifer and location of the Westland ASR field site (black square).

10.3. The ASR-facility

The Westland ASR system has been installed to infiltrate the rainwater surplus from 270,0000 m2 of greenhouse roof into a local shallow aquifer (23 - 37 m below sea level (m BSL)) with negligible lateral displacement. Part of the water is recovered in times of demand. For this purpose, two multiple partially penetrating wells (MPPW) were initially installed (Figure 10.3 and Figure 10.4), such that water can be infiltrated preferably at the aquifer base, and recovered at the aquifer top to increase the recovery efficiency. These ASR wells (AW1 and AW2) were installed in 2012 using reverse-circulation rotary drilling. The elevations of the filter screens are given in Table 10.1. Bentonite clay was applied to seal the ASR boreholes (type: Micolite300). The ASR wells use a 3.2 m high standpipe to provide infiltration pressure. Rainwater can be pre-treated and infiltrated with a total rate of 40 m^3/h, and recovered with a total rate of 50 m^3/h.

In a later stage of the pilot at the Westland site, ASR-Coastal was combined with a Freshkeeper and reverse osmosis ('ASRRO') to maximize the recovery of infiltrated freshwater surpluses (Figure 10.1).

In the improved set-up, two wells are used to feed two separate RO-facilities. One is the original brackish water RO ('BWRO') plant present at the site, which has been active since

2006. This well abstracts water from the whole aquifer thickness at the fringe of the freshwater body, thereby feeding the BWRO with a mixture of water qualities. This BWRO-plant was designed to be fed by 40 m^3/h of brackish groundwater to produce 20 m^3/h (480 m^3/d) of freshwater, which results in an equal stream of concentrate at an RO-recovery of 50%. The membrane concentrate is disposed in a deeper aquifer (Figure 10.1).

The ASR-wells were connected to an additional RO-plant (ASRRO) to desalinate mixed water recovered from the bottom of the ASR well below the freshwater bubble, similar to the Freshkeeper set-up (Deliverables D1.2 and D1.3). Both RO-systems produce supplementary high-quality water (total freshwater production of 22 m^3/h) and are used in combination with concentrate disposal in a deep aquifer, resulting in a net freshwater mining in the groundwater system.

10.4. Monitoring wells

Five bailer drilled boreholes (MW1-5, Figure 10.3 and Figure 10.4) were realised around the ASR system. These monitoring wells allowed to determine the distribution of and interaction between the fresh- and saltwater bodies during operation of the ASR-Coastal system. The depths of these monitoring well screens are included in Table 10.1. Bentonite (type: Micolite300) clay was applied to seal monitoring boreholes, where aquitards were pierced and in between various piezometers.

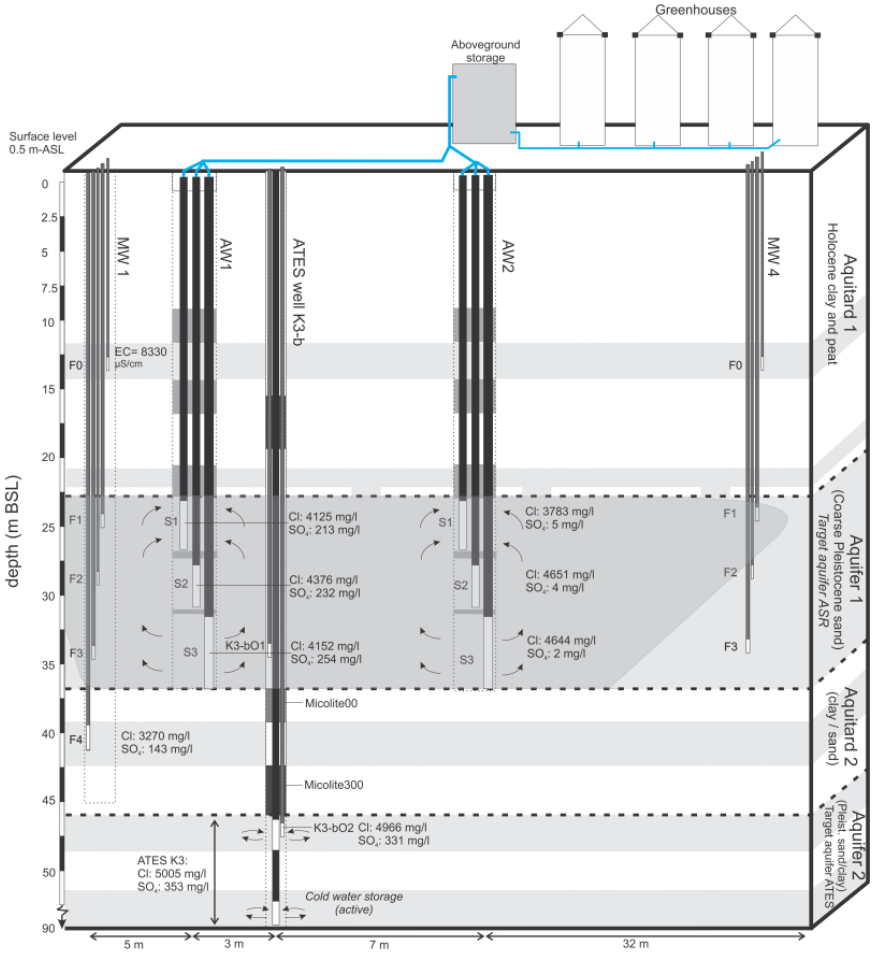

Figure 10.3: Cross-section of the Westland ASR site schematizing the geology, ASR wells, ATES well, and the typical hydrochemical composition of the native groundwater. Horizontal distances are not to scale.

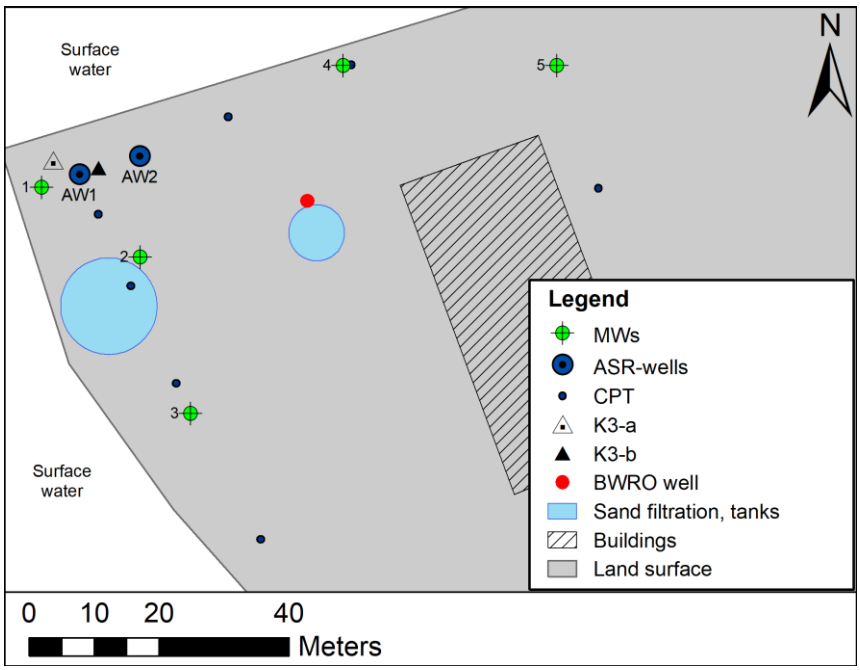

Figure 10.4: Schematic plan view of the ASR-Coastal set-up at the Westland field site.

Table 10.1: Elevations of the MPPW-ASR wells screens (AW#-S#) and the monitoring well screens (MW#-S#) of the Westland ASR-Coastal system (Figure 10.3 and Figure 10.4).

Monitoring Well-Screens	Well screen top (m BSL)	Well screen bottom (m BSL)
AW1-S1	-23.09	-26.59
AW1-S2	-27.59	-30.59
AW1-S3	-31.59	-36.44
AW2-S1	-23.09	-26.59
AW2-S2	-27.59	-30.59
AW2-S3	-31.59	-36.44
MW1-S0	-12.94	-13.94
MW1-S1	-23.94	-24.94
MW1-S2	-28.94	-29.94
MW1-S3	-33.94	-34.94
MW1-S4	-40.94	-41.94
MW2-S0	-11.78	-12.78
MW2-S1	-23.78	-24.78
MW2-S2	-28.78	-29.78
MW2-S3	-33.78	-34.78
MW3-S0	-12.77	-13.77
MW3-S1	-23.77	-24.77
MW3-S2	-28.77	-29.77
MW3-S3	-33.77	-34.77
MW4-S0	-12.78	-13.78
MW4-S1	-24.78	-25.78
MW4-S2	-29.78	-30.78
MW4-S3	-34.78	-35.78
MW5-S0	-12.77	-13.77
MW5-S1	-23.77	-24.77
MW5-S2	-28.77	-29.77
MW5-S3	-33.77	-34.77

10.5. Photographic impression

A photographic impression of the ASR-Coastal set-up in Westland is presented in Figure 10.5 and Figure 10.6.

Figure 10.5: ASR well field (left) and slow sand filter (right).

Figure 10.6: Installation for infiltration and recovery of the rainwater (top) and the desalination of water recovered with high salinities (via the Freshkeeper) (bottom).

11. Characterization of the target aquifer

11.1. Approach

A detailed characterization of the target aquifer was obtained by:

- Taking samples from the bailer of MW1-5.
- Preparing the samples using the method of Konert and Vandenberghe (1997).
- Using a HELOS/KR laser particle sizer (Sympatec GmbH, Germany) to derive the grain size distributions of the prepared samples in the range of 0.12 - 2000 µm.
- Correcting the obtained grain size distribution for the gravel contribution by oven-drying samples containing gravel and sieving them with a 1600 µm sieve to obtain the fraction > 2000 µm, taking elongated particles into account.
- Using Bear (1972) to initially assess the hydraulic conductivity (K) of the target aquifer from the measured grain size distribution. The hydraulic conductivity of the target aquifer was also derived from head responses at monitoring wells upon pumping. The hydraulic conductivity of the deeper subsurface was derived from a pumping test at approximately 500 m from the ASR wells.

A detailed characterization of the native groundwater in the target aquifer was obtained by:

- Recording the electrical conductivities in the aquifer at two locations (MW1 and MW2) prior to ASR operation (November 28, 2012) by geophysical borehole logging using a Robertson DIL-39 probe ('EM-39') (McNeill et al., 1990). This allows to determine the exact location of the fresh-salt interface.
- Sampling at all ASR and monitoring well screens prior to ASR operation (November and December, 2012), and analysing the samples for the same parameters as during the water quality monitoring (see Chapter 13.2).

11.2. Aquifer characterization

The target aquifer for ASR (Aquifer 1) is 14 m thick and consists of coarse fluvial sands (average grain size: 400 µm) with a hydraulic conductivity (K) of 30 – 100 m/d. Aquifer 2 (target aquifer for ATES) has a thickness of more than 40 m, but is subdivided into two parts at the ATES well (K3) by a 20 m thick layer of clayey sand and clay. The K-value of the fine sands in Aquifer 2 is 10 to 12 m/d and is in line with the estimated K-value from grain size distribution (Mos Grondmechanica, 2006).

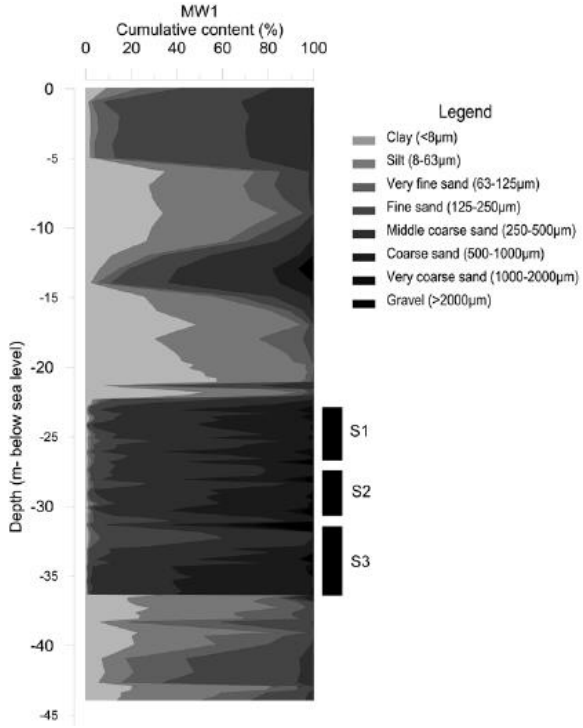

Figure 11.1: Cumulative grain size distribution observed at MW1 (at 5 m from ASR well 1). S1-S3 mark the depth intervals of the individual ASR well screens in the target aquifer.

11.3. Native groundwater characterization

The groundwater is brackish, with observed Cl concentrations ranging from 3,793 to 4,651 mg/l in the target aquifer (Aquifer 1; Table 11.1) and approximately 5,000 mg/l in Aquifer 2 (Figure 10.3). This means that with the accepted Cl-concentrations during recovery, only around 1% of admixed ambient groundwater is allowed. A sand layer in Aquitard 2 contains slightly fresher water (Cl = 3,270 mg/l). SO_4 is a useful tracer to identify the saltwater from Aquifer 1 and 2: it is virtually absent in Aquifer 1 (presumably younger groundwater, infiltrated when the Holocene cover was already thick), whereas it is high in Aquifer 2 (older water, infiltrated through a thinner clay cover which limited SO_4-reduction, see Stuyfzand (1993) for more details). Concentrations of 300 to 400 mg/L SO_4 were observed in this deeper aquifer. HCO_3 (approximately 1300 mg/L in Aquifer 1 and 600 mg/L in Aquifer 2) was another suitable tracer, yet less distinct. The average characteristics of the native groundwater in the target aquifer prior to ASR operation are given in Table 11.1.

Table 11.1: Typical hydrogeochemical composition of native brackish groundwater in the target aquifer (Aquifer 1), based on average concentrations in the ASR-wells and monitoring wells on November 6 and December 12, 2012. EC-25 Field is the electrical conductivity measured in the field with a reference temperature of 25°C. The presence of NO_3 can be a result of nitrification during storage and/or analysis, as a consequence of necessary dilution in the lab. Dissolved oxygen and phosphate were not sampled at this time.

Sample code	Target aquifer (at 29.4m depth)
	Nov – Dec 2012
EC-25 Field (µS/cm)	12054
Temperature (°C)	11.6
pH (Field)	7.4
Na (mg/L)	2129.8
K (mg/L)	83.9
Ca (mg/L)	423.7
Mg (mg/L)	321.0
Fe (mg/L)	8.7
Mn (mg/L)	1.1
NH_4 (mg NH_4/L)	9.76
Cl (mg/L)	4496.8
SO_4 (mg SO_4/L)	57.2
HCO_3 (mg HCO_3/L)	1196.6
NO_3 (mg N/L)	1.2
As (µg/L)	1.4
Zn (µg/L)	71.6

12. Groundwater model set-up

12.1. Model set-up

Groundwater transport modelling with SEAWAT (Langevin et al., 2007) was initially executed to simulate the ASR operation and to validate the added value of the MPPW-ASR(RO) set-up at the Westland field site. A schematization of the computer model is shown in Figure 12.1 and the hydrogeological properties that were applied are given in Table 12.1. For more information regarding the groundwater flow and transport model, the reader is referred to Zuurbier and Stuyfzand (2017).

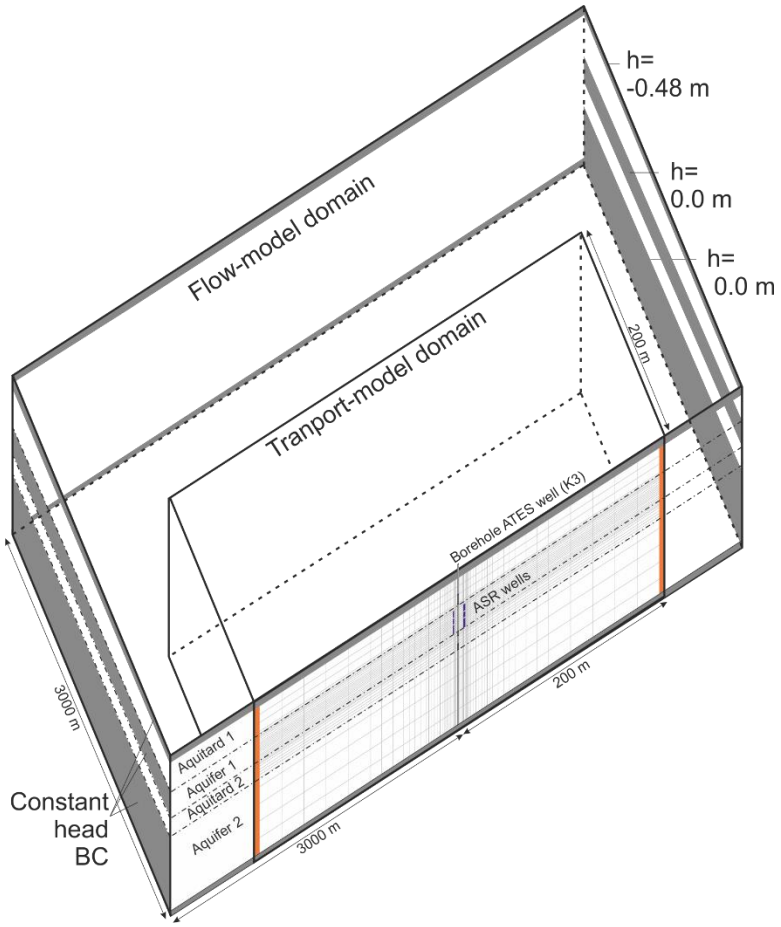

Figure 12.1: Set-up of the groundwater transport model (half-domain) of the Westland ASRRO system. 'BC' refers to the boundary condition and 'h' to hydraulic head.

12.2. Modelling strategy

A two-stage approach was applied by first modelling two individual ASR(RO) systems to study their performance and interaction on a local scale. In a later stage of the research, the model was used to test potential pathways for deeper groundwater to reach the target aquifer and to explore the characteristics of a potential conduit via scenario modelling. The final model includes this conduit, because it is able to simulate the real situation the best.

This model is compared with field measurements to validate its capability to predict the future performance at the field site.

Table 12.1: Hydrogeological properties of the geological layers in the Westland SEAWAT model. 'VANI' = vertical anisotropy ratio, K_h = horizontal hydraulic conductitivity, S_s = specific storage, n = porosity.

Geological Layer	Model Layers	Layer Base (m BSL)	K_h (m/d)	VANI (K_h/K_v)	S_s (m^{-1})	n (-)	Initial Conc. (mg Cl /L)	Initial Conc. (mg SO_4/L)
Aquitard 1	6	22.3	0.2 – 1	100	10^{-4}	0.2	2000 - 3000	4
Aquifer 1 (target aquifer)	12 3	33.7 36.4	35 100	1	10^{-7}	0.3	4000 - 4800	4
Aquitard 2 (clay-sand)	8	47.5	0.05 - 10	1 - 10	10^{-4}	0.2 - 0.3	3200	160
Aquifer 2 (deep aquifer)	6	96	12	1	10^{-6}	0.3	4100 - 7900	331 - 375

13. Monitoring during operation (2012-2017)

13.1. Water quantity

Calibrated, electronic water meters were coupled to the programmable logic controller (PLC) of the ASR system to record the operation per well screen.

13.2. Water quality

Water samples were frequently obtained at the infiltration water inlet, the ASR-wells, the monitoring wells, and the water used for the RO-system and the resulting concentrate. All samples were analysed in the field in a flow-through cell for EC (GMH 3410, Greisinger, Germany), pH, temperature (Hanna 9126, Hanna Instruments, USA), and dissolved oxygen (DO) (Odeon Optod, Neotek-Ponsel, France). The samples were filtrated using 0.45 µm cellulose acetate membranes (Whatman FP-30, UK) in the field and sent to the VU University Water Lab (2012-2015) and the WUR University Water Lab (2015-2017). Here, the macrochemical composition was analysed. Samples were stored in two 10-ml plastic vials, of which one was acidified with 100 µl 65% HNO_3 (Suprapur, Merck International) for analysis of cations (Na, K, Ca, Mg, Mn, Fe, S, Si, P, and trace elements) using ICP-OES (Varian 730-ES ICP OES, Agilent Technologies, U.S.A.). The other 10 ml vial was used for analysis of F, Cl, Br, NO_2, NO_3, PO_4, and SO_4 using the Dionex DX-120 IC (Thermo Fischer Scientific Inc., USA), and NH_4 using the LabMedics Aquakem 250 (Stockport, UK). All samples were cooled to 4°C and stored dark immediately after sampling. At the WUR university, 100 ml samples with filtrated samples were used for ICP-AES (Al, Ca, Fe, K, Mg, Mn, Na, P, S, Zn, Si) and ICP-MS (As) upon Aqua-Regia extraction, Segmented Flow Analyzer (NH_4, NO_3+NO_2, PO_4), Flow Injection Analyzer (Cl), and Shimadzu analyzer (TC, IC).

13.3. Hydrological effects

CTD-divers (Schlumberger Water Services, Delft, The Netherlands) were used for electronic recording of conductivity, temperature, and pressure in the target aquifer at MW1 (S1, S2, and S3) and MW2 (S1 and S2).

13.4. Geophysical measurements

Electrical conductivity profiles were constructed for MW1, MW2, and MW3 by geophysical borehole logging (EM-39) during different phases of consecutive ASR cycles in 2013 and 2016. Changes in formation conductivity outside the standpipe of the well should indicate a change in electrical conductivity of the groundwater, as the lithology remains constant (Metzger and Izbicki, 2013). Therefore, these profiles can be used to determine the development and distribution of the freshwater body during operation of the ASR-Coastal system in Westland.

14. Results: Monitoring

14.1. Water quantity analysis

The ASR-Coastal system at the Westland site recovered around 22.5% of the infiltrated freshwater between 2012-2017. The recovery improved after the Freshkeeper was implemented (2014) and then varied as a consequence of the infiltration volume (winter water surplus).

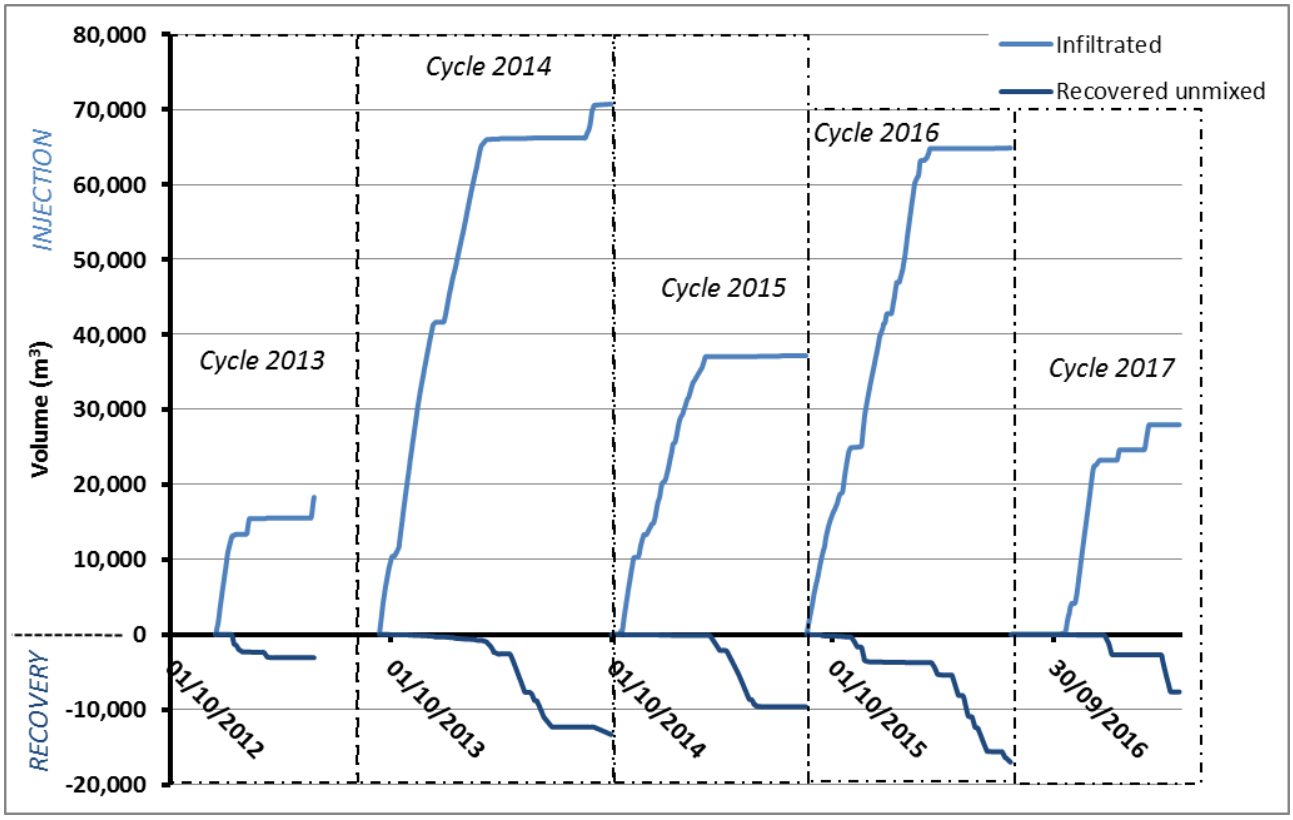

Figure 14.1: Infiltrated and recovered volumes per cycle versus time (data on a daily basis)

Table 14.1: Infiltrated and recovered volume at ASR-Coastal Westland

Cycle	Absolute infiltration (m^3)	Absolute recovery (m^3)	Recovery efficiency ASR (%)	Freshkeeper
2013*	18,313	3,082	16.8%	NO
2014	70,710	13,320	18.8%	YES
2015	37,166	9,625	25.7%	YES
2016	64,846	15,855	24.5%	YES
2017**	27,968	7,482	26.8%	YES
Total	219,003	49,306	22.5%	

**Started half-way December 2012. No Freshkeeper added to the MPPW-ASR system*

*** Cycle until April 26, 2017: maximal direct recovery was attained.*

The production of freshwater via ASRRO and BWRO is listed in Table 14.2. The final recovery of freshwater from the brackish feed water was below 50% as a consequence of clogging of the RO membranes. For more information on this matter, the reader is referred to DESSIN deliverable D33.

Table 14.2: Abstraction of brackish groundwater as feedwater for the ASRRO and BWRO plant and transformation to freshwater and concentrate upon RO-treatment

Cycle	Abstracted brackish / Feedwater ASRRO	Produced freshwater ASRRO	Re-injected / Concentrate ASRRO	Reco-very	Feedwater BWRO	Produced freshwater BWRO	Concentrate BWRO	Reco-very
2014*	10,226	0	10,226	0%	33,480	13,392	20,088	40%
2015	15,661	6,841	8,820	44%	61,771	19,415	42,356	31%
2016	28,192	11,547	16,645	41%	28,196	12,095	16,664	43%
Total	54,079	18,388	35,691	34%	123,447	44,902	79,108	36%

**ASRRO plant not in operation yet, brackish groundwater from Freshkeeper directly re-injected*

14.2. Water quality analysis: infiltration water

The average water quality of the infiltration water was derived by taking the average of 20 samples taken between 2012 and 2017 (Table 14.3). The variation of the infiltration water quality can be derived from (Figure 14.2-Figure 14.4). The infiltrated water is typically very fresh and oxic. EC and pH are relatively constant, but the temperature has a seasonal variation.

All average concentrations of the infiltrated freshwater remain below the legal limits set by the Water Act of The Netherlands in 2017, except for Zn. Zn often exceeded 100 µg/l, which resulted in an average infiltration concentration above the legal limits. Since concentrations of Zn in the freshwater reaching the surrounding monitoring wells remained <10 µg/l, it was presumed that Zn was adsorbed in the vicinity of the ASR-wells. A better removal of Zn in the pre-treatment facility should be attained.

Table 14.3: Observed infiltration water quality averaged over 20 measurements between 2012 and 2017, tabulated together with the legal limits set by the Water Act of The Netherlands in 2017. EC-25 Field is the electrical conductivity measured in the field with a reference temperature of 25°C.

Sample code	Average	Legal limits
	2012-2017	Water Act, The Netherlands, 2017
EC-25 Field (µS/cm)	38	-
Temperature (°C)	8.7	-
pH (Field)	7.1	-
DO (mg/L)	9.5	-
Na (mg/L)	5.0	120
K (mg/L)	0.3	-
Ca (mg/L)	1.9	-
Mg (mg/L)	0.7	-
Fe (mg/L)	0.0	-
Mn (mg/L)	0.1	-
NH_4 (mg NH_4/L)	0.19	3.2
Cl (mg/L)	6.5	200
SO_4 (mg SO_4/L)	2.3	150
HCO_3 (mg HCO_3/L)	7.7	-
NO_3 (mg N/L)	3.0	24.8
PO_4-t (mg P/L)	0.1	1.25
As (µg/L)	1.3	10
Zn (µg/L)	171.8	65

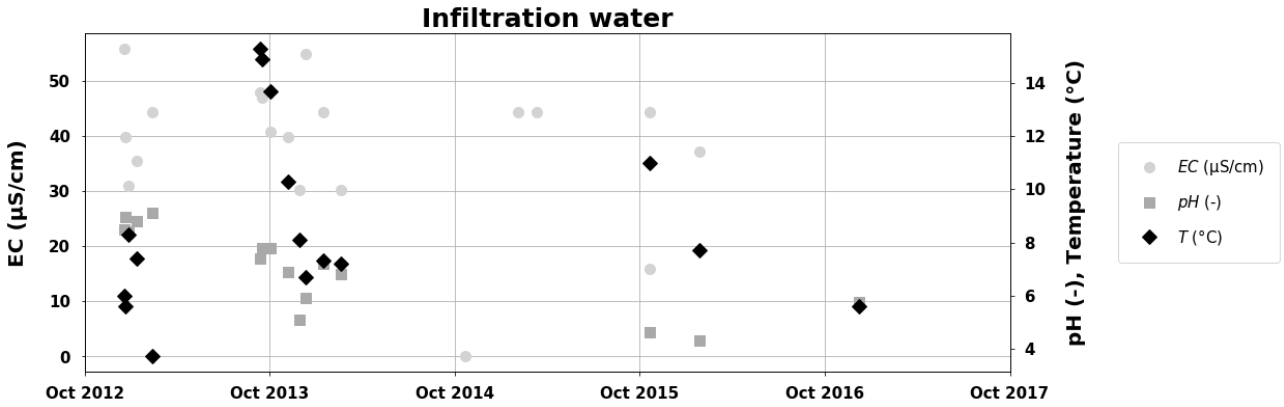

Figure 14.2: Electrical conductivity (EC in µS/cm), pH (-), and temperature (Temp in °C) of the freshwater used for infiltration in the ASR-Coastal set-up.

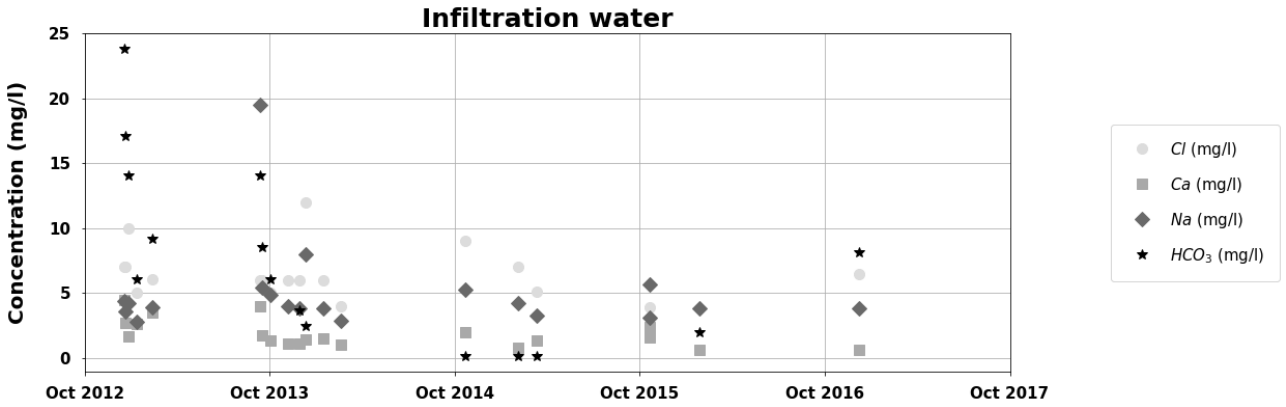

Figure 14.3: Concentrations of Cl, Ca, Na, and HCO_3 in the freshwater used for infiltration in the ASR-Coastal set-up.

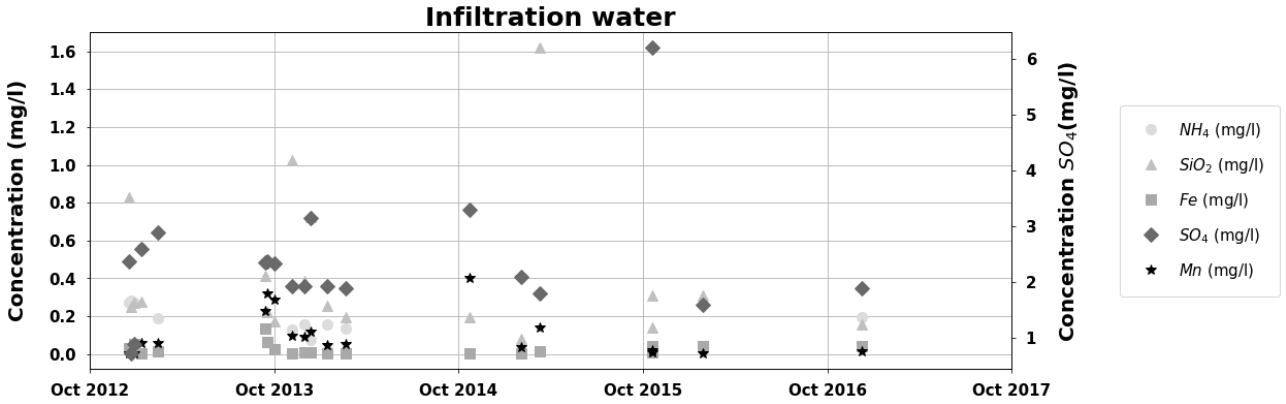

Figure 14.4: Concentrations of NH_4, SiO_2, Fe, SO_4, and Mn in the freshwater used for infiltration in the ASR-Coastal set-up.

14.3. Water quality analysis: recovered freshwater (AW2.1, AW2.2)

For quality assurance of the freshwater recovered through the upper two well screens of AW2 that were used for recovery in times of demand, the hydrogeochemical composition of this water was monitored over time (Figure 14.5 - Figure 14.10). The data clearly visualizes the initial recovery of freshwater (very similar to infiltration water, but now anoxic and with higher SO_4, Ca, and HCO_3 concentrations). In 2016 and 2017, the recovery at AW2.1 and AW2.2 was prolonged to feed the ASRRO-plant with relatively fresh water. This explains the increasing concentrations at the end of the recovery season.

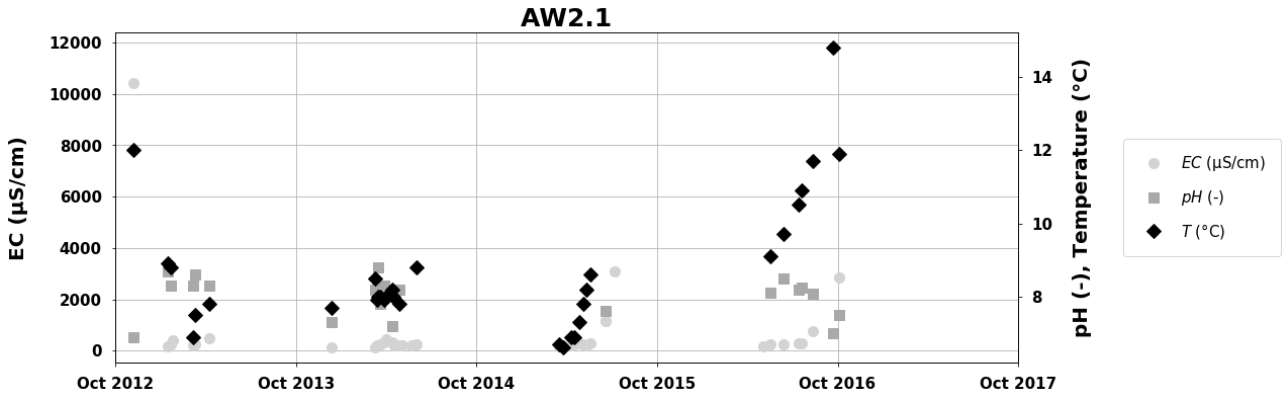

Figure 14.5: Electrical conductivity (EC in µS/cm), pH (-), and temperature (Temp in °C) of water recovered through AW2-S1.

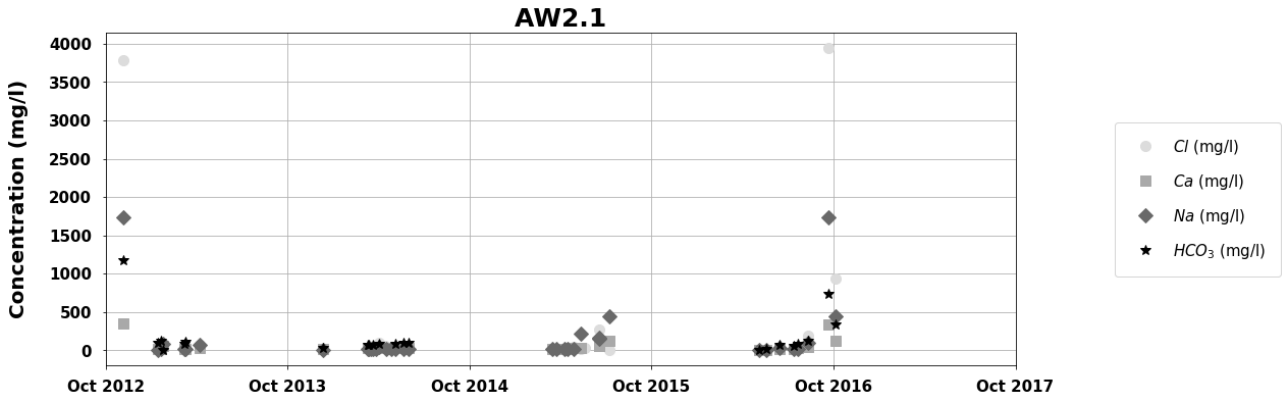

Figure 14.6: Concentrations of Cl, Ca, Na, and HCO_3 in water recovered through AW2-S1.

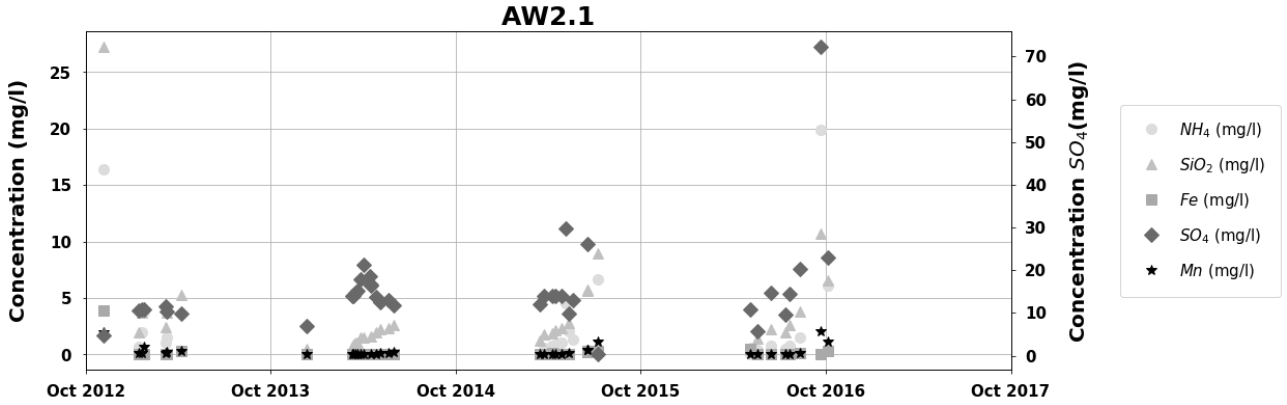

Figure 14.7: Concentrations of NH_4, SiO_2, Fe, SO_4, and Mn in water recovered through AW2-S1.

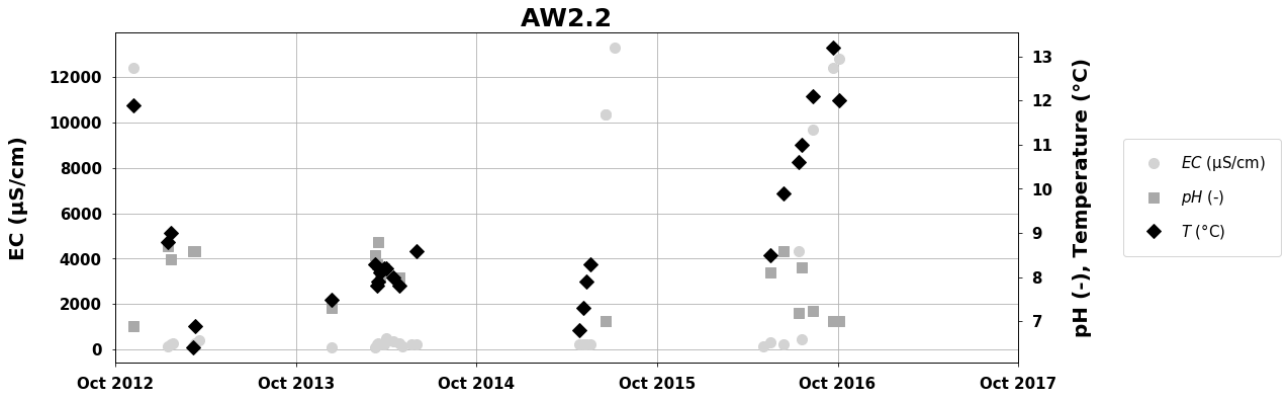

Figure 14.8: Electrical conductivity (EC in µS/cm), pH (-), and temperature (Temp in °C) of water recovered through AW2-S2.

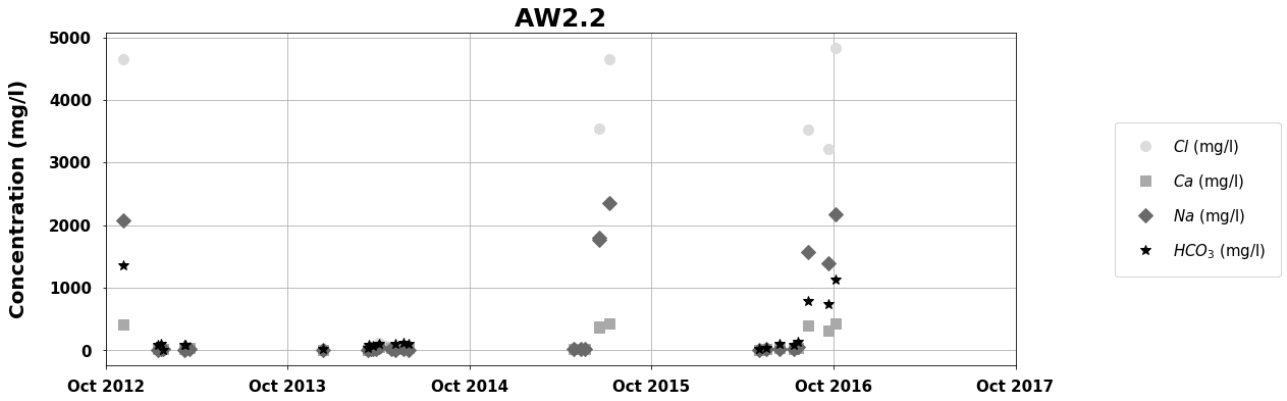

Figure 14.9: Concentrations of Cl, Ca, Na, and HCO_3 in water recovered through AW2-S2.

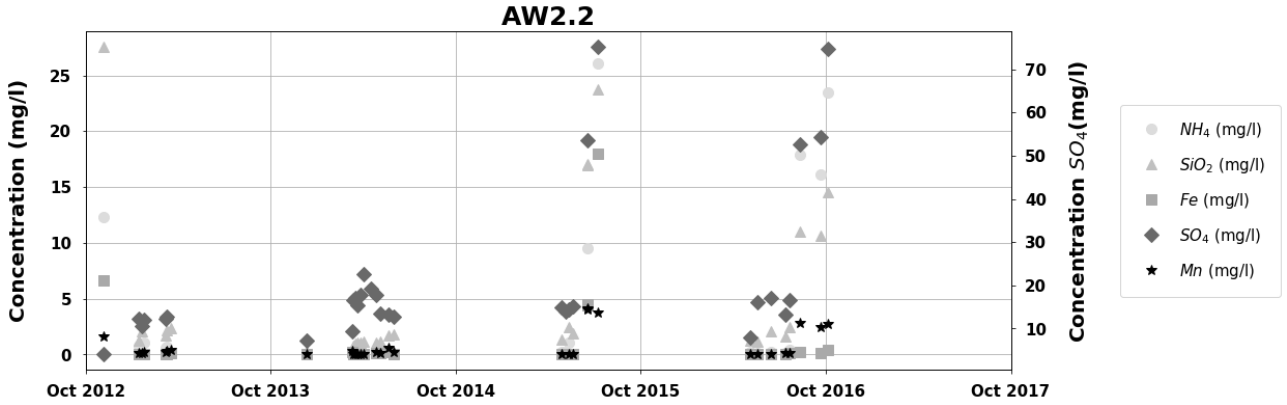

Figure 14.10: Concentrations of NH_4, SiO_2, Fe, SO_4, and Mn in water recovered through AW2-S2.

14.4. Water quality analysis: recovered brackish water (AW1.3 and AW2.3)

The brackish water that feeds the ASRRO system while the deepest wells work as a 'Freshkeeper' typically has a low salinity at the start, which increases as the season

continues. Later in the recovery season, also Fe and Mn can attain high concentration here.

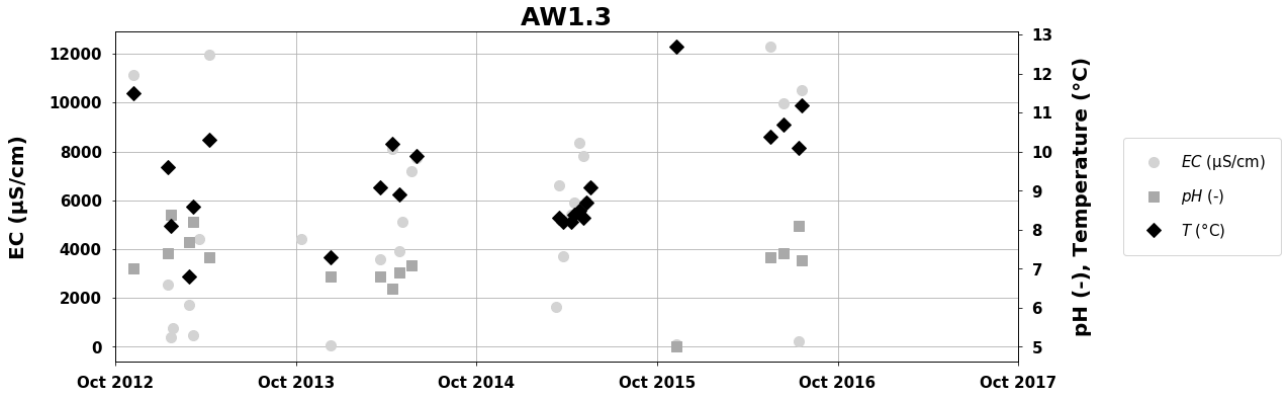

Figure 14.11: Electrical conductivity (EC in µS/cm), pH (-), and temperature (Temp in °C) of water observed at AW1-S3.

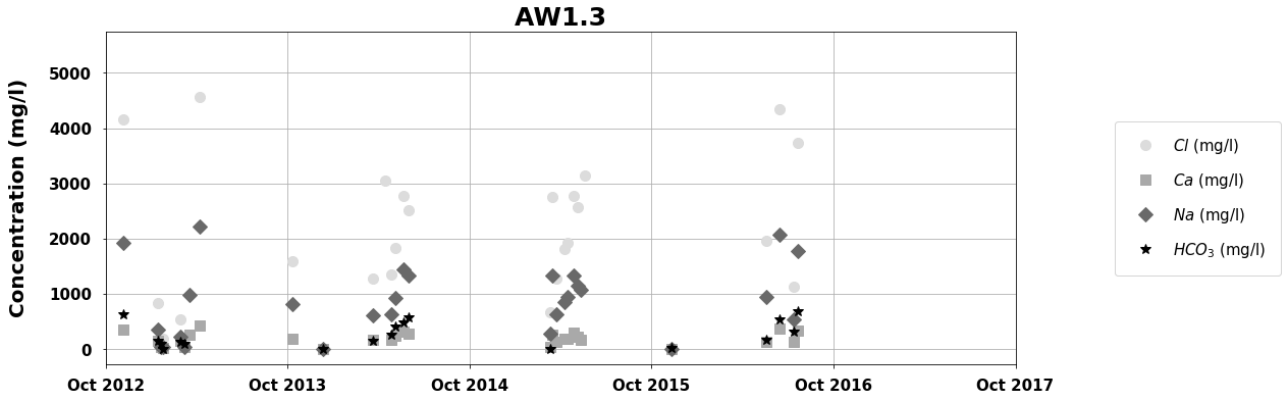

Figure 14.12: Concentrations of Cl, Ca, Na, and HCO_3 in water observed at AW1-S3.

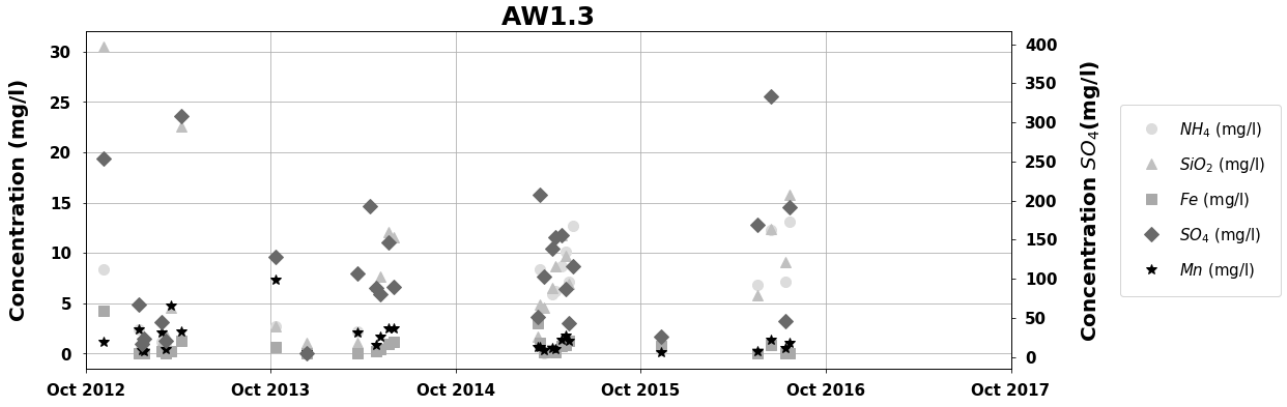

Figure 14.13: Concentrations of NH_4, SiO_2, Fe, SO_4, and Mn in water observed at AW1-S3.

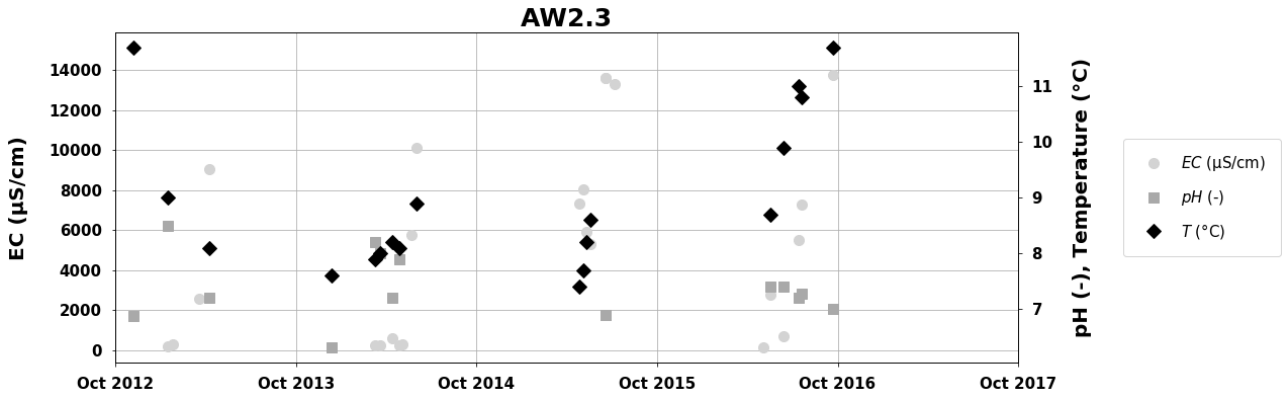

Figure 14.14: Electrical conductivity (EC in µS/cm), pH (-), and temperature (Temp in °C) of water observed at AW2-S3.

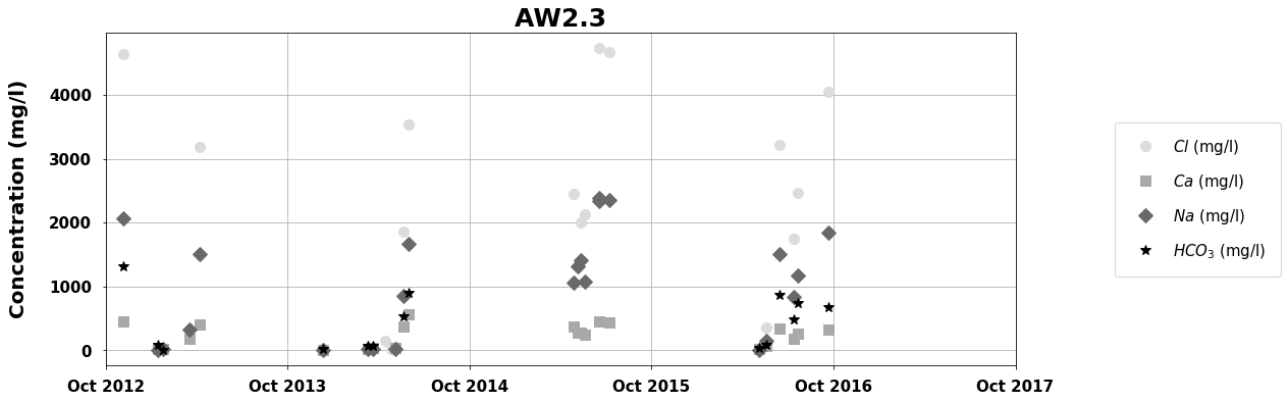

Figure 14.15: Concentrations of Cl, Ca, Na, and HCO_3 in water observed at AW2-S3.

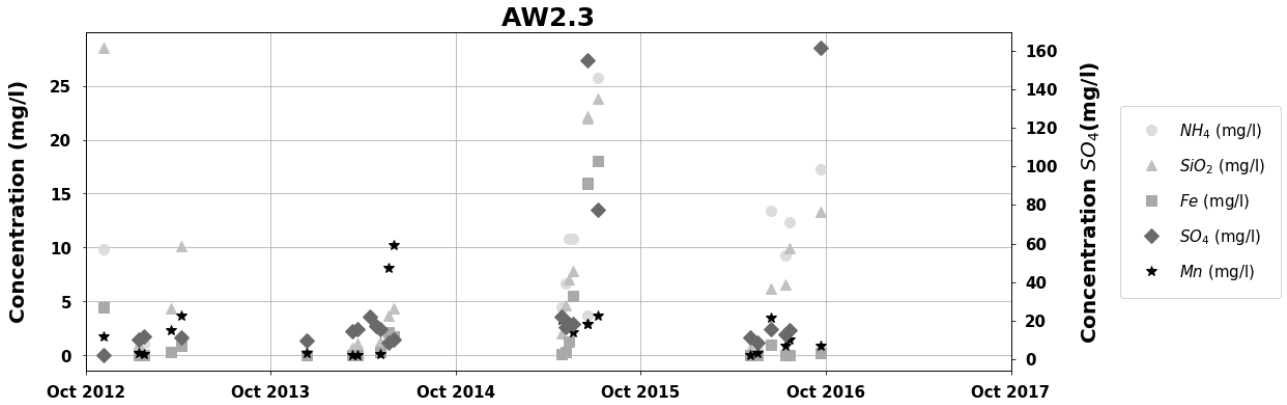

Figure 14.16: Concentrations of NH_4, SiO_2, Fe, SO_4, and Mn in water observed at AW2-S3.

14.5. Geophysical measurements: EM-39

Geophysical logging of the subsurface with EM-39 provided detailed information about the local (MW1, MW2, and MW3) changes at the interface of freshwater and saltwater (Figure 14.17 and Figure 14.18). Based on the results, it can be concluded that:

1. The coarser fractions of the aquifer are freshened first as a result of the infiltration of freshwater.
2. The clayey aquitard does not freshen yet, or very slowly;
3. Freshening of the aquifer also occurs up to MW3, located at a distance of 40 m from the ASR-well.
4. Freshwater remained present at the top of the target aquifer and to a lesser extent at the bottom of the aquifer. This is presumably due to the buoyancy effect.
5. During recovery, freshwater remains present in the aquifer top, forming a horizontal freshwater barrier.
6. Every year, the target aquifer becomes more fresh because the volume of unrecovered freshwater increases after subsequent ASR-cycles.

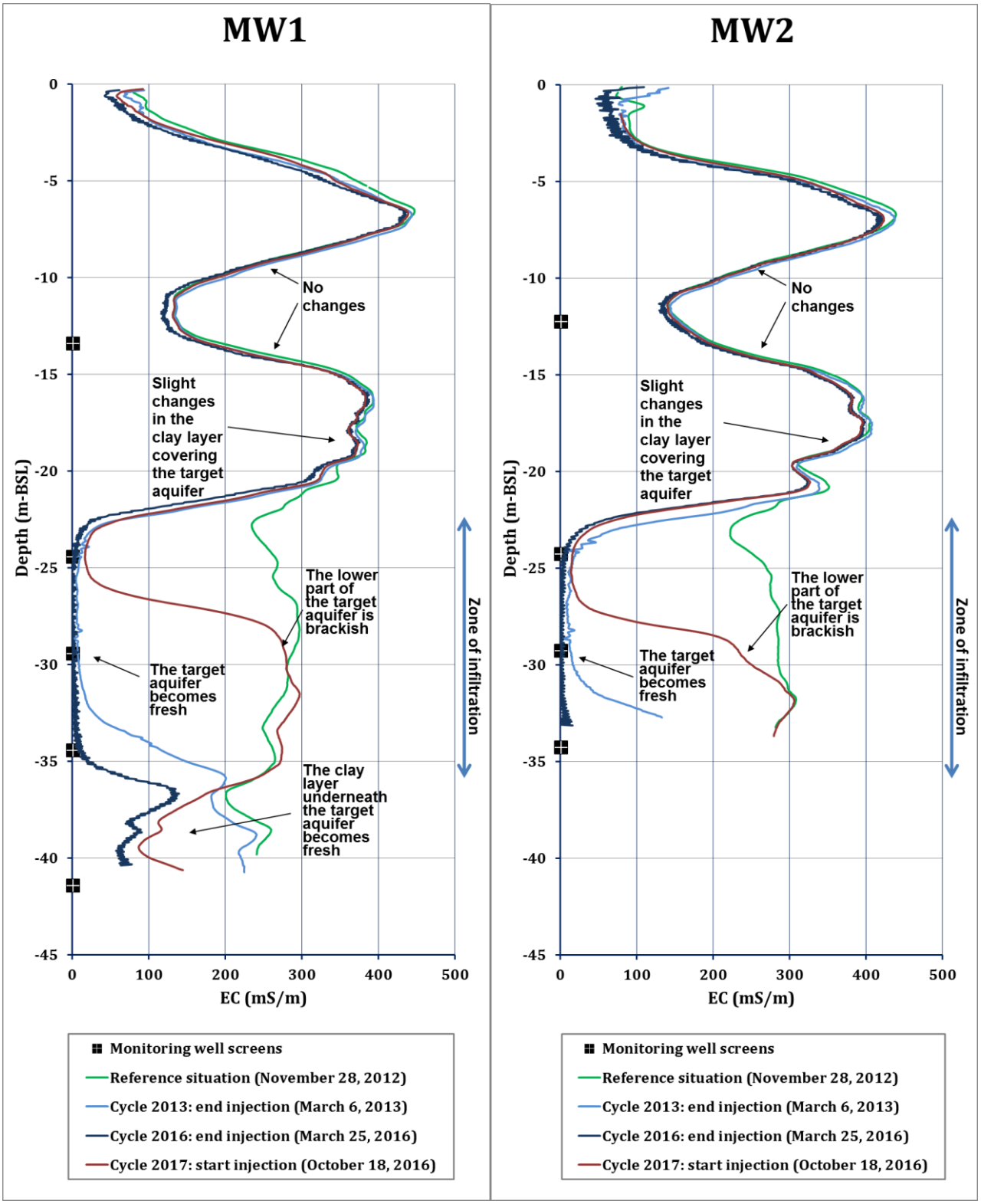

Figure 14.17: Conductivity profile (EC [mS/m] vs. Depth [m BSL]) measured in MW1 (left) and MW2 (right) during different phases of the ASR operation in Westland.

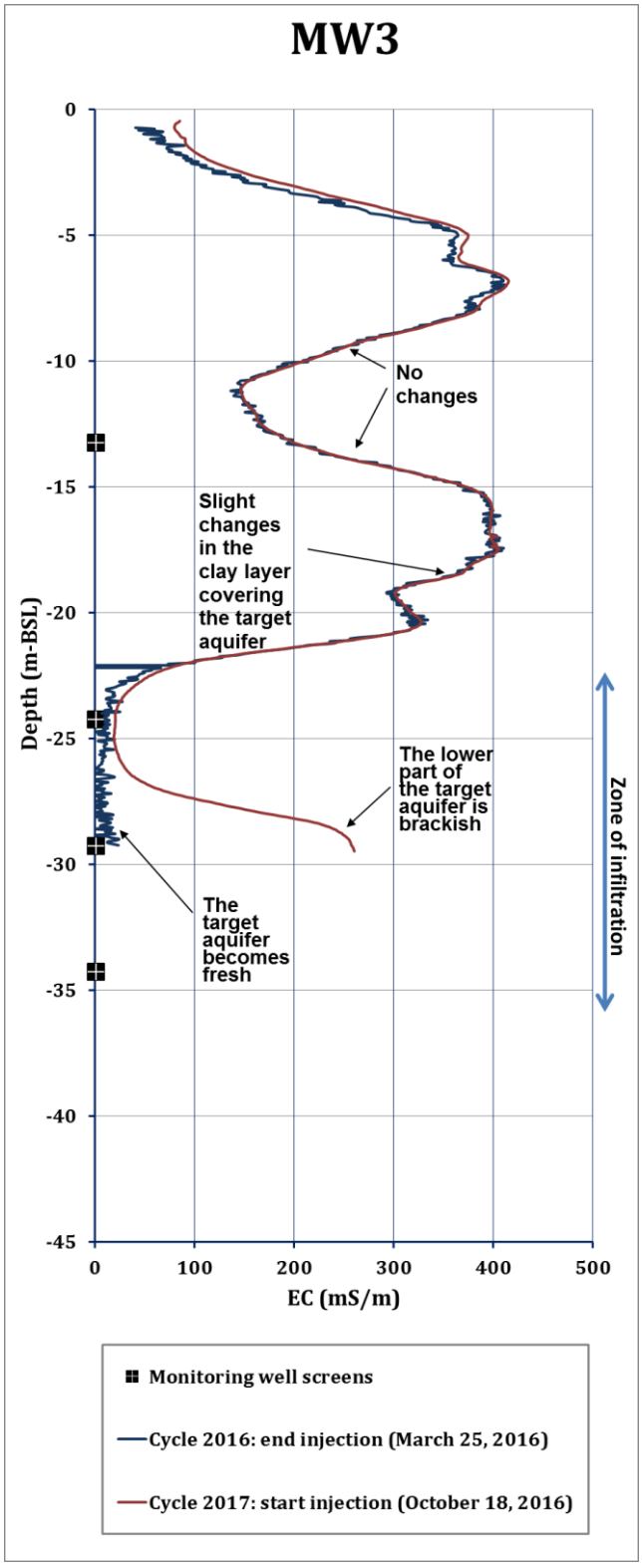

Figure 14.18: Conductivity profile (EC [mS/m] vs. Depth [m-BSL]) measured in MW3 during different phases of the ASR operation in Westland.

15. Results: Modelling

During finalisation of this report, the complex SEAWAT groundwater model of the Westland ASR-site between 2012 and 2017 was still running (requires runtime of multiple weeks). These results will be reported later.

In earlier reports (Zuurbier and Paalman, 2014; Zuurbier and Stuyfzand, 2017), the modelling of the first two cycles was reported. Here, it was shown that leakage of saltwater from the deeper Aquifer 2 disturbed the recovery of the infiltrated rainwater (Figure 15.1). Recovery efficiencies remained therefore <25%, whereas they would be 30-40% without the borehole leakage (Figure 15.2).

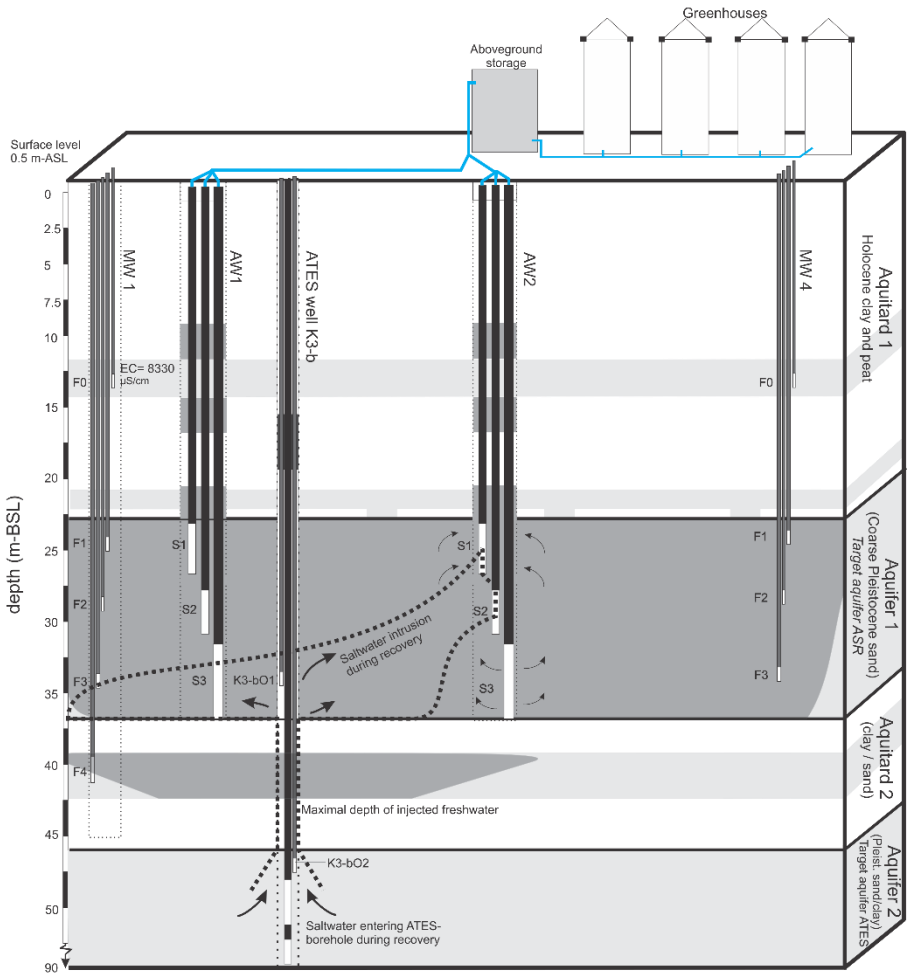

Figure 15.1: Leakage of deeper saltwater via a close-by borehole during recovery, salinizing the ASR wells.

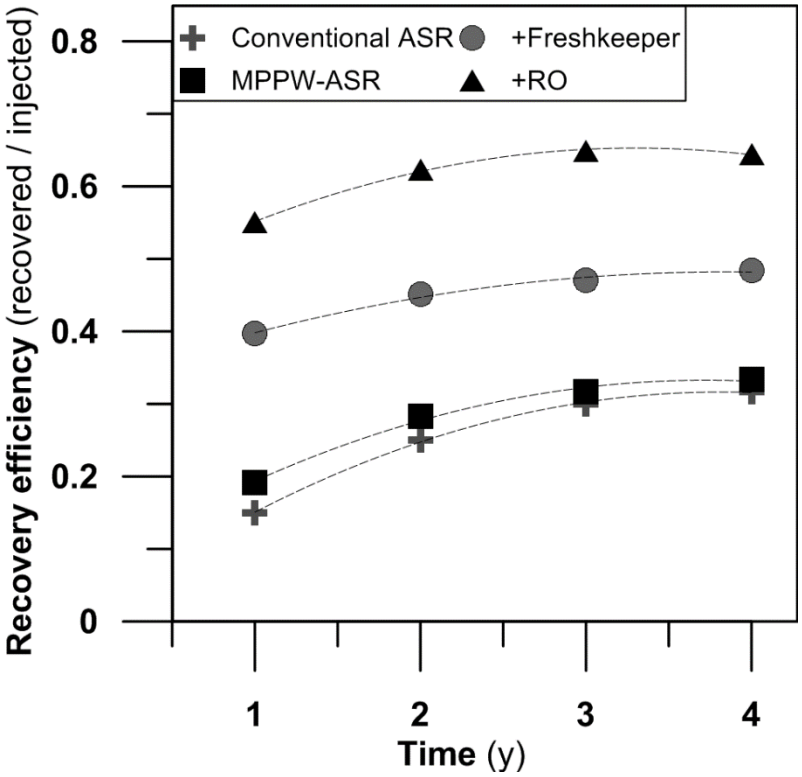

Figure 15.2: Recovery efficiencies of the Westland ASR-Coastal system without the borehole leakage. Scenarios with a conventional ASR well (one well screen), ASR-Coastal ('MPPW-ASR'), addition of a Freshkeeper to delay salinization ('+Freshkeeper'), and with desalination of the abstracted brackish water ('+RO')

16. Automated control unit

At the Westland site, an automated control unit was implemented to increase the efficiency of the ASR-Coastal operation (Figure 16.1), including the use of the Freshkeeper well for brackish water interception. The following aspects were automated:

- Start/stop of the infiltration, based on the level in the rainwater collection tank, using setpoints;
- Backflush of the rapid sand filter (based on reading pressure sensors inlet/outlet);
- Abstraction rate of the Freshkeeper wells (AW1.3 and AW2.3) using frequency-controlled pumps. The abstraction rate of AW2.3 was based on the EC read at AW2.2 (the deepest well screen for freshwater recovery). AW1.3 automatically operated with a fixed rate during abstraction to intercept the deeper saltwater leaking via an old borehole;
- Daily upload of all pumping data via ftp to feed the dashboards.

In April 2017, this program was tested during recovery in a dry spell. It was found that:

- the automated control unit functioned as planned and correctly increased the interception below the recovery by the Freshkeeper, as marked by the abstracted volume at AW2.3, which increased during the recovery phase due to the encroachment of more saline groundwater (Figure 16.2);
- frequent alternations in pumping rate due to variations in EC were not occurring: changes in EC are slow enough to react to;
- the automated control unit kept abstracting once the maximum EC in the recovered water was exceeded, despite giving an alarm. The automated control unit was therefore modified such that recovery will be ceased upon exceedance of the maximum EC;
- after implementing the automated control unit, manual operation of the abstraction pumps was not possible, but is required for maintenance, sampling, etc.

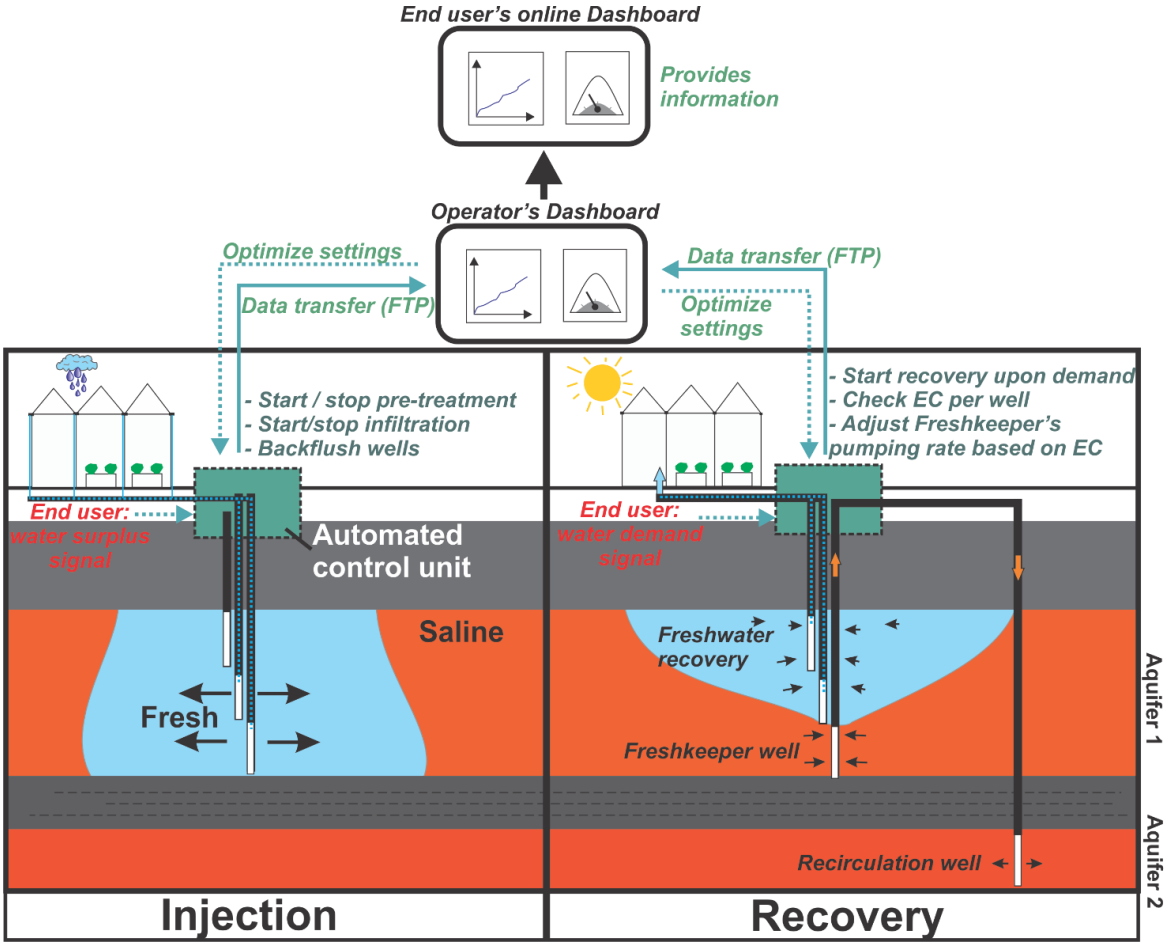

Figure 16.1: Automated control unit implemented at the ASR-Coastal site Westland

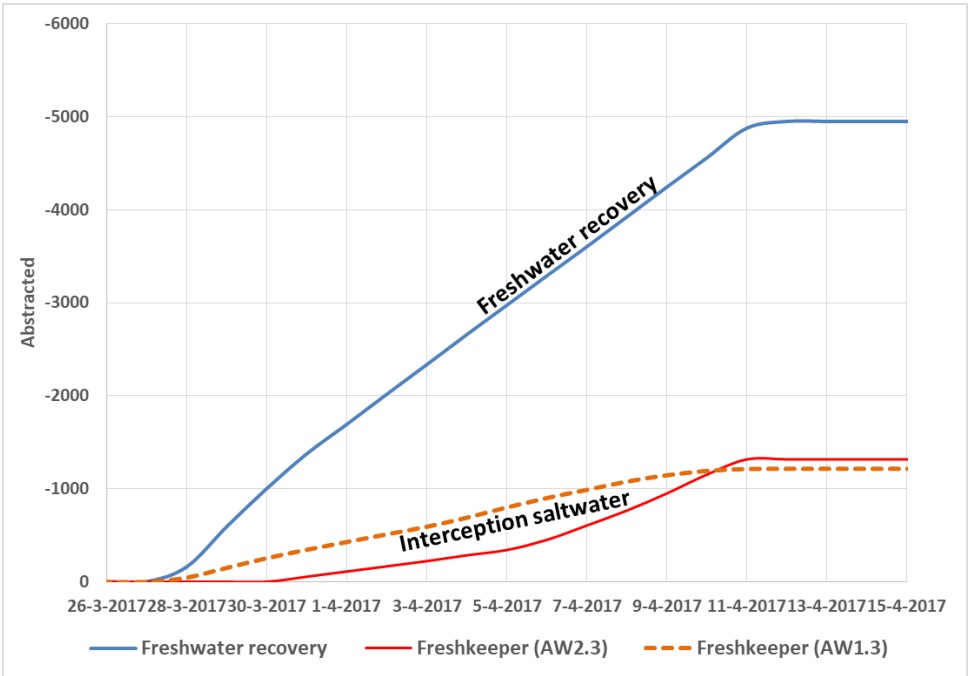

Figure 16.2: Production of freshwater (AW2.1, AW2.2) and interception of saltwater with the freshkeepers (AW1.3, AW2.3) during test phase of the automated control unit

17. Pre-treatment and well clogging

17.1. Functioning of the pre-treatment

At the Westland site, the slow sand-filter was cleaned three times between 2012 and 2017. This was done by manually removing the accumulated fine particles and organic matter (‘schmutzdecke’) on top of the sand. This was done by simply displacing this material to the sides of the sand filter bed with a rake.

During long stand-still periods (summer, dry spells), water was recirculated over the sand filter. Especially in summer, the schmutzdecke degraded under absence of fresh rainwater added to the filter. Additionally, it was found that the floater box (Figure 17.1) and the distribution system suffered from biofouling in these summer periods, more than at the Nootdorp ASR-Coastal site (which was also infiltrating in summer periods).

Figure 17.1: Biogrowth in the floater box at ASR-Coastal site Westland

17.2. Condition of the ASR wells

In general, the ASR wells maintained their capacity, except for the first weeks of infiltration at the end of the summer, after many months without infiltration. In these first weeks, a rapid decrease in infiltration capacity was generally observed, despite regular backflushes of the ASR well (Figure 17.2).

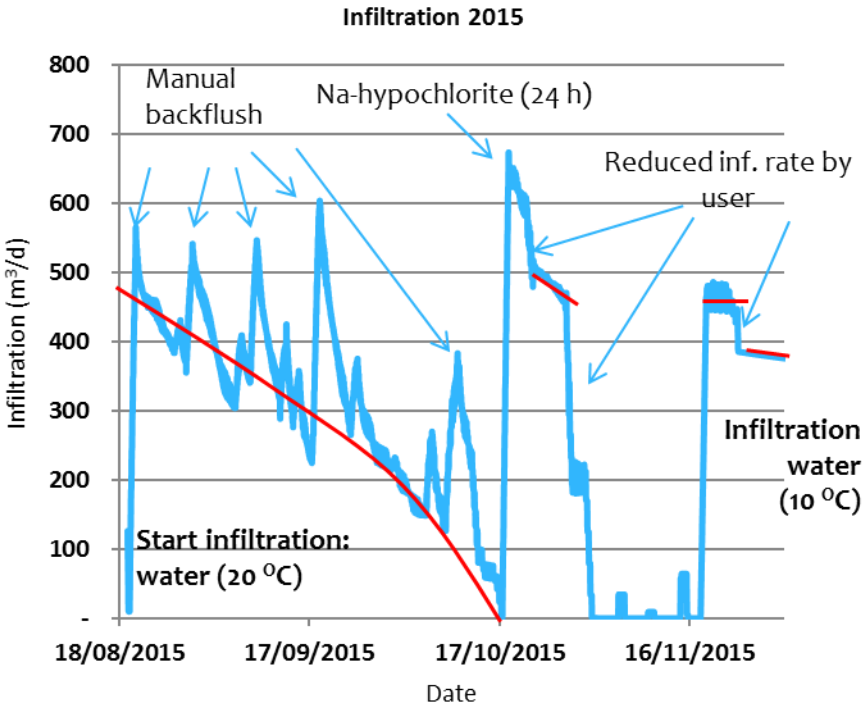

Figure 17.2: Infiltration rate of the ASR wells (AW1, AW2 (summed capacity) at the Westland site: start season 2015/2016.

Treatment with 120 L Na-hypochlorite (12.5%) was required to restore the (constant) infiltration capacity of the wells. The following strategy was thereby applied:

1. Mixing of 20 L Na-hypochlorite with around 1.5 m^3 of infiltration water in the floater box + standpipe;
2. Infiltration of this water at one selected well layer at the time;
3. Infiltration of clean water for around 30 seconds to push the Na-hypochlorite completely into the infiltration well;
4. 24 hours of stand-still;
5. Start of abstraction with the maximum pumping rate. Water pumped to waste;
6. 2 hours of frequent alternations: infiltration / recovery.

Upon on this treatment, the whole infiltration system was clearly cleaner (Figure 17.3) and the first water that was abstracted had a very high turbidity (Figure 17.4). After the treatment, the infiltration rate remained significantly higher and virtually constant (especially in the winter season), even without backflushing the wells (Figure 17.2). The

results suggest that due to a high biological activity (and high temperature) in the water and a reduced functionality of the slow sand filter after long periods of stand-still make the system vulnerable to clogging at the start of the infiltration season. As a result, yearly cleaning of the infiltration system including the ASR wells may be a requirement. The costs were added to the operational costs (Chapter 18).

Figure 17.3: Floater box during and after the treatment with Na-hypochlorite.

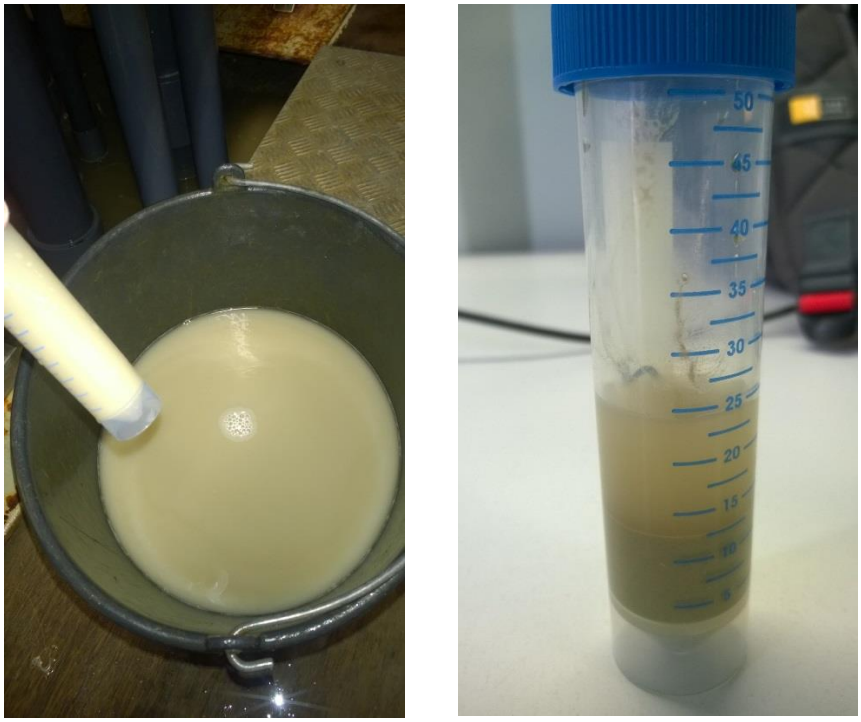

Figure 17.4: Abstracted water during clean pumping after 24 ha stand-still with Na-hypochlorite

18. Cost analysis ASR-Coastal Westland

The costs of the ASR-Coastal system in Westland were analysed, taking into account:

- The true costs required to build the current installation;
- National subsidies for investment in sustainable technologies like ASR (MIA/Vamil);
- Operational and energy costs;
- Depreciation (in 10 years);
- Re-investments to keep the scheme running (pumps).
- Tax shield: as a consequence of depreciation, less profit tax has to be payed;
- Financing (incl. interest);
- Costs discounted at a discount rate of 3%;
- An economic lifespan of 20 years (wells, pipelines, central control unit should make this without re-investments);
- The total production of freshwater during the lifespan,

The alternative (an aboveground basin) was also analysed with the same model, taking into account the loss of net income by the claim on aboveground agricultural land (greenhouse) into account (

Table 18.1).

It was found that the ASR-Coastal system produces cheaper water (Table 18.2) than the current alternative for storage (above ground basins), which is primarily due to the longer lifetime and the absence of loss of production by a spatial claim. Initial investments and operational costs are higher, compared to the alternative. Piped river water is available from the drinking water distribution system, but is also more expensive per m^3 and relatively saline (39 mg/l Na and 58 mg/l Cl).

The business case for ASR-Coastal Westland would have been a lot better, if the recovery efficiency wouldn't be as low as 25% due to the borehole leakage close to the ASR wells. Based on previous models, this set-up would then attain a recovery efficiency of around 40% and the cost price would decrease to 0.54 eur/m^3.

Table 18.1: Input for ASR-Coastal Westland cost analysis

Parameter	Unit	Input
Freshmaker		
Lifespan ASR system	yr	20
Yearly recovery	m^3/yr	15 000
Yearly infiltration	m^3/yr	60 000
Depreciation period	yr	10
Discount rate	%	3
Energy price	€/kWh	0.16
Maintenance/monitoring	€/yr	1900
Initial investment	€	235 000
Basin		
Lifespan Basin	yr	15
Depreciation period	yr	10
Loss of net income	€/m^2	3.6
Basin volume	m^3	15 000
Basin surface	m^2	6 650
Costs for realisation	€/m^3	6.15
Loan duration	yr	5
Interest	%	3

Table 18.2: Cost price of the produced irrigation water at the ASR-Coastal Westland site

Water source	ASR-Coastal	Aboveground basin	Piped water
Costs / m^3	0.84	1.63	0.90
Costs / m^3 (without borehole leakage)	0.54		

19. Conclusions ASR-Coastal Nootdorp & Westland

Two ASR-Coastal field sites with distinct characteristics (Table 19.1), but the same basic ASR-Coastal strategy (water could be infiltrated and recovered via various independently operated well screens in different segments of the aquifer to increase the recovery of freshwater) were thoroughly documented during 5-6 years of operation.

The Nootdorp ASR-Coastal system functioned rather smoothly and was always able to supply sufficient irrigation water to the local horticulturist. The required maintenance was limited and the recovered water quality was very constant after Cycle 1 and met the owners demands. With total costs of 0.59 euro/m^3, the ASR-Coastal system provided a significantly cheaper source of high-quality freshwater compared to alternatives. The owner will keep using the system as its only source for irrigation water.

The Westland ASR-Coastal system functioned satisfactorily, but clearly suffered from saltwater leakage via a nearby older borehole, which reduced the recovery efficiency from 40% to 22.5%. Therefore, the system was not able to meet the yearly demand of the local horticulturist. Additionally, yearly cleaning of the infiltration system and ASR wells was required at the start-up of the system after long periods without infiltration. Despite these additional obstructions, the total costs were acceptable (0.84 euro/m^3). The owner will keep using the system as additional supply, together with aboveground rainwater storage and brackish water reverse osmosis.

The two sites show that the ASR-Coastal technique is mature and robust, and can be further implemented. It also shows that local conditions and mode of operation can lead to differences in performance and operational costs and should be taken into account.

Table 19.1: Characteristics of ASR-Coastal Nootdorp and Westland

Characteristic	Nootdorp	Westland
Cl in target aquifer	150 – 1 100 mg/l	~4 500 mg/l
Thickness target aquifer	28 m	17 m
Specific conditions	Clayey intervals half-way the aquifer	Leakage of deep saltwater via an older borehole
# wells	1	2
# layer per well	4	3
Freshkeeper	No	Yes
Infiltration	Dynamic, every rainfall event ~14 000 m^3/yr	Only August – March ~7 200 m^3/yr
Recovery	Dynamic, whenever any demand 7 500 – 16 000 m^3/yr	Only March – August 28 000 – 70 000 m^3/yr
Recovery efficiency	53.4%	22.5%
Pre-treatment	Slow sand filtration	Slow sand filtration
Required well cleaning	None	Yearly cleaning with Na-hypochlorite

20. References

Bear, J., 1972. Dynamics of fluids in porous media. American Elsevier, New York, U.S.A.

Busschers, F.S. et al., 2005. Sedimentary architecture and optical dating of Middle and Late Pleistocene Rhine-Meuse deposits – fluvial response to climate change, sea-level fluctuation and glaciation. Netherlands Journal of Geosciences, 84(1): 25-41.

Konert, M., Vandenberghe, J., 1997. Comparison of laser grain size analysis with pipette and sieve analysis: a solution for the underestimation of the clay fraction. Sedimentology, 44(3): 523-535.

Langevin, C.D., Thorne, D.T., Dausman, A.M., Sukop, M.C., Guo, W., 2007. SEAWAT version 4: a computer program for simulation of multi-species solute and heat transport. In: U.S.G.S. (Ed.), Techniques and Methods, book 6, Reston, Virginia, USA.

McNeill, J.D., Bosnar, M., Snelgrove, J.B., 1990. Technical Note 25: Resolution of an Electromagnetic Borehole logger for Geotechnical and groundwater applications.

Metzger, L.F., Izbicki, J.A., 2013. Electromagnetic-Induction Logging to Monitor Changing Chloride Concentrations. Ground water, 51(1): 108-121.

Mos Grondmechanica, 2006. Interpretation pilot drilling for ATES system grower's association Prominent at Groeneweg-II, Mos Grondmechanica, Rotterdam.

Oele, E. et al., 1983. Surveying The Netherlands: sampling techniques, maps and their implications. Geologie en Mijnbouw, 62: 355-372.

Stuyfzand, P.J., 1993. Hydrochemistry and Hydrology of the Coastal Dune area of the Western Netherlands, Vrije Universiteit, Amsterdam, The Netherlands, 366 pp.

Stuyfzand, P.J., 2008. Base Exchange Indices as Indicators of Salinization or Freshening of (Coastal) Aquifers Saltwater Intrusion Meeting. IFAS Research, Napels, Florida, USA, pp. 262-265.

Zuurbier, K.G., Hartog, N., Stuyfzand, P.J., 2016. Reactive transport impacts on recovered freshwater quality during multiple partially penetrating wells (MPPW-)ASR in a brackish heterogeneous aquifer. Applied Geochemistry, 71: 35-47.

Zuurbier, K.G., Paalman, M., 2014. Field trial aquifer storage and recovery in saline groundwater (Pilot ASR Prominent) (in Dutch), Knowledge for Climate, Utrecht.

Zuurbier, K.G., Stuyfzand, P.J., 2017. Consequences and mitigation of saltwater intrusion induced by short-circuiting during aquifer storage and recovery in a coastal subsurface. Hydrol. Earth Syst. Sci., 21(2): 1173-1188.

Zuurbier, K.G., Zaadnoordijk, W.J., Stuyfzand, P.J., 2014. How multiple partially penetrating wells improve the freshwater recovery of coastal aquifer storage and recovery (ASR) systems: A field and modeling study. Journal of Hydrology, 509(0): 430-441.

21. APPENDIX 1: Water quality analysis: observed groundwater Nootdorp

The hydrogeochemical composition of brackish water observed at the lower two well screens of the ASR-well was monitored in phases when the system had a net recovery, as otherwise young, infiltrated rainwater would be sampled. These well screens were not used for recovery itself, as this would result in an early salinization of the ASR-well by the surrounding brackish groundwater. At AW1.3, this salinization was only observed during sampling in 2013. Between 2015-2017, the well remained fresh. The deeper AW1.4, however, shows clear salinization every spring and summer.

The hydrogeochemical composition of brackish water observed at the well screens of MW1 and MW2 that are situated within the target aquifer was also monitored.

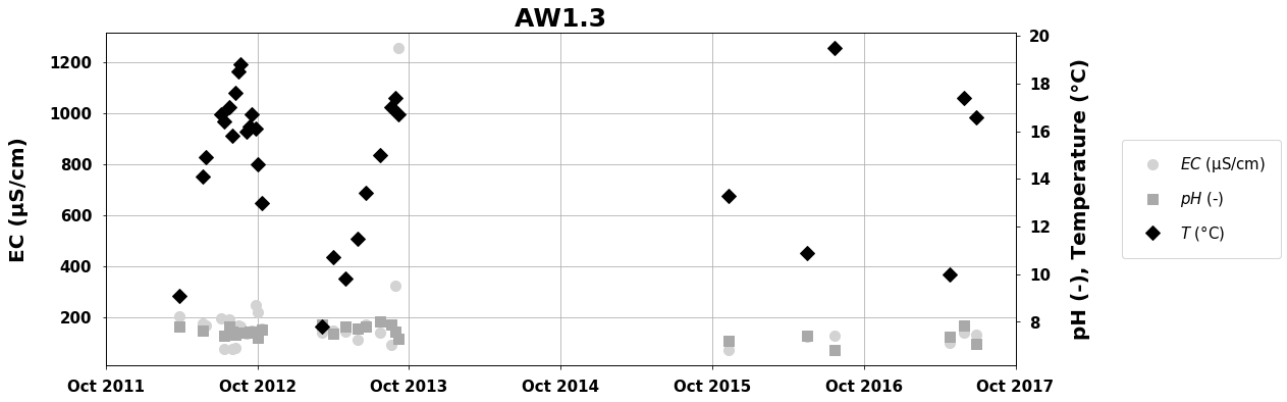

Figure 21.1: Electrical conductivity (EC in µS/cm), pH (-), and temperature (Temp in °C) of water observed at AW3.

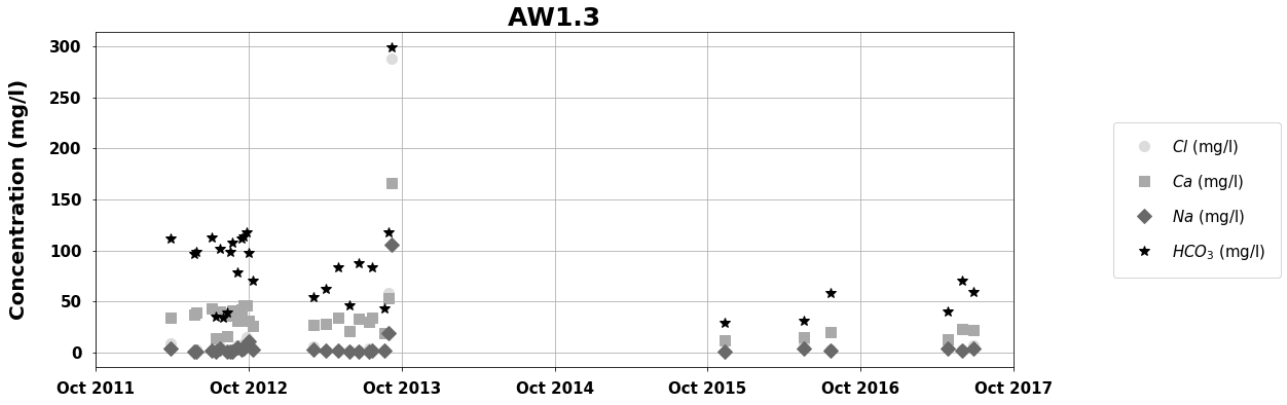

Figure 21.2: Concentrations of Cl, Ca, Na, and HCO_3 in water observed at AW3.

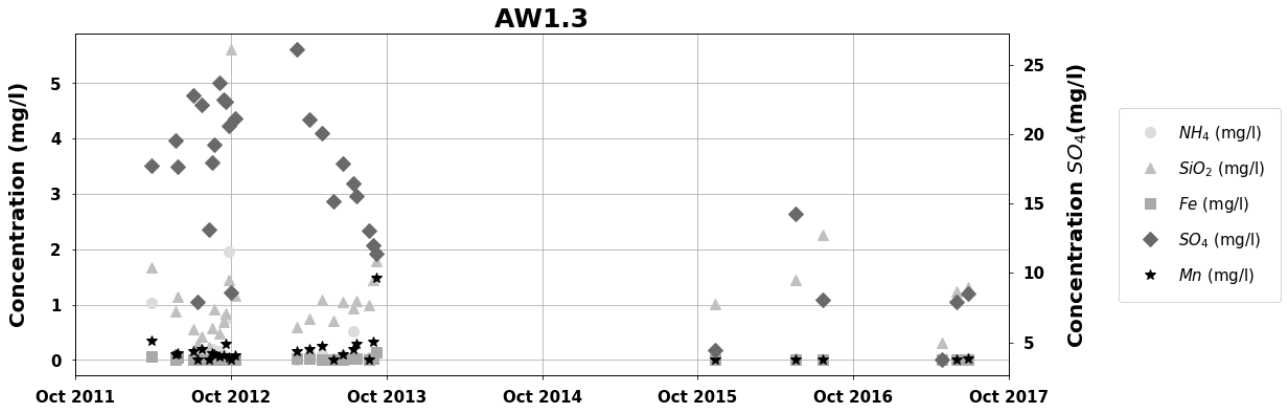

Figure 21.3: Concentrations of NH_4, SiO_2, Fe, SO_4, and Mn in water observed at AW3.

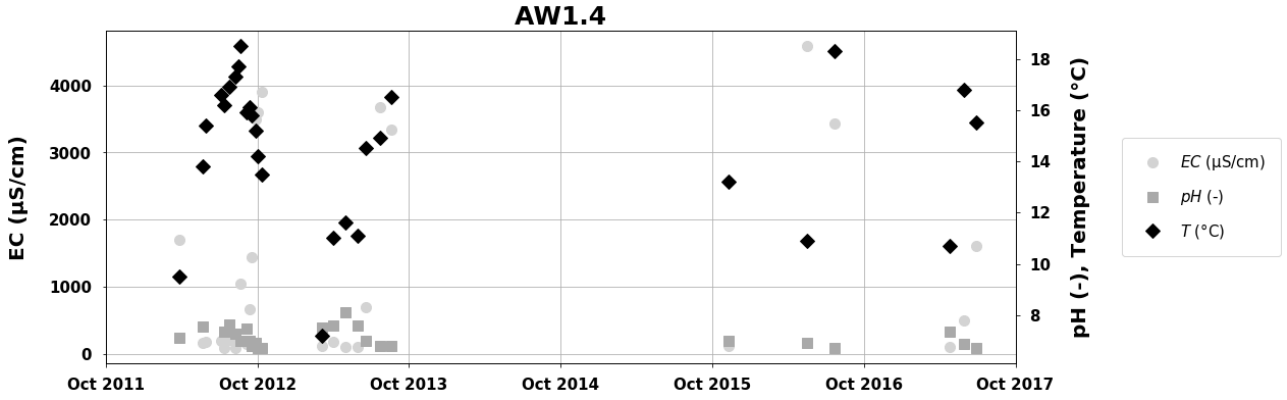

Figure 21.4: Electrical conductivity (EC in µS/cm), pH (-), and temperature (Temp in °C) of water observed at AW4.

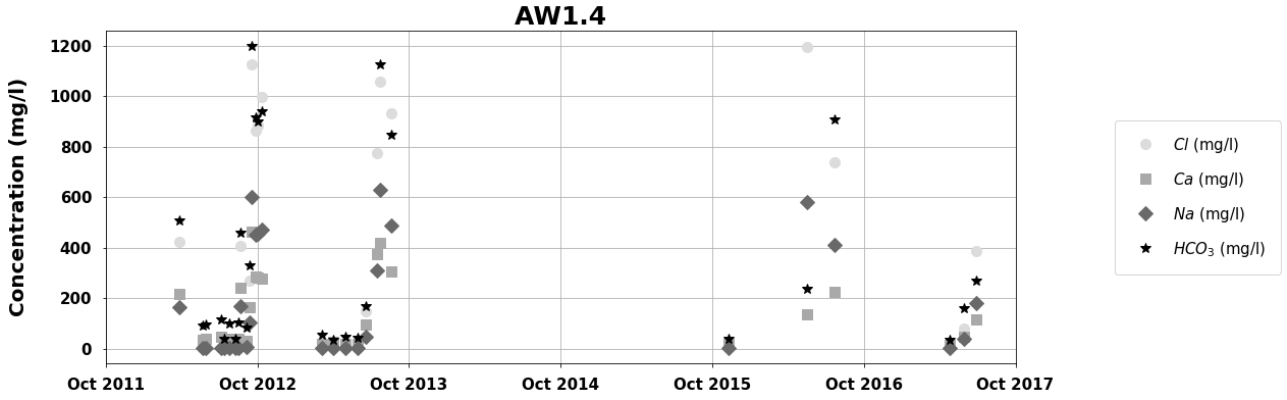

Figure 21.5: Concentrations of Cl, Ca, Na, and HCO_3 in water observed at AW4.

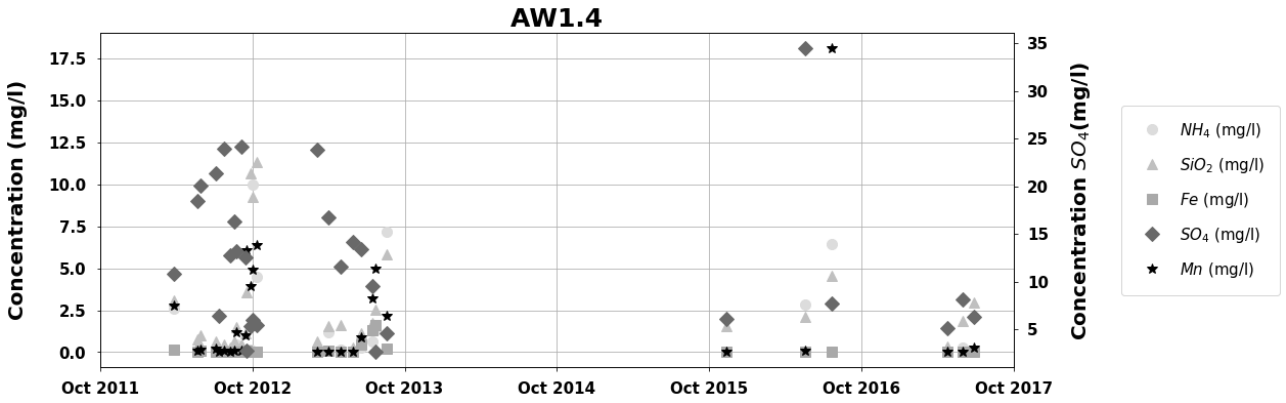

Figure 21.6: Concentrations of NH_4, SiO_2, Fe, SO_4, and Mn in water observed at AW4.

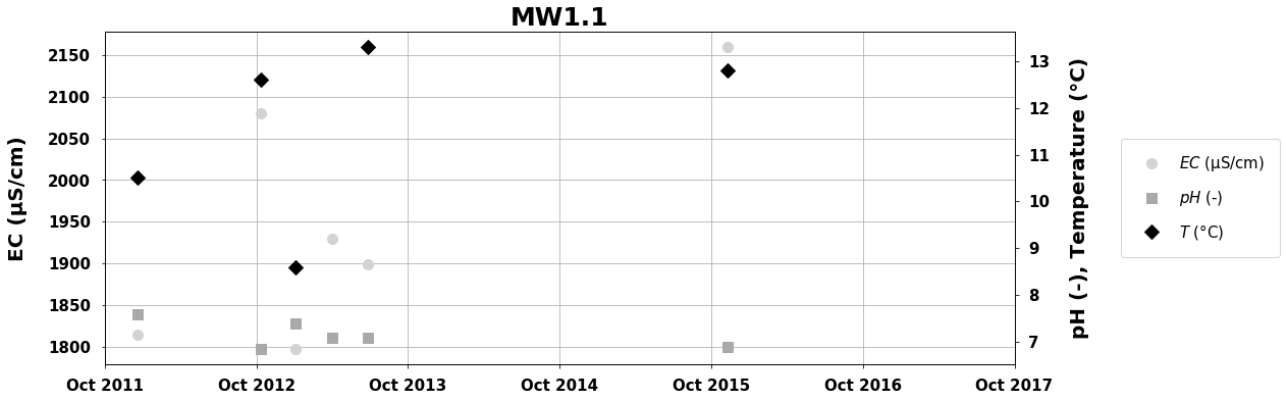

Figure 21.7: Electrical conductivity (EC in µS/cm), pH (-), and temperature (Temp in °C) of water observed at MW1-S1.

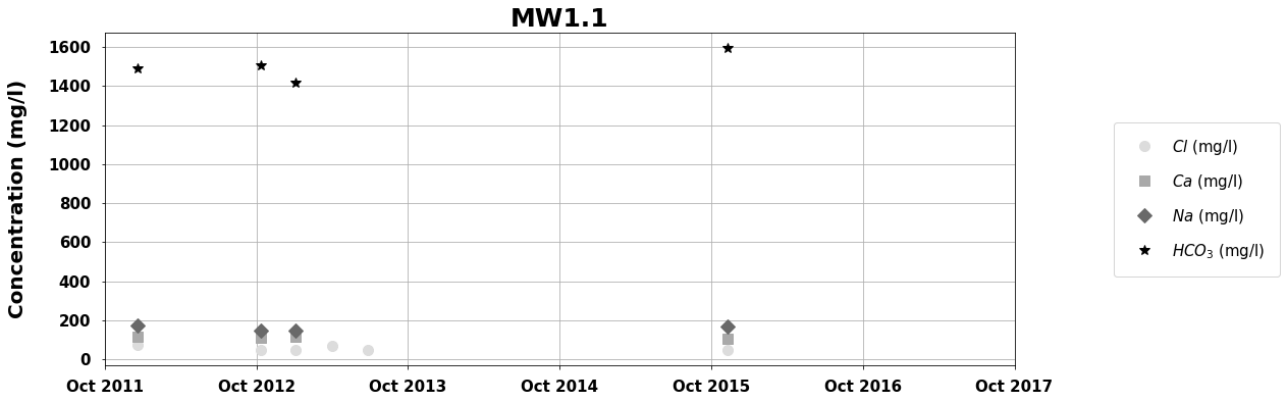

Figure 21.8: Concentrations of Cl, Ca, Na, and HCO_3 in water observed at MW1-S1.

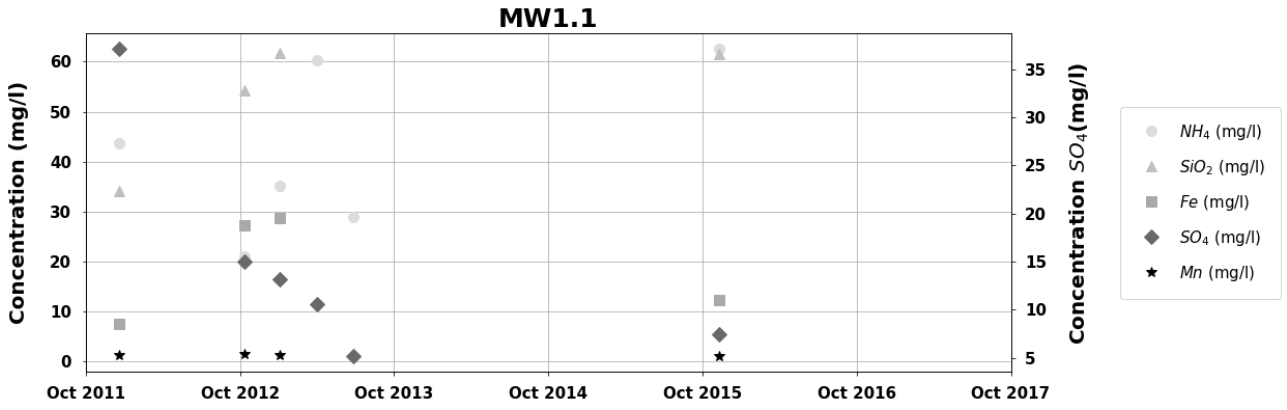

Figure 21.9: Concentrations of NH_4, SiO_2, Fe, SO_4, and Mn in water observed at MW1-S1.

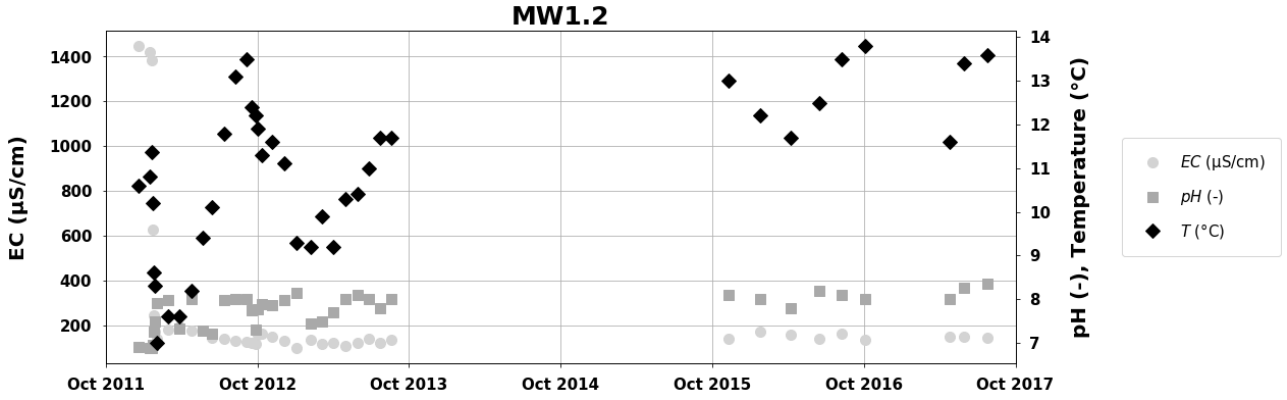

Figure 21.10: Electrical conductivity (EC in µS/cm), pH (-), and temperature (Temp in °C) of water observed at MW1-S2.

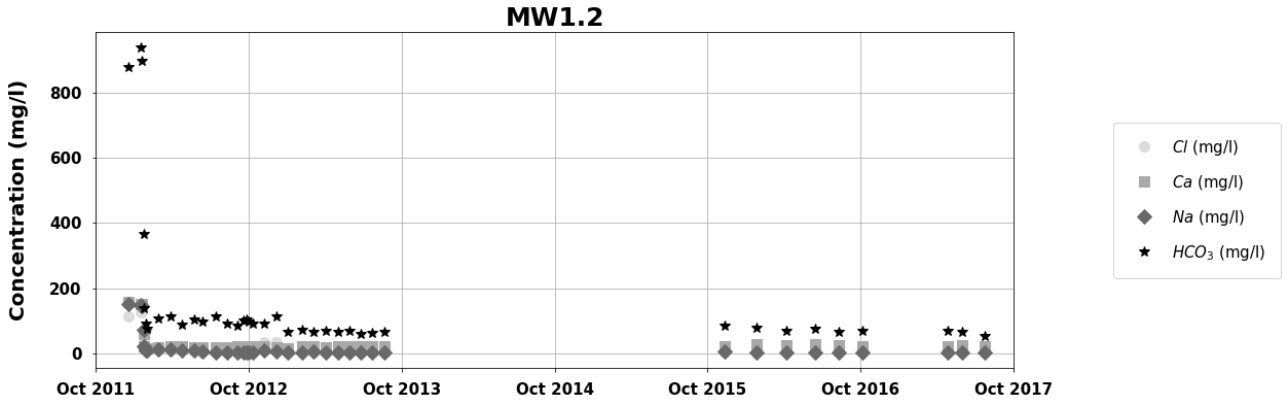

Figure 21.11: Concentrations of Cl, Ca, Na, and HCO_3 in water observed at MW1-S2.

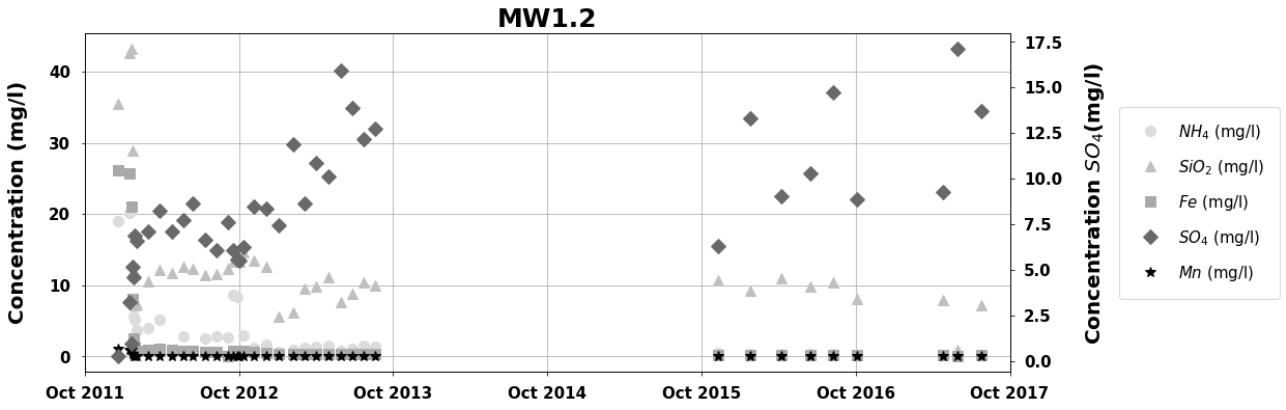

Figure 21.12: Concentrations of NH_4, SiO_2, Fe, SO_4, and Mn in water observed at MW1-S2.

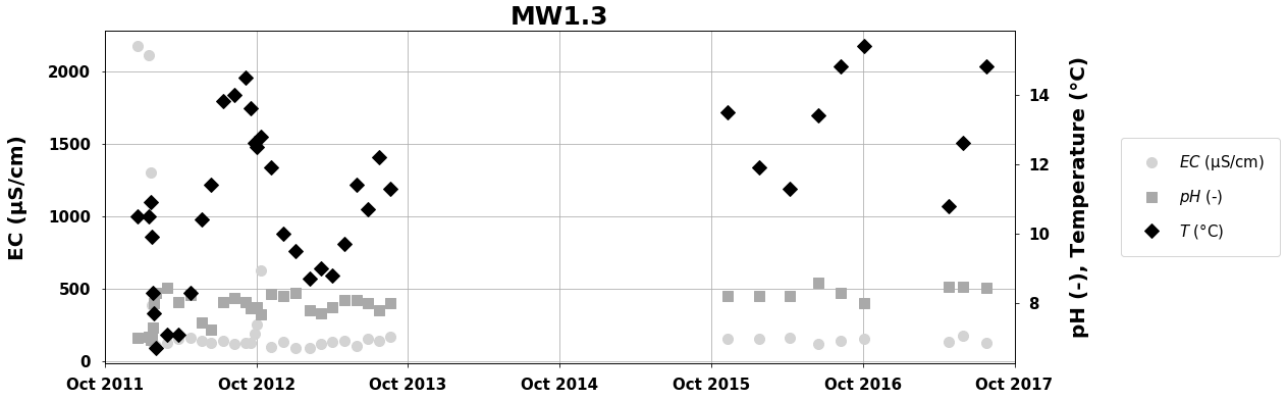

Figure 21.13: Electrical conductivity (EC in µS/cm), pH (-), and temperature (Temp in °C) of water observed at MW1-S3.

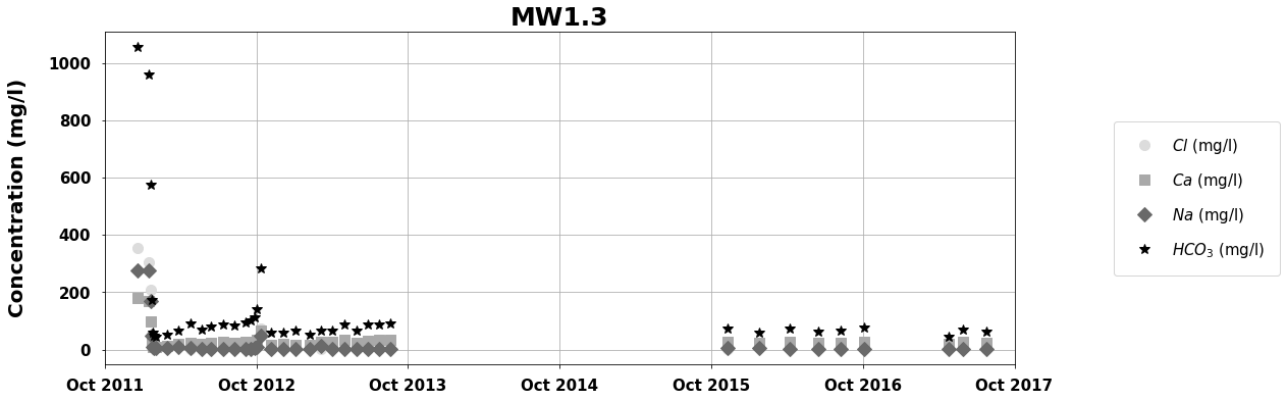

Figure 21.14: Concentrations of Cl, Ca, Na, and HCO_3 in water observed at MW1-S3.

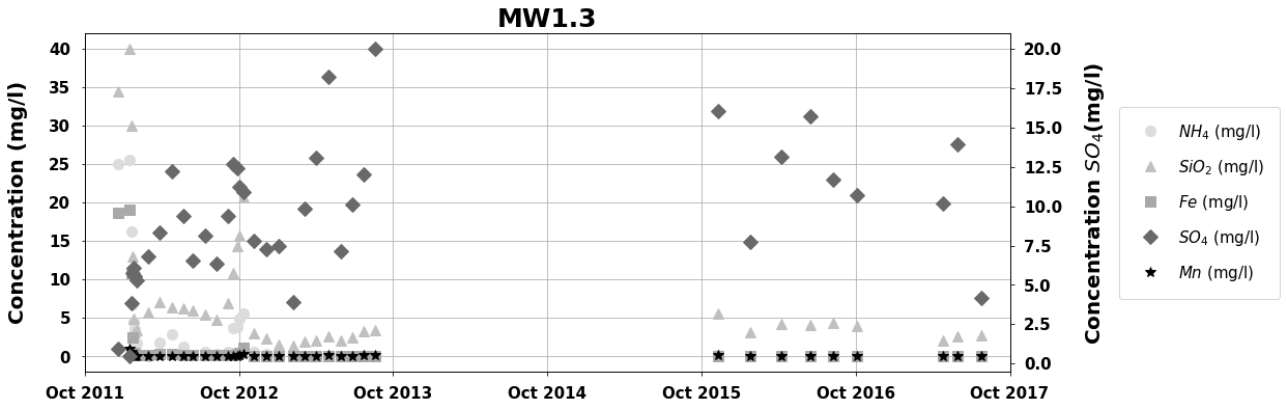

Figure 21.15: Concentrations of NH_4, SiO_2, Fe, SO_4, and Mn in water observed at MW1-S3.

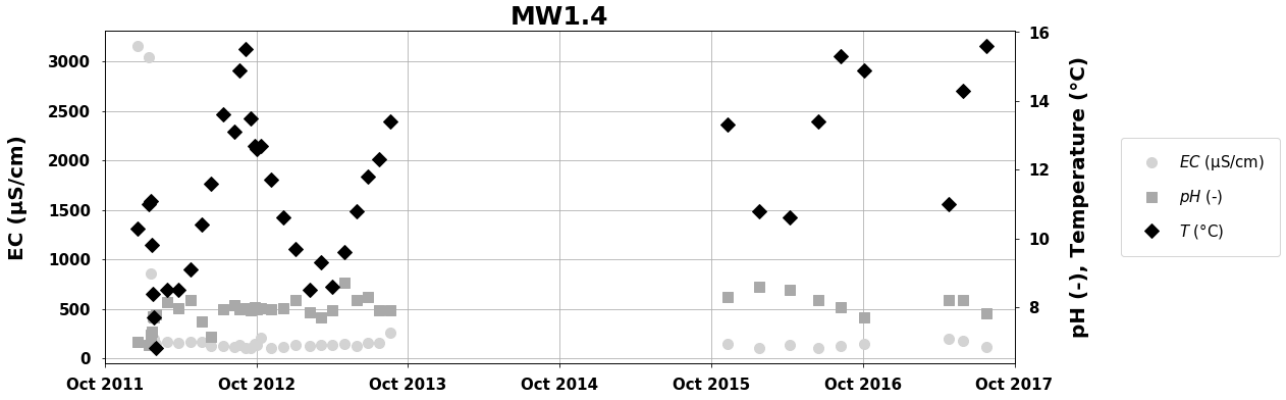

Figure 21.16: Electrical conductivity (EC in µS/cm), pH (-), and temperature (Temp in °C) of water observed at MW1-S4.

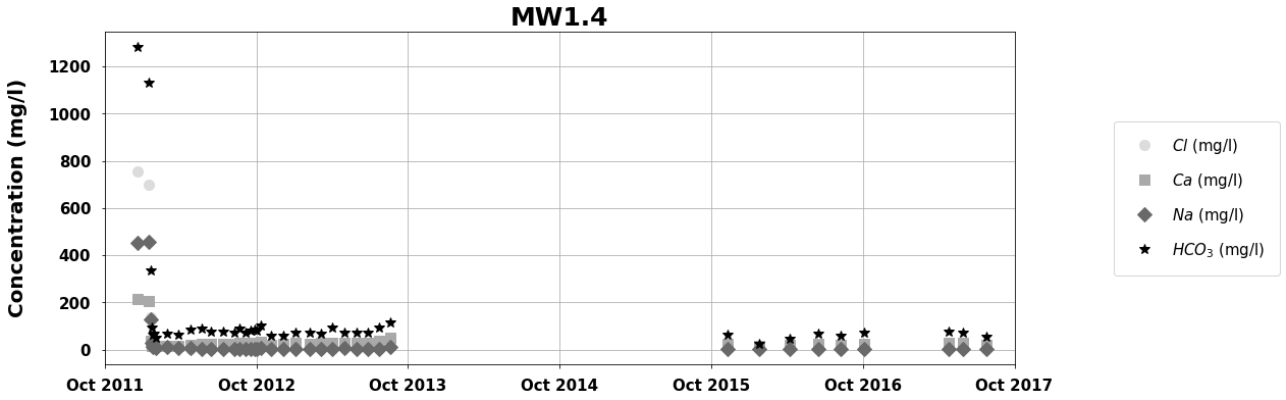

Figure 21.17: Concentrations of Cl, Ca, Na, and HCO_3 in water observed at MW1-S4.

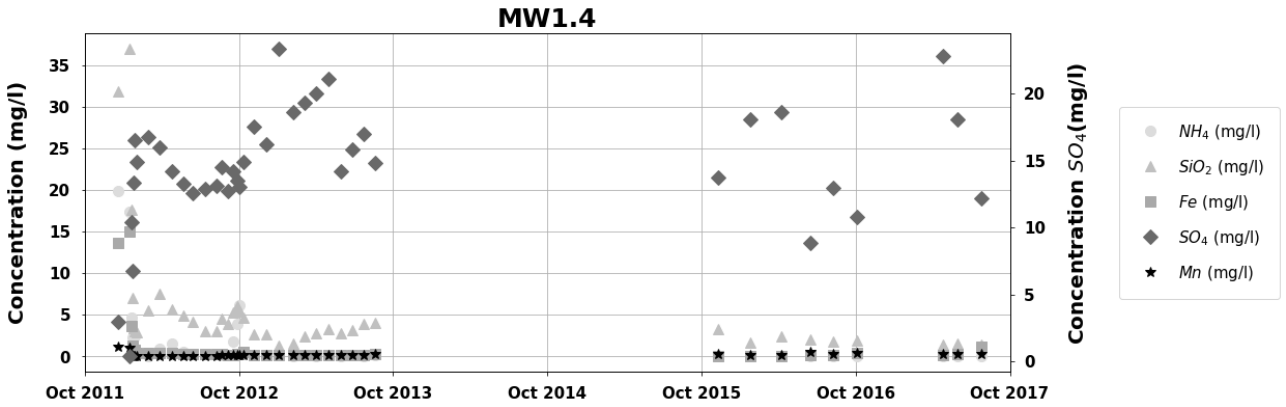

Figure 21.18: Concentrations of NH_4, SiO_2, Fe, SO_4, and Mn in water observed at MW1-S4.

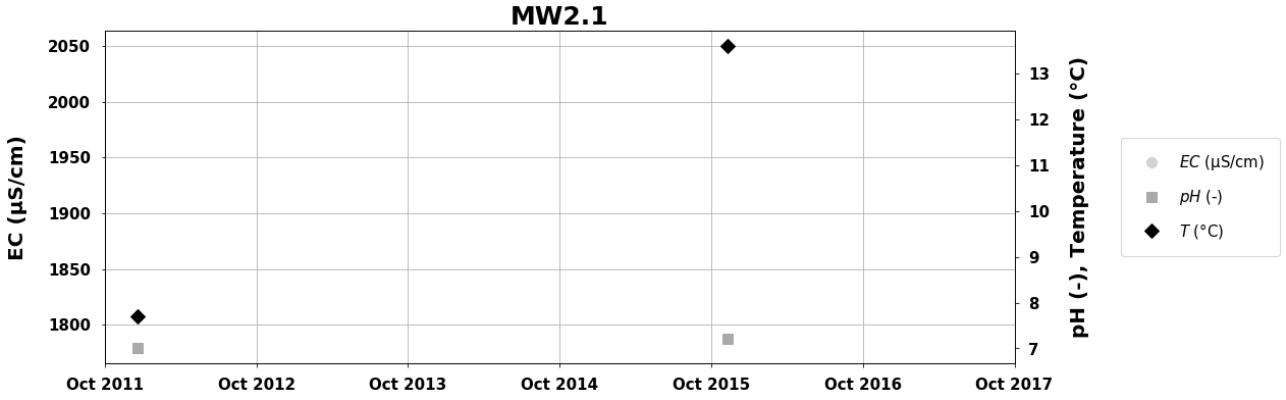

Figure 21.19: Electrical conductivity (EC in µS/cm), pH (-), and temperature (Temp in °C) of water observed at MW2-S1.

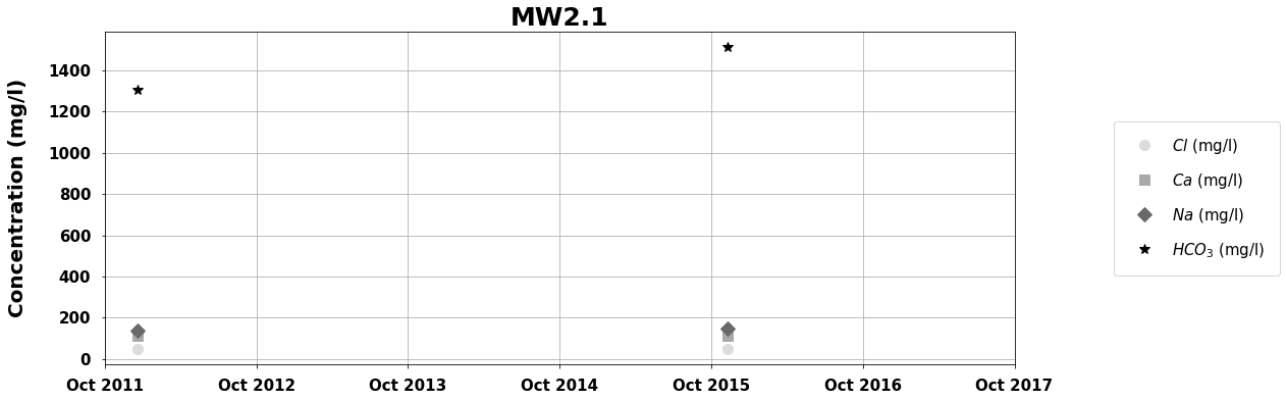

Figure 21.20: Concentrations of Cl, Ca, Na, and HCO_3 in water observed at MW2-S1.

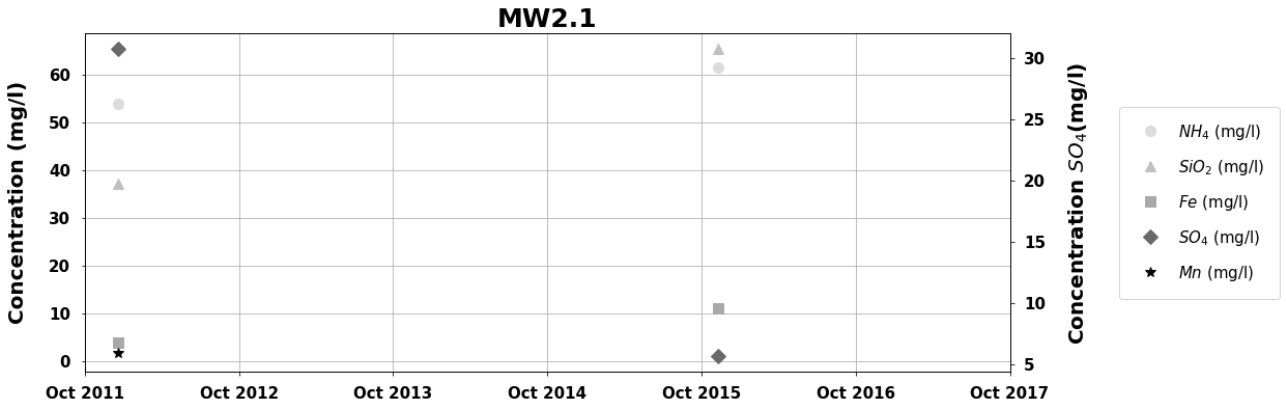

Figure 21.21: Concentrations of NH_4, SiO_2, Fe, SO_4, and Mn in water observed at MW2-S1.

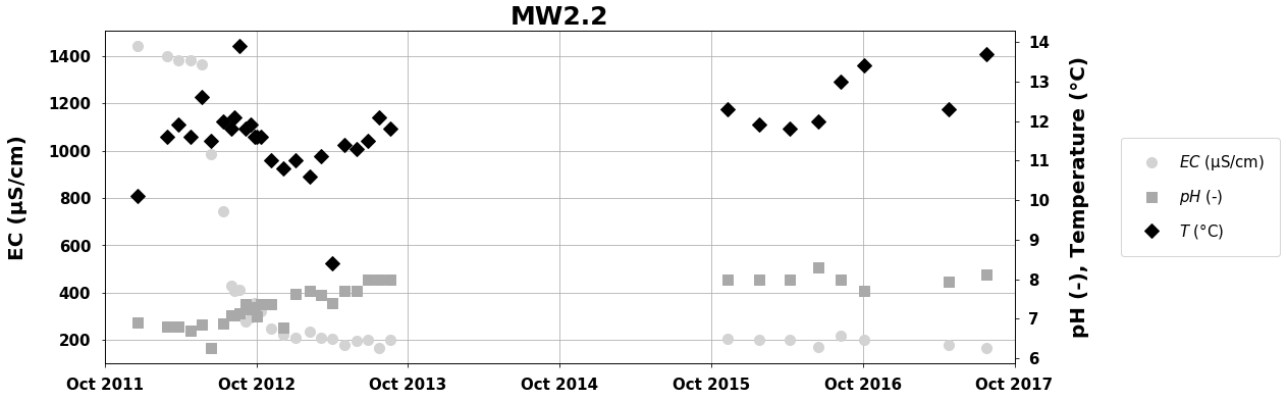

Figure 21.22: Electrical conductivity (EC in µS/cm), pH (-), and temperature (Temp in °C) of water observed at MW2-S2.

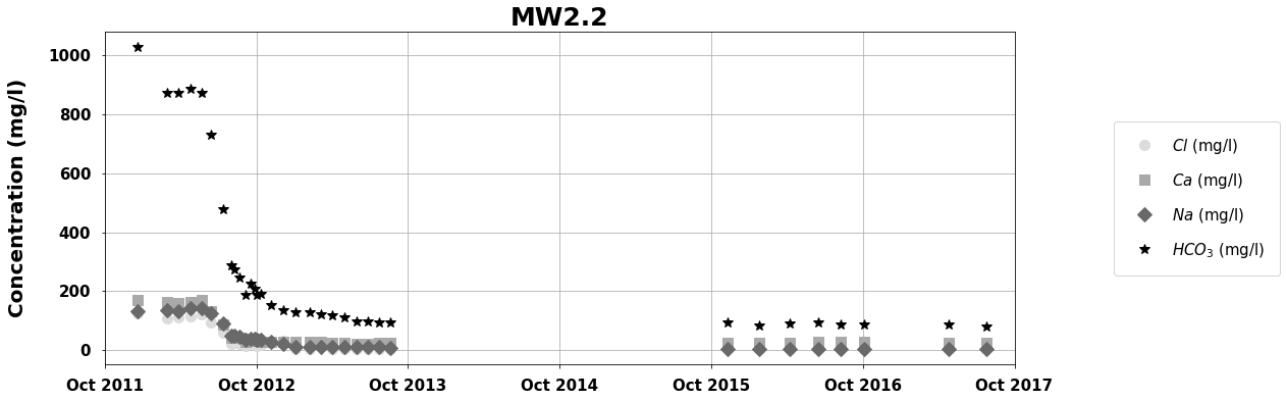

Figure 21.23: Concentrations of Cl, Ca, Na, and HCO_3 in water observed at MW2-S2.

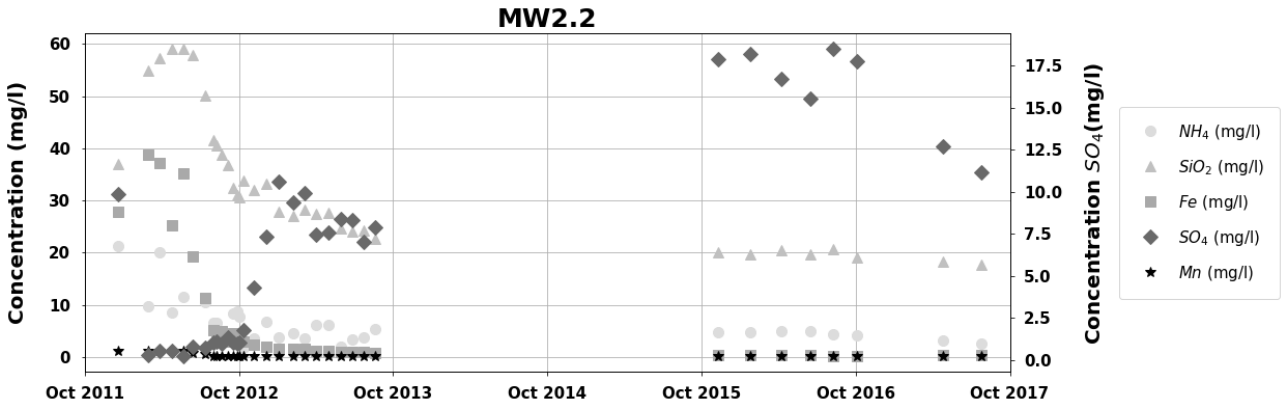

Figure 21.24: Concentrations of NH_4, SiO_2, Fe, SO_4, and Mn in water observed at MW2-S2.

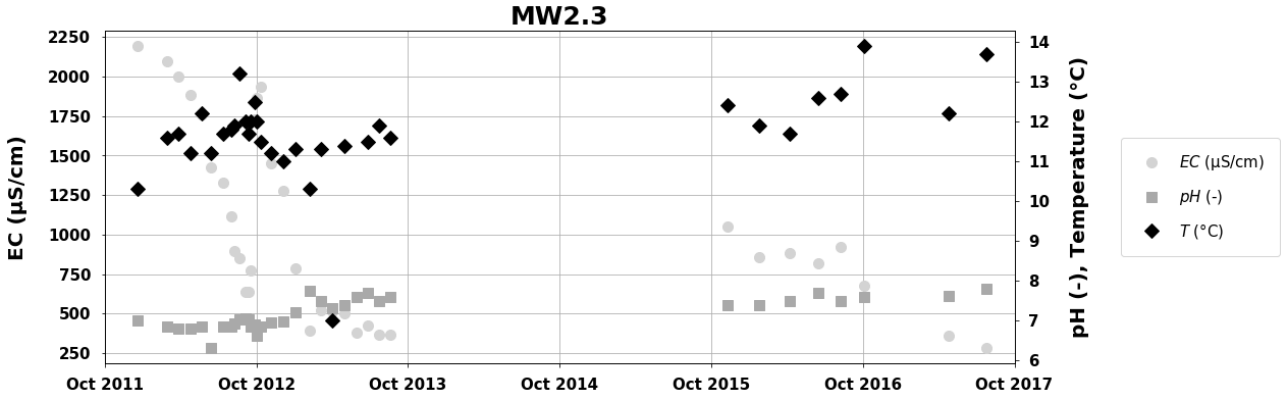

Figure 21.25: Electrical conductivity (EC in µS/cm), pH (-), and temperature (Temp in °C) of water observed at MW2-S3.

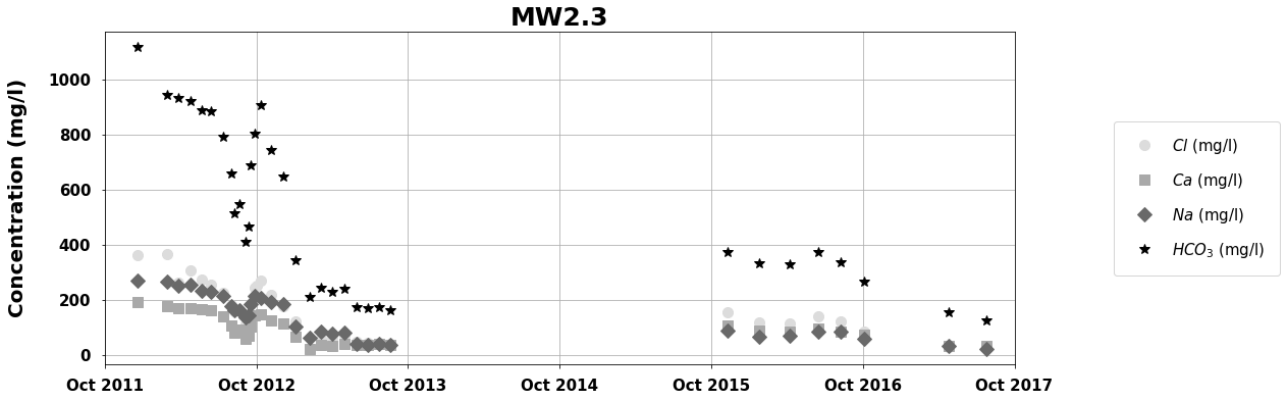

Figure 21.26: Concentrations of Cl, Ca, Na, and HCO_3 in water observed at MW2-S3.

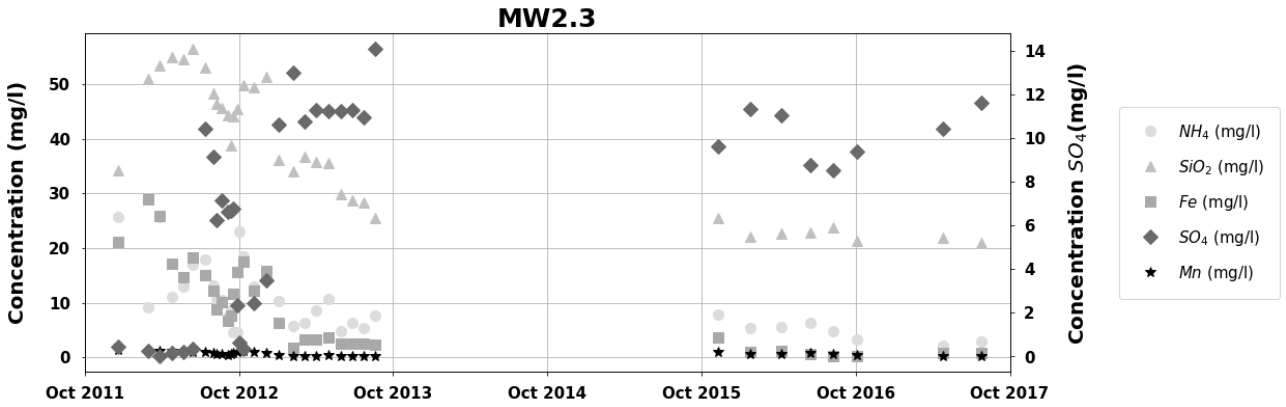

Figure 21.27: Concentrations of NH_4, SiO_2, Fe, SO_4, and Mn in water observed at MW2-S3.

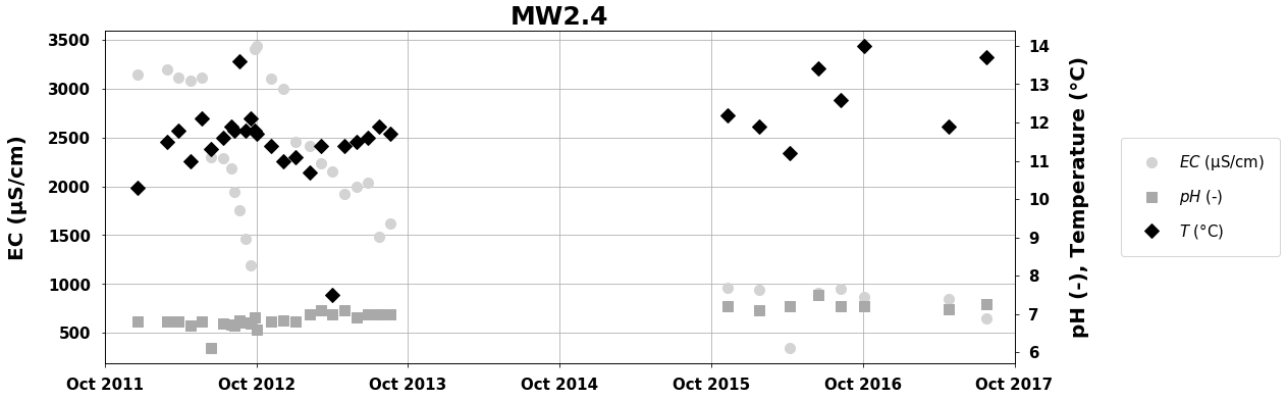

Figure 21.28: Electrical conductivity (EC in µS/cm), pH (-), and temperature (Temp in °C) of water observed at MW2-S4.

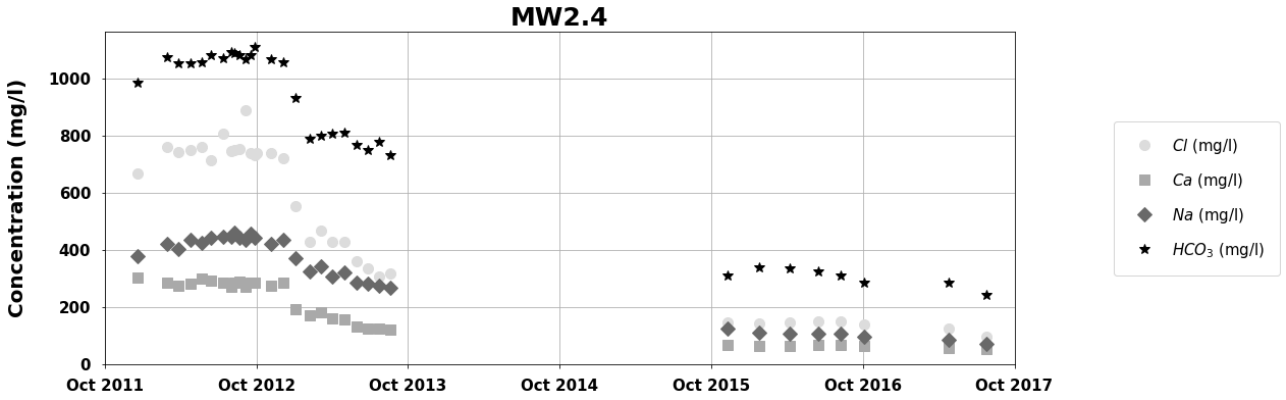

Figure 21.29: Concentrations of Cl, Ca, Na, and HCO_3 in water observed at MW2-S4.

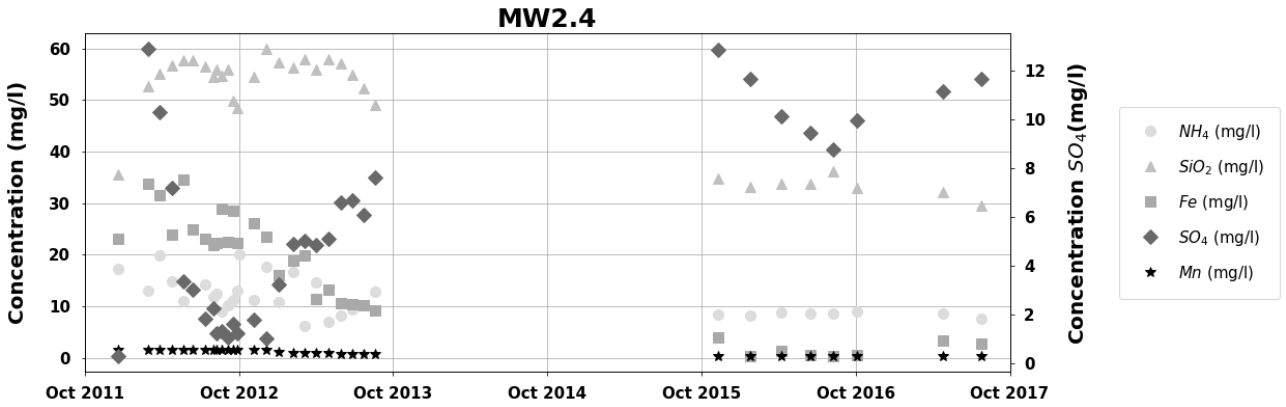

Figure 21.30: Concentrations of NH_4, SiO_2, Fe, SO_4, and Mn in water observed at MW2-S4.

22. APPENDIX 2: Water quality analysis: observed groundwater Westland

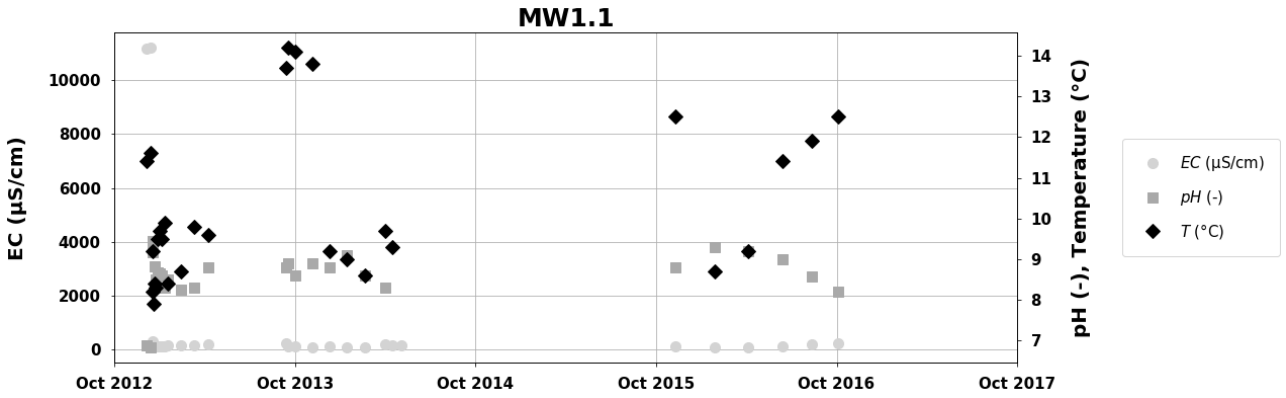

Figure 22.1: Electrical conductivity (EC in µS/cm), pH (-), and temperature (Temp in °C) of water observed at MW1-S1.

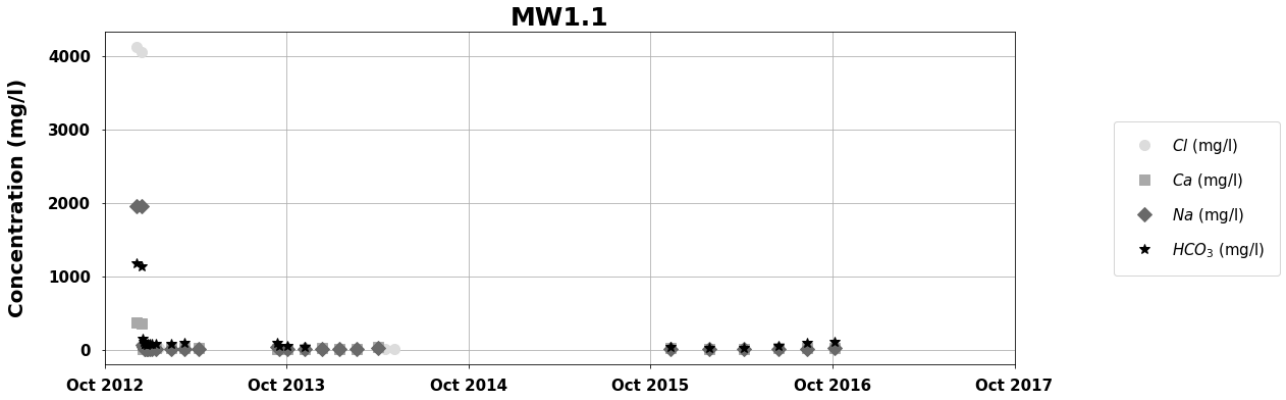

Figure 22.2: Concentrations of Cl, Ca, Na, and HCO_3 in water observed at MW1-S1.

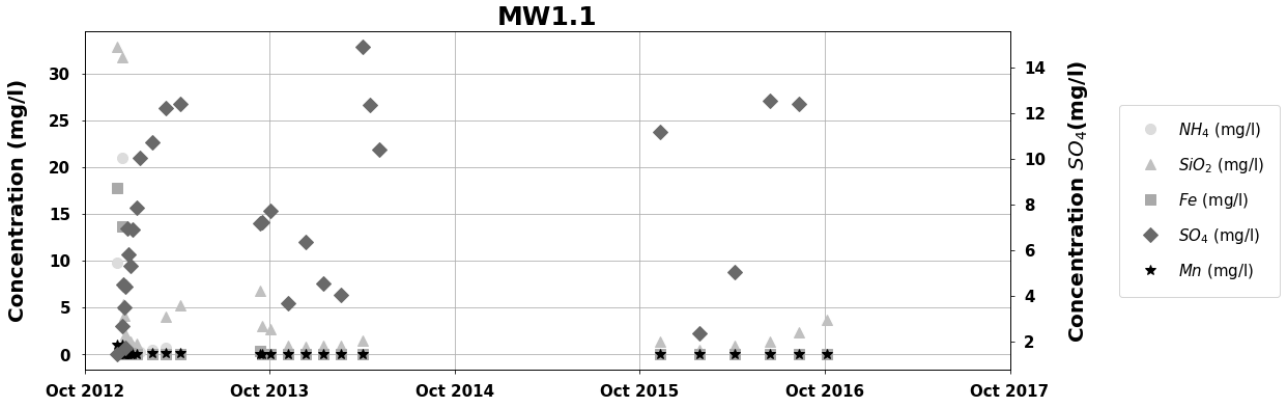

Figure 22.3: Concentrations of NH_4, SiO_2, Fe, SO_4, and Mn in water observed at MW1-S1.

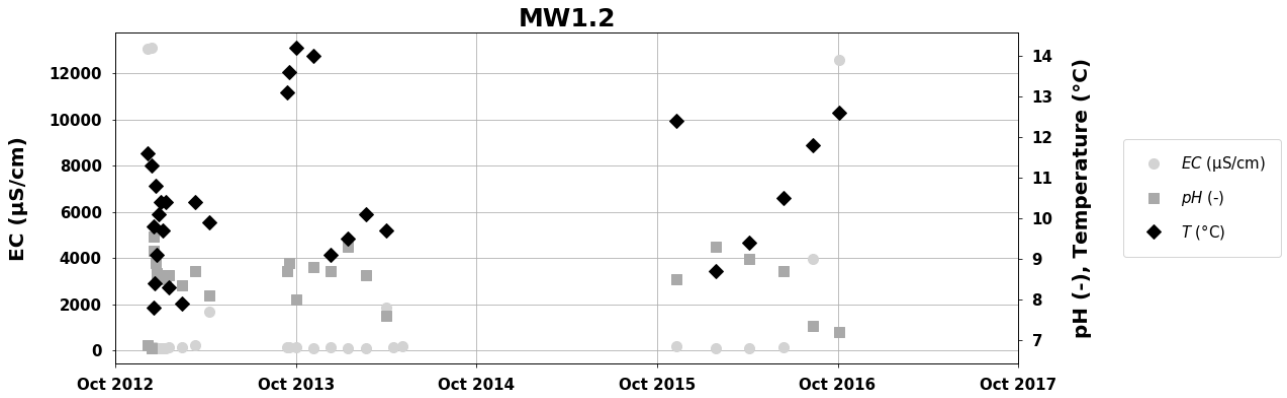

Figure 22.4: Electrical conductivity (EC in µS/cm), pH (-), and temperature (Temp in °C) of water observed at MW1-S2.

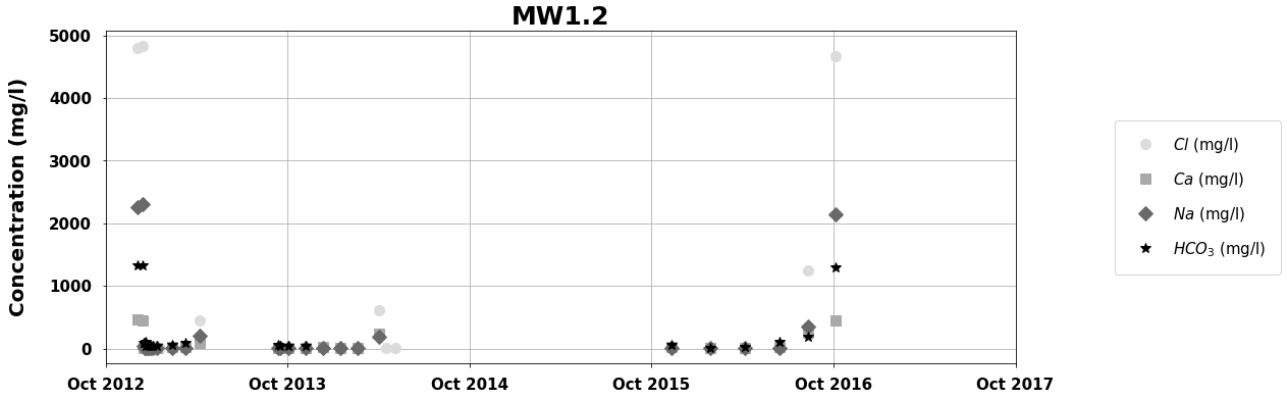

Figure 22.5: Concentrations of Cl, Ca, Na, and HCO_3 in water observed at MW1-S2.

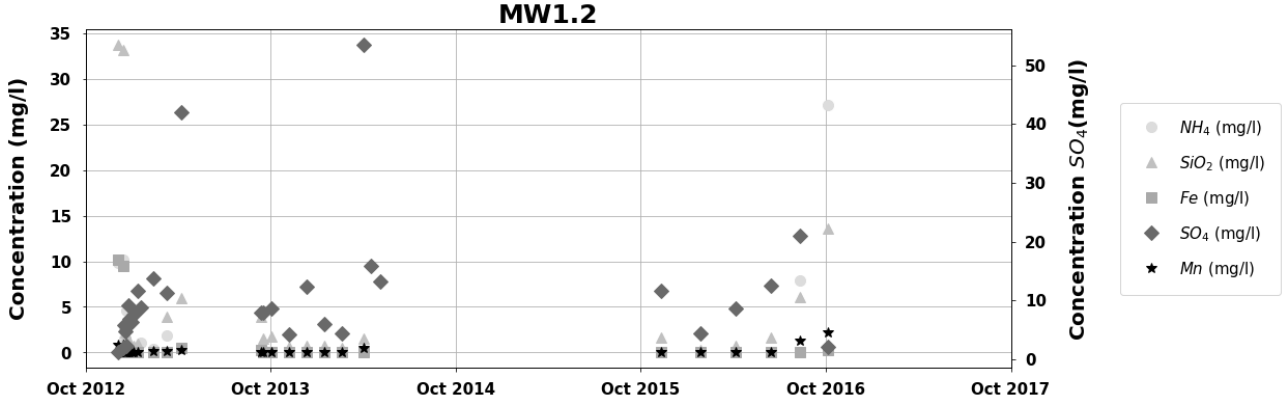

Figure 22.6: Concentrations of NH_4, SiO_2, Fe, SO_4, and Mn in water observed at MW1-S2.

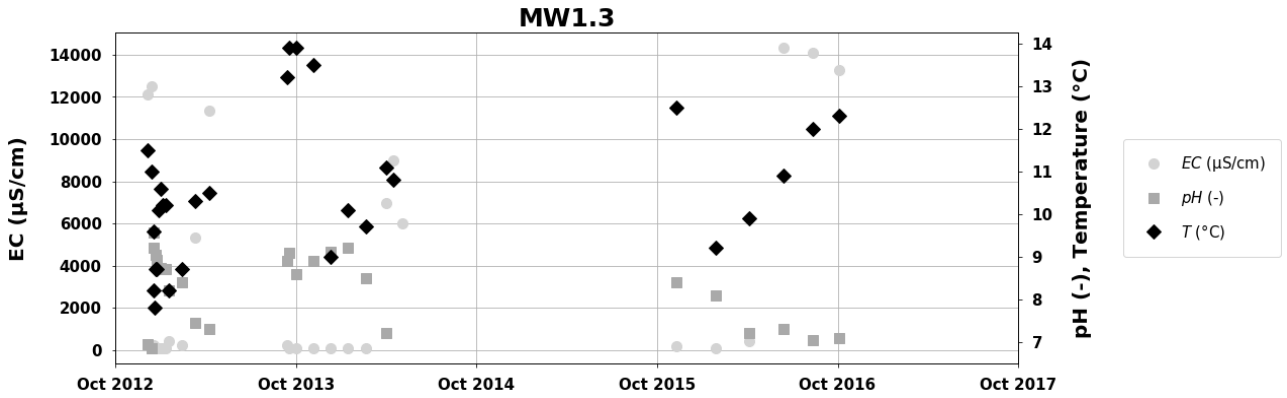

Figure 22.7: Electrical conductivity (EC in µS/cm), pH (-), and temperature (Temp in °C) of water observed at MW1-S3.

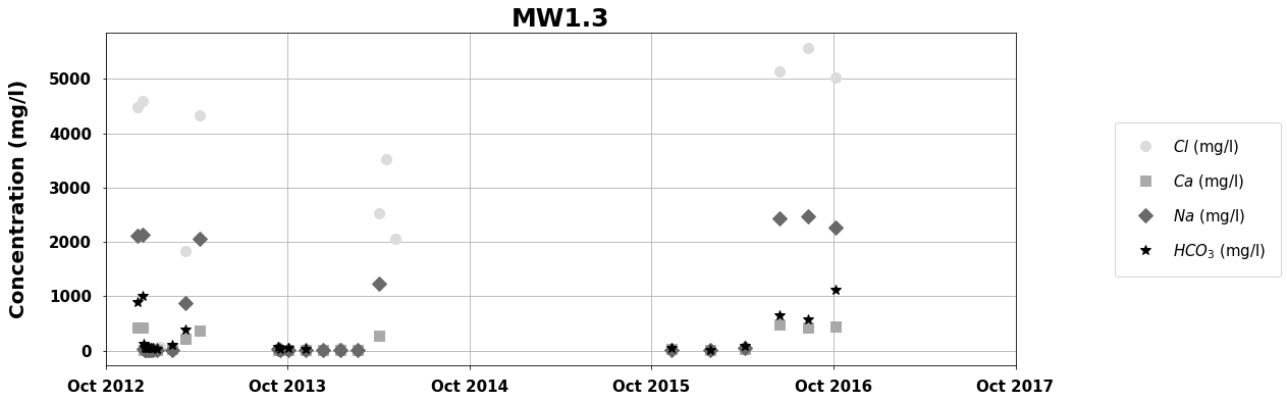

Figure 22.8: Concentrations of Cl, Ca, Na, and HCO_3 in water observed at MW1-S3.

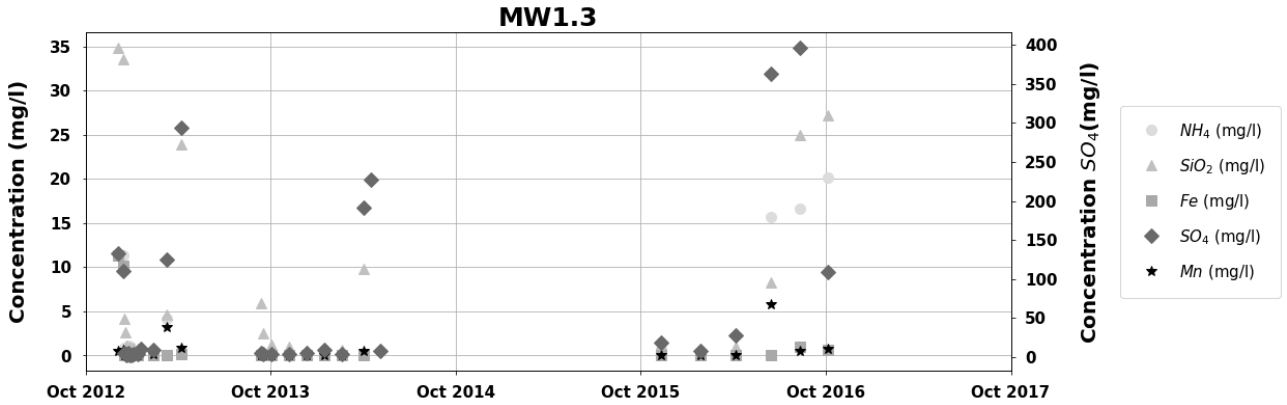

Figure 22.9: Concentrations of NH_4, SiO_2, Fe, SO_4, and Mn in water observed at MW1-S3.

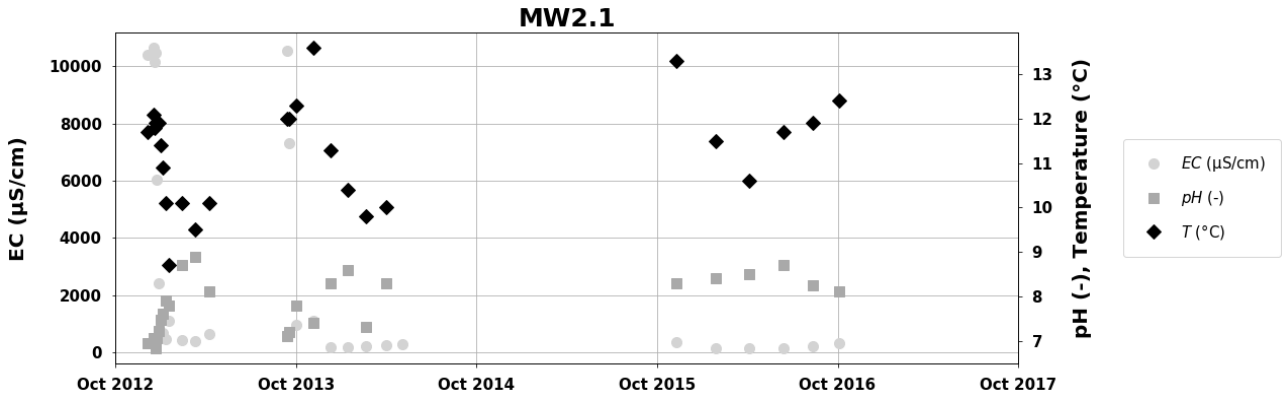

Figure 22.10: Electrical conductivity (EC in µS/cm), pH (-), and temperature (Temp in °C) of water observed at MW2-S1.

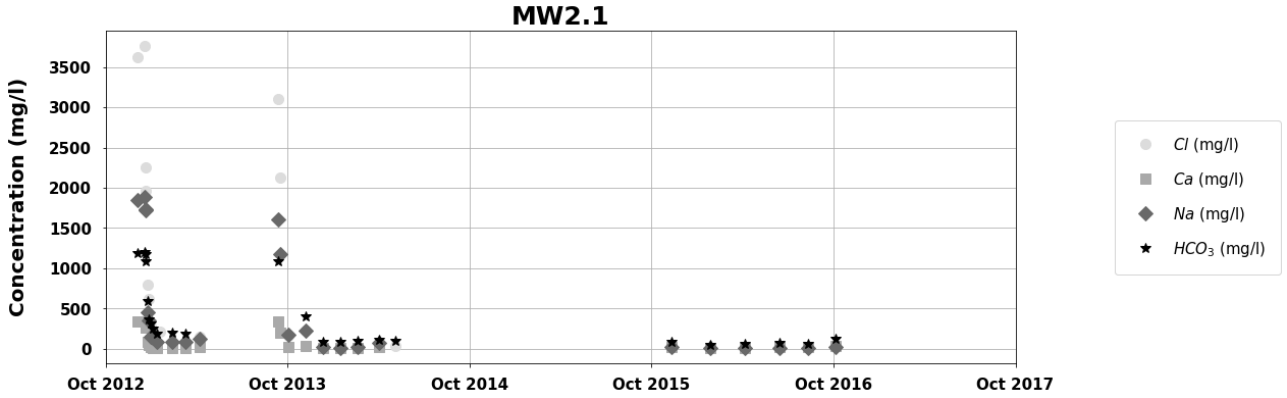

Figure 22.11: Concentrations of Cl, Ca, Na, and HCO_3 in water observed at MW2-S1.

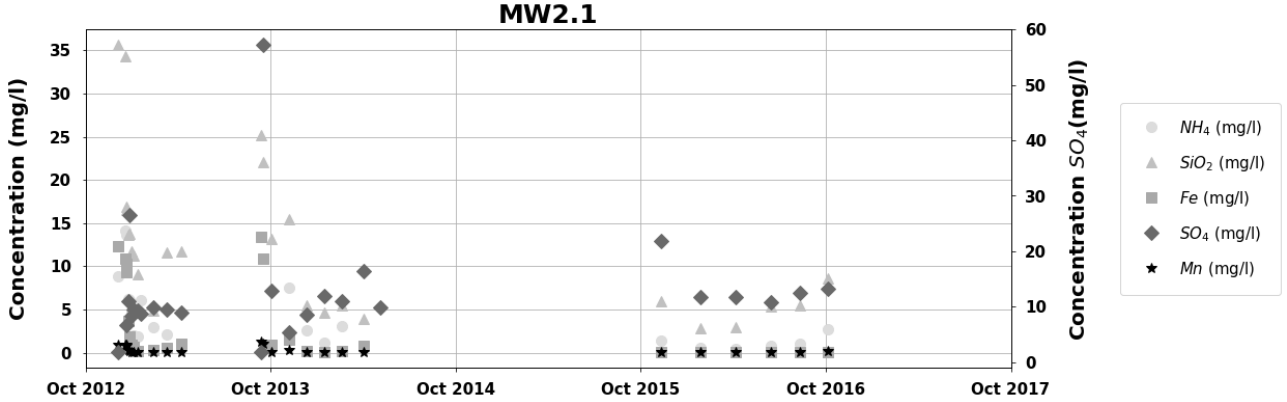

Figure 22.12: Concentrations of NH_4, SiO_2, Fe, SO_4, and Mn in water observed at MW2-S1.

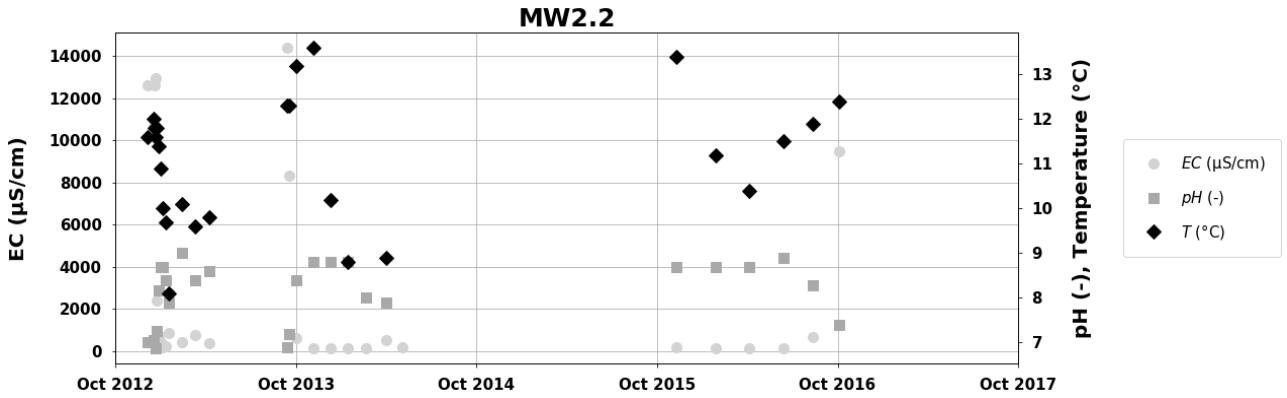

Figure 22.13: Electrical conductivity (EC in µS/cm), pH (-), and temperature (Temp in °C) of water observed at MW2-S2.

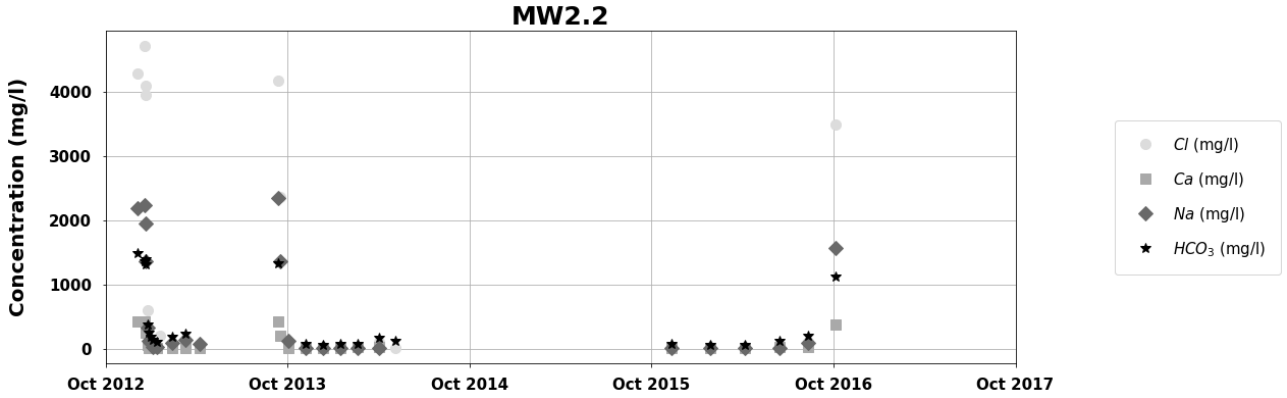

Figure 22.14: Concentrations of Cl, Ca, Na, and HCO_3 in water observed at MW2-S2.

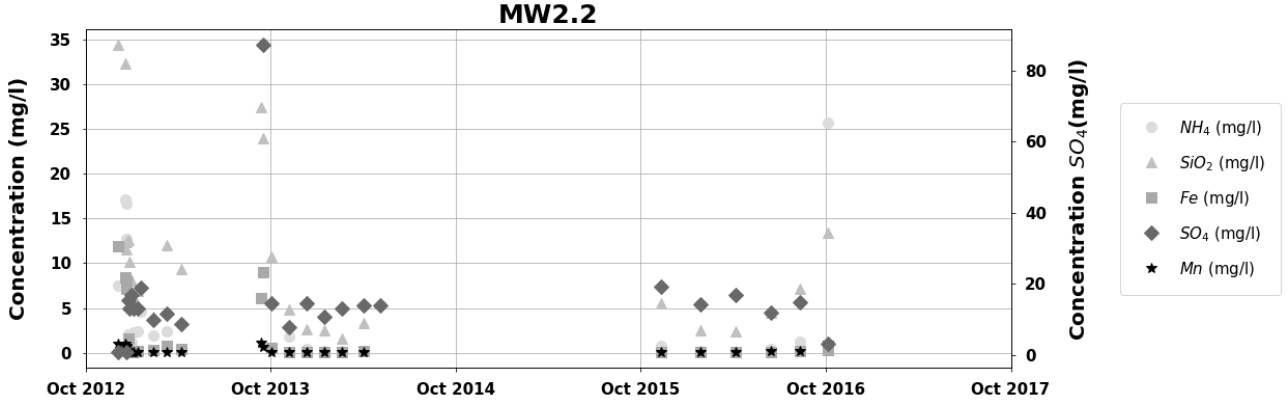

Figure 22.15: Concentrations of NH_4, SiO_2, Fe, SO_4, and Mn in water observed at MW2-S2.

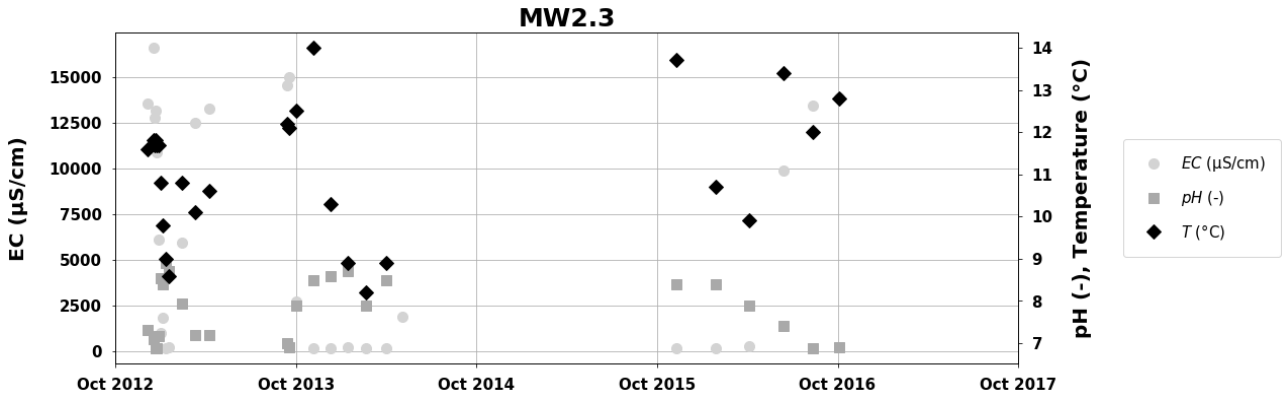

Figure 22.16: Electrical conductivity (EC in µS/cm), pH (-), and temperature (Temp in °C) of water observed at MW2-S3.

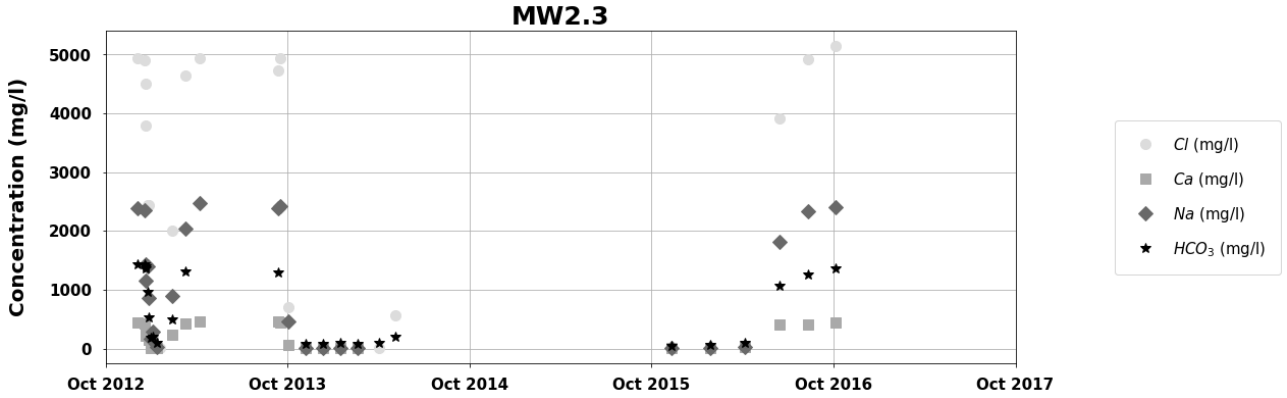

Figure 22.17: Concentrations of Cl, Ca, Na, and HCO_3 in water observed at MW2-S3.

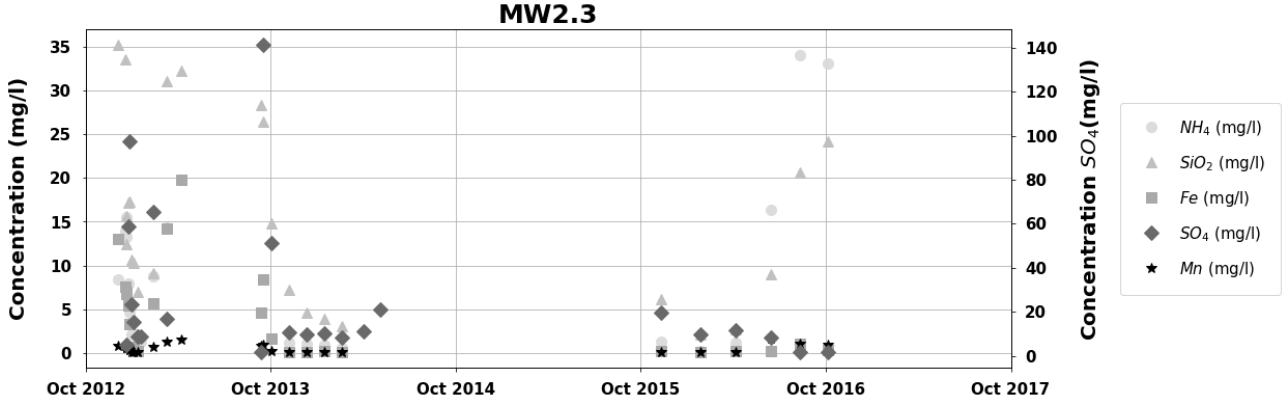

Figure 22.18: Concentrations of NH_4, SiO_2, Fe, SO_4, and Mn in water observed at MW2-S3.